5-2023

Unveiling the Ancestral Function of a Neuroendocrine Regulator, POU-I/Pit1: Insights from Gene Expression Analysis in the Sea Anemone Nematostella vectensis

Miguel Agostinho Pina da Silva
University of Arkansas-Fayetteville

Unveiling the Ancestral Function of a Neuroendocrine Regulator, POU-I/Pit1:
Insights from Gene Expression Analysis in the Sea Anemone *Nematostella vectensis*

A thesis submitted in partial fulfillment
of the requirements for the degree of
Master of Science in Cell and Molecular Biology

by

Miguel Agostinho Pina da Silva
University of Aveiro
Bachelor of Science in Biology, 2018

May 2023
University of Arkansas

This thesis is approved for recommendation to the Graduate Council.

Nagayasu Nakanishi, Ph.D.
Thesis Director

Erica Westerman, Ph.D.
Committee Member

Timothy Evans, Ph.D.
Committee Member

Vibha Srivastava, Ph.D.
Committee Member

Woodrow Shew, Ph.D.
Committee Member

Abstract

Cnidaria (i.e., sea anemones, jellyfish, corals) and Bilateria (i.e., vertebrates, sea stars, fruit flies), are sister groups that diverged around 600 million years ago. Despite the long evolutionary time, many cellular differentiation mechanisms, cell types, tissues and behaviors are conserved. Such as neurons, mechanosensory hair cells, feeding behaviors, peristaltic movements, and sleep. Recent advances in genomics, molecular biology and microscopy have fueled an increased interest in understanding cnidarian nervous and neuroendocrine systems. Understanding the developmental mechanisms and the mode of operation of Cnidarian nervous systems helps to reconstruct the ancestral nervous system of the last common ancestor of Cnidaria and Bilateria. Thus, also shedding light in fundamental aspects of Bilaterian nervous systems. Here, the 'starlet sea anemone' *Nematostella vectensis*, a powerful cnidarian model organism was used to address the gene expression pattern of Pit1, a conserved gene shared between Cnidaria and Bilateria.

In Chapter 1, a method to extract DNA and genotype embryos of *Nematostella* without sacrificing the animal was established, with possible application to other non-sea anemone cnidarians. Early genotyping is fundamental for addressing phenotypes during development, thus opening the door to study the function of any gene of interest during larval pre-metamorphic stages.

In Chapter 2, the expression pattern of Pit1 and detailed cellular morphology of Pit1-positive cells was characterized for the first time in *Nematostella*. Complex neuronal networks and diverse sensory cells were found. Furthermore, the foundation for future functional studies of Pit1 was laid by establishing stable CRISPR-Cas9 knockout and transgenic reporter lines.

Acknowledgments

I want to thank my Professor and Mentor Dr. Nagayasu Nakanishi, for his unwavering support and close guidance, for all the teachings in so many aspects of science and life, for his constructive and diligent feedback and all the transferred experience and expertise, and for the opportunity to join his lab and work closely with him. I also want to thank all the Professors in my Committee, Dr. Erica Westerman, Dr. Timothy Evans, Dr. Vibha Srivastava, and Dr. Woodrow Shew for all the clear advice and feedback, and for vouching for my academic and professional success. I want to thank all my laboratory colleagues, Ndotimi Apulu, Julia Baranyk, Sakura Rieck, Ethan Ozment, Dr. Arianna Tamvacakis and Jianhong Zhou, for the good teamwork, and for the good moments spent together. Furthermore, I want to thank the University of Arkansas for these very instructive years in my personal and professional life and for supporting my graduate studies and research. Additionally, I want to thank Dr. Lora Shadwick that guided me through my first semester teaching at the University of Arkansas and to all other great Professors that I had the pleasure to work and teach with, Dr. Ines Pinto, Dr. Michael Lehmann, Dr. Nagayasu Nakanishi, Dr. Tim Evans, Dr. Adam Paré, Dr. Lewis and Tammy Lorince. Also, I want to thank all my previous Professors that gave me the foundations, motivation, and inspiration to pursue the academic path, Prof. Mário Pacheco, and Prof. Ana Maria Rodrigues, from the University of Aveiro, Prof. Miquel Arnedo, from the University of Barcelona, and Prof. Martine Maan, from the University of Groningen.

Dedication

I want to dedicate my thesis to my siblings, Filipe, and Susana, for their unwavering support and for serving as a source of academic and professional inspiration. To my mother Amália, and to my father Amílcar, for providing me a childhood with a very close contact with nature and meticulous observation of its phenomena, from the observation of the tides and its effect on inter-tidal organisms, to the mesmerizing bioluminescence in the lagoon often seen at night. For the Jacque Cousteau books, the atlases, and the national geographic collections that definitely marked my fascination for the natural world and the natural sciences. To the transforming life experiences that sparked my interest in understanding the mysteries and origins of the mind, the evolution of sensory biology, and the emergent phenomena of reality. To Thainá, whom I met in Fayetteville and who changed my life for the better by being a source of strength, focus, and inspiration.

Table of Contents

List of Published Papers

Silva MAP, Nakanishi N. Genotyping of Sea Anemone during Early Development. J Vis Exp. 2019 May 13;(147). doi: 10.3791/59541. PMID: 31132068. (Chapter 1).

INTRODUCTION

Nervous systems allow animals to quickly gather, process and store information. It allows humans to comprehend complex concepts, think abstractly, communicate using intricate written and spoken languages and to perform mental time travel (i.e., to recall the past and prospect the future across long stretches of time) (DeLong, 1981; Klein, 2013; Ramirez, 2018; Schacter & Addis, 2007; Suddendorf et al., 2018; Suddendorf & Corballis, 1997, 2007; Szpunar et al., 2014; Tonegawa et al., 2015; Zhu et al., 2022). To better understand the fundamental aspects of our mind and its diverse modes of operation, it is essential to understand the origins, evolution and functioning of nervous systems across the animal kingdom (mind evolution: Bolhuis & Wynne, 2009; Buss, 2009; Carter, 1898; Gutfreund, 2018; Popper, 1978; Premack, 2007); (*modi operandi*: Borjigin et al., 2013; Eichenlaub et al., 2014; Irwin et al., 2020; Kanaya et al., 2020; Kondziella, 2020; Mutz & Javadi, 2017; Peinkhofer et al., 2019; Raffone et al., 2019; Schwartz & Maquet, 2002; Tang et al., 2009; Vicente et al., 2022; Voss et al., 2009).

> *In the distant future … psychology will be based on a new foundation, that of the necessary acquirement of each mental power and capacity by gradation. Much light will be thrown on the origin of man and his history*
>
> – Charles Darwin (1859, pg. 488)

Cnidaria (i.e., sea anemones, jellyfish, corals) and Bilateria (i.e., primates, octopuses, insects) are sister groups that diverged around 600 million years ago before the Cambrian explosion (Erwin et al., 2011; Medina et al., 2001; Narbonne, 2005). Despite the long evolutionary time distance, many developmental mechanisms, cell types, tissues, and behaviors are conserved, including neuronal differentiation mechanisms and neuronal cell types (Boero et al., 2007; Galliot, 2000; Gold et al., 2014; Kanaya et al., 2020; Leclère & Röttinger, 2017; Marlow et al., 2009; Nakanishi et al., 2012, 2015; Ozment et al., 2021; Tarrant, 2005; Tournière et al., 2020). Thus, I here make the case that

unveiling fundamental aspects of Cnidarian neurobiology will allow for a more profound understanding of the origins and modes of operation of the putative Cnidarian-Bilaterian mind (Boly et al., 2013; Bosch et al., 2017 Cabanac et al., 2009; Edelman & Seth, 2009; Feinberg & Mallatt, 2013; Griffin, 1999; Mashour & Alkire, 2013; Ota et al., 2022; Shevlin, 2021).

The 'starlet sea anemone' *Nematostella vectensis* is a powerful Cnidarian model organism with a sequenced genome (Putnam et al., 2007), a translucent body propitious for whole-body staining, and several established techniques such as CRISPR-Cas9, transgenesis, in-situ hybridization, RNA-seq, ChIP-seq and live imaging (DuBuc et al., 2016; Ikmi et al., 2014; Renfer et al., 2010; Steinmetz et al., 2012; Schwaiger et al., 2014).

Pit1 (*pituitary specific transcription factor*) is present across the animal tree of life, and well described in vertebrates (Gold et al., 2014; Ingraham et al., 1988), where it functions as a main regulator of development and hormone synthesis of the anterior pituitary gland, essential for growth, metabolism and reproduction (Cohen et al., 1996; Godfrey, 1993; Ho et al., 2015; Lin, 1993; McNamara et al., 2021; Scully & Rosenfeld, 2002; Shewchuk et al., 2006). Furthermore, it plays crucial roles in sensory hair cell maturation of the inner ear, essential for hearing (Fang et al., 2012; Mustapha et al., 2009; Sundaresan et al., 2016).

Considering the lack of knowledge of this gene outside of Bilateria we set to address its expression pattern, the cellular characteristic of Pit1-positive cells and its function in *Nematostella vectensis*.

In Chapter 1, a method for genotyping early embryos of *Nematostella*, without sacrificing the life of the animal, was developed. Thus, allowing for the characterization of mutant phenotypes during larval stages. Furthermore, this method can be applied to other cnidarians as long as the embryos are capable of regeneration after surgery (Silva & Nakanishi, 2019).

In Chapter 2, the gene expression pattern of Pit1 was described during the development of *Nematostella* at embryonic, larval, metamorphic, and polyp stages. Pit1-positive neurons were found across the animal's body, particularly in the endoderm of the body column in vast neuronal networks, and in the ectoderm of tentacles, in sensory cells with diverse morphologies. Some of the detected sensory cells have hair cell specific features such as a single cilium surrounded by stereocilia and actin rootlets in the apex of the cell. The method developed in Chapter 1 was applied to screen knockout mutants of CRISPR-Cas9 Pit1 at early embryonic stages. Furthermore, a transgenic reporter line with the fluorescent protein Kaede under the control of Pit1 promoter, was created. The established knockout lines and transgenic reporter lines will allow for future validation of the function of Pit1 in *Nematostella vectensis*.

Our findings indicate that Pit1 is present in sensory neurons of *Nematostella* and, taken together with comparative studies from the 'moon jellyfish' *Aurelia* which shows expression in sensory cells (Nakanishi et al., 2010), we can extrapolate that Pit1 is present in sensory cells across Cnidaria. Furthermore, in the lancelet *Branchiostma floridae* Pit1 is expressed in the Hatschek's pit which is hypothesized to have chemosensory functions (Candiani et al., 2008).

Taken together this suggests a conserved expression of Pit1 in sensory cells across Bilateria and Cnidaria. Further elucidating the function of Pit1 in regulating cellular differentiation in Cnidaria and the nature of Pit1 cells in early chordates and other bilaterians is essential to unravel the ancestral function of Pit1 between Cnidaria and Bilateria. Doing so will provide a glimpse into the role of Pit1 in the ancestral nervous system of the last common ancestor, which constitutes the foundation for the emergence of our minds.

REFERENCES

Ahissar, E., & Assa, E. (2016). Perception as a closed-loop convergence process. *ELife*, *5*, e12830. https://doi.org/10.7554/eLife.12830

Boero, F., Schierwater, B., & Piraino, S. (2007). Cnidarian milestones in metazoan evolution. Integrative and Comparative Biology, 47(5), 693–700. https://doi.org/10.1093/icb/icm041

Bolhuis, J. J., & Wynne, C. D. L. (2009). Can evolution explain how minds work? Nature, 458(7240), 832–833. https://doi.org/10.1038/458832a

Boly, M., Seth, A. K., Wilke, M., Ingmundson, P., Baars, B., Laureys, S., Edelman, D. B., & Tsuchiya, N. (2013). Consciousness in humans and non-human animals: Recent advances and future directions. Frontiers in Psychology, 4.https://doi.org/10.3389/fpsyg.2013.00625

Borjigin, J., Lee, U., Liu, T., Pal, D., Huff, S., Klarr, D., Sloboda, J., Hernandez, J., Wang, M. M., & Mashour, G. A. (2013). Surge of neurophysiological coherence and connectivity in the dying brain. Proceedings of the National Academy of Sciences, 110(35), 14432–14437. https://doi.org/10.1073/pnas.1308285110

Bosch, T. C. G., Klimovich, A., Domazet-Lošo, T., Gründer, S., Holstein, T. W., Jékely, G., Miller, D. J., Murillo-Rincon, A. P., Rentzsch, F., Richards, G. S., Schröder, K., Technau, U., & Yuste, R. (2017). Back to the Basics: Cnidarians Start to Fire. Trends in Neurosciences, 40(2), 92–105. https://doi.org/10.1016/j.tins.2016.11.005

Buss, D. M. (2009). The great struggles of life: Darwin and the emergence of evolutionary psychology. American Psychologist, 64(2), 140–148. https://doi.org/10.1037/a0013207

Cabanac, M., Cabanac, A. J., & Parent A. (2009). The emergence of consciousness in phylogeny. Behavioural Brain Research, 198(2), 267-272. https://doi.org/10.1016/j.bbr.2008.11.028.

Candiani, S., Holland, N. D., Oliveri, D., Parodi, M., & Pestarino, M. (2008). Expression of the amphioxus Pit-1 gene (AmphiPOU1F1/Pit-1) exclusively in the developing preoral organ, a putative homolog of the vertebrate adenohypophysis. Brain Research Bulletin, 75(2–4), 324–330. https://doi.org/10.1016/j.brainresbull.2007.10.023

Carter, M. H. (1898). Darwin's Idea of Mental Development. The American Journal of Psychology, 9(4), 534. https://doi.org/10.2307/1412189

Cohen, L. E., Wondisford, F. E., & Radovick, S. (1996). ROLE OF PIT-1 IN THE GENE EXPRESSION OF GROWTH HORMONE, PROLACTIN, AND THYROTROPIN. Endocrinology and Metabolism Clinics of North America, 25(3), 523–540. https://doi.org/10.1016/S0889-8529(05)70339-X

Darwin, C., 1809-1882. (1859). On the origin of species by means of natural selection, or preservation of favoured races in the struggle for life. London :John Murray,

DeLong, A. J. (1981). Phenomenological Space-Time: Toward an Experiential Relativity. Science, 213(4508), 681–683. https://doi.org/10.1126/science.7256273

Edelman, D. B., & Seth, A. K. (2009). Animal consciousness: a synthetic approach. Trends in neurosciences, 32(9), 476–484. https://doi.org/10.1016/j.tins.2009.05.008

Eichenlaub, J.-B., Nicolas, A., Daltrozzo, J., Redouté, J., Costes, N., & Ruby, P. (2014). Resting Brain Activity Varies with Dream Recall Frequency Between Subjects. Neuropsychopharmacology, 39(7), 1594–1602. https://doi.org/10.1038/npp.2014.6

Erwin, D. H., Laflamme, M., Tweedt, S. M., Sperling, E. A., Pisani, D., & Peterson, K. J. (2011). The Cambrian Conundrum: Early Divergence and Later Ecological Success in the Early History of Animals. Science, 334(6059), 1091–1097. https://doi.org/10.1126/science.1206375

Fang, Q., Giordimaina, A. M., Dolan, D. F., Camper, S. A., & Mustapha, M. (2012). Genetic Background of Prop1 df Mutants Provides Remarkable Protection Against Hypothyroidism-Induced Hearing Impairment. Journal of the Association for Research in Otolaryngology, 13(2), 173–184. https://doi.org/10.1007/s10162-011-0302-3

Feinberg, T. E., & Mallatt, J. (2013). The evolutionary and genetic origins of consciousness in the Cambrian Period over 500 million years ago. Frontiers in Psychology, 4, Article 667. https://doi.org/10.3389/fpsyg.2013.00667

Galliot, B. (2000). Conserved and divergent genes in apex and axis development of cnidarians. Current Opinion in Genetics & Development, 10(6), 629–637. https://doi.org/10.1016/S0959-437X(00)00141-6

Godfrey, P. (1993). GHRH receptor of little mice contains a missense mutation in the extracellular domain that disrupts receptor function. Nature Genetics, 4(3), 227–232. https://doi.org/10.1038/ng0793-227

Gold, D. A., Gates, R. D., & Jacobs, D. K. (2014). The Early Expansion and Evolutionary Dynamics of POU Class Genes. Molecular Biology and Evolution, 31(12), 3136–3147. https://doi.org/10.1093/molbev/msu243

Griffin, D. R. (1999). Nonhuman Minds. Philosophical Topics, 27(1), 233–254.

Gutfreund, Y. (2018). The Mind-Evolution Problem: The Difficulty of Fitting Consciousness in an Evolutionary Framework. Frontiers in Psychology, 9, 1537. https://doi.org/10.3389/fpsyg.2018.01537

Ho, Y., Cooke, N. E., & Liebhaber, S. A. (2015). An Autoregulatory Pathway Establishes the Definitive Chromatin Conformation at the Pit-1 Locus. Molecular and Cellular Biology, 35(9), 1523–1532. https://doi.org/10.1128/MCB.01283-14

Ingraham, H. A., Albert, V. R., Chen, R., & Crenshaw, E. B. (1988). A Family of Pou-Domain and Pit-1 Tissue-Specific Transcription Factors in Pituitary and Neuroendocrine Development.

Irwin, K., Amaral, M., & Chester, D. (2020) The Self-Simulation Hypothesis Interpretation of Quantum Mechanics. Entropy (Basel), 22(2), 247. https://doi.org/10.3390/e22020247

Kanaya, H. J., Park, S., Kim, J., Kusumi, J., Krenenou, S., Sawatari, E., Sato, A., Lee, J., Bang, H., Kobayakawa, Y., Lim, C., & Itoh, T. Q. (2020). A sleep-like state in Hydra unravels conserved sleep mechanisms during the evolutionary development of the central nervous system. Science Advances, 6(41), eabb9415. https://doi.org/10.1126/sciadv.abb9415

Klein, S. B. (2013). The complex act of projecting oneself into the future: The complex act of projecting oneself into the future. Wiley Interdisciplinary Reviews: Cognitive Science, 4(1), 63–79. https://doi.org/10.1002/wcs.1210

Kondziella, D. (2020). The Neurology of Death and the Dying Brain: A Pictorial Essay. Frontiers in Neurology, 11, 736. https://doi.org/10.3389/fneur.2020.00736

Leclère, L., & Röttinger, E. (2017). Diversity of Cnidarian Muscles: Function, Anatomy, Development and Regeneration. Frontiers in Cell and Developmental Biology, 4. https://doi.org/10.3389/fcell.2016.00157

Lin, S. C. (1993). Molecular basis of the little mouse phenotype and implications for cell type-specific growth. Nature, 364(6434), 208–213. https://doi.org/doi: 10.1038/364208a0

Marlow, H. Q., Srivastava, M., Matus, D. Q., Rokhsar, D., & Martindale, M. Q. (2009). Anatomy and development of the nervous system of Nematostella vectensis, an anthozoan cnidarian. Developmental Neurobiology, 69(4), 235–254. https://doi.org/10.1002/dneu.20698

Mashour, G. A., & Alkire, M. T. (2013). Evolution of consciousness: phylogeny, ontogeny, and emergence from general anesthesia. Proceedings of the National Academy of Sciences of the United States of America, 110 Suppl 2, 10357–10364. https://doi.org/10.1073/pnas.1301188110

Medina, M., Collins, A. G., Silberman, J. D., & Sogin, M. L. (2001). Evaluating hypotheses of basal animal phylogeny using complete sequences of large and small subunit rRNA. Proceedings of the National Academy of Sciences, 98(17), 9707–9712. https://doi.org/10.1073/pnas.171316998

Mustapha, M., Fang, Q., Gong, T.-W., Dolan, D. F., Raphael, Y., Camper, S. A., & Duncan, R. K. (2009). Deafness and Permanently Reduced Potassium Channel Gene Expression and Function in Hypothyroid Pit1 dw Mutants. The Journal of Neuroscience, 29(4), 1212–1223. https://doi.org/10.1523/JNEUROSCI.4957-08.2009

Mutz, J., & Javadi, A.-H. (2017). Exploring the neural correlates of dream phenomenology and altered states of consciousness during sleep. Neuroscience of Consciousness, 2017(1). https://doi.org/10.1093/nc/nix009

Nakanishi, N., Camara, A. C., Yuan, D. C., Gold, D. A., & Jacobs, D. K. (2015). Gene Expression Data from the Moon Jelly, Aurelia, Provide Insights into the Evolution of the Combinatorial Code Controlling Animal Sense Organ Development. PLOS ONE, 10(7), e0132544. https://doi.org/10.1371/journal.pone.0132544

Nakanishi, N., Renfer, E., Technau, U., & Rentzsch, F. (2012). Nervous systems of the sea anemone Nematostella vectensis are generated by ectoderm and endoderm and shaped by distinct mechanisms. Development, 139(2), 347–357. https://doi.org/10.1242/dev.071902

Nakanishi, N., Yuan, D., Hartenstein, V., & Jacobs, D. K. (2010). Evolutionary origin of rhopalia: Insights from cellular-level analyses of Otx and POU expression patterns in the developing rhopalial nervous system: Otx and POU expression patterns in Aurelia. Evolution & Development, 12(4), 404–415. https://doi.org/10.1111/j.1525-142X.2010.00427.x

Narbonne, G. M. (2005). THE EDIACARA BIOTA: Neoproterozoic Origin of Animals and Their Ecosystems. Annual Review of Earth and Planetary Sciences, 33(1), 421–442. https://doi.org/10.1146/annurev.earth.33.092203.122519

Ota, K., Suzuki, D.G. & Tanaka, S. (2022). Phylogenetic Distribution and Trajectories of Visual Consciousness: Examining Feinberg and Mallatt's Neurobiological Naturalism. Journal for General Philosophy of Science, 53, 459–476. https://doi.org/10.1007/s10838-021-09591-1

Ozment, E., Tamvacakis, A. N., Zhou, J., Rosiles-Loeza, P. Y., Escobar-Hernandez, E. E., Fernandez-Valverde, S. L., & Nakanishi, N. (2021). Cnidarian hair cell development illuminates an ancient role for the class IV POU transcription factor in defining mechanoreceptor identity. ELife, 10, e74336. https://doi.org/10.7554/eLife.74336

Peinkhofer, C., Dreier, J. P., & Kondziella, D. (2019). Semiology and Mechanisms of Near-Death Experiences. Current Neurology and Neuroscience Reports, 19(9), 62. https://doi.org/10.1007/s11910-019-0983-2

Popper, K. (1978). Natural Selection and the Emergence of Mind. Dialectica, 32(3–4), 339–355. https://doi.org/10.1111/j.1746-8361.1978.tb01321.x

Premack, D. (2007). Human and animal cognition: Continuity and discontinuity. Proceedings of the National Academy of Sciences, 104(35), 13861–13867. https://doi.org/10.1073/pnas.0706147104

Raffone, A., Marzetti, L., Del Gratta, C., Perrucci, M. G., Romani, G. L., & Pizzella, V. (2019). Toward a brain theory of meditation. In Progress in Brain Research (Vol. 244, pp. 207–232). Elsevier. https://doi.org/10.1016/bs.pbr.2018.10.028

Ramirez, S. (2018). Crystallizing a memory. Science, 360(6394), 1182–1183. https://doi.org/10.1126/science.aau0043

Schacter, D. L., & Addis, D. R. (2007). The cognitive neuroscience of constructive memory: Remembering the past and imagining the future. Philosophical Transactions of the Royal

Society B: Biological Sciences, 362(1481), 773–786. https://doi.org/10.1098/rstb.2007.2087

Schwartz, S., & Maquet, P. (2002). Sleep imaging and the neuro-psychological assessment of dreams. Trends in Cognitive Sciences, 6(1), 23–30. https://doi.org/10.1016/S1364-6613(00)01818-0

Scully, K. M., & Rosenfeld, M. G. (2002). Pituitary Development: Regulatory Codes in Mammalian Organogenesis. Science, 295(5563), 2231–2235. https://doi.org/10.1126/science.1062736

Shevlin, H. (2021). Non-human consciousness and the specificity problem: A modest theoretical proposal. Mind & Language, 36, 297–314.

Shewchuk, B. M., Ho, Y., Liebhaber, S. A., & Cooke, N. E. (2006). A Single Base Difference between Pit-1 Binding Sites at the hGH Promoter and Locus Control Region Specifies Distinct Pit-1 Conformations and Functions. Molecular and Cellular Biology, 26(17), 6535–6546. https://doi.org/10.1128/MCB.00267-06

Silva, M. A. P., & Nakanishi, N. (2019). Genotyping of Sea Anemone during Early Development. Journal of Visualized Experiments, 147, 59541. https://doi.org/10.3791/59541

Smith, C. U. M. (1978). Charles Darwin, the origin of consciousness, and panpsychism. Journal of the History of Biology, 11(2), 245–267. https://doi.org/10.1007/BF00389301

Suddendorf, T., Bulley, A., & Miloyan, B. (2018). Prospection and natural selection. Current Opinion in Behavioral Sciences, 24, 26–31. https://doi.org/10.1016/j.cobeha.2018.01.019

Suddendorf, T., & Corballis, M. C. (1997). Mental time travel and the evolution of the human mind. Genetic, Social, and General Psychology Monographs, 123(2), 133–167.

Suddendorf, T., & Corballis, M. C. (2007). Mental time travel across the disciplines: The future looks bright. Behavioral and Brain Sciences, 30(3), 335–345. https://doi.org/10.1017/S0140525X0700221X

Sundaresan, S., Balasubbu, S., & Mustapha, M. (2016). Thyroid hormone is required for the pruning of afferent type II spiral ganglion neurons in the mouse cochlea. Neuroscience, 312, 165–178. https://doi.org/10.1016/j.neuroscience.2015.11.020

Szpunar, K. K., Spreng, R. N., & Schacter, D. L. (2014). A taxonomy of prospection: Introducing an organizational framework for future-oriented cognition. Proceedings of the National Academy of Sciences, 111(52), 18414–18421. https://doi.org/10.1073/pnas.1417144111

Tang, Y.-Y., Ma, Y., Fan, Y., Feng, H., Wang, J., Feng, S., Lu, Q., Hu, B., Lin, Y., Li, J., Zhang, Y., Wang, Y., Zhou, L., & Fan, M. (2009). Central and autonomic nervous system interaction is altered by short-term meditation. Proceedings of the National Academy of Sciences, 106(22), 8865–8870. https://doi.org/10.1073/pnas.0904031106

Tarrant, A. M. (2005). Endocrine-like Signaling in Cnidarians: Current Understanding and Implications for Ecophysiology. Integrative and Comparative Biology, 45(1), 201–214. https://doi.org/10.1093/icb/45.1.201

Tonegawa, S., Liu, X., Ramirez, S., & Redondo, R. (2015). Memory Engram Cells Have Come of Age. Neuron, 87(5), 918–931. https://doi.org/10.1016/j.neuron.2015.08.002

Tournière, O., Dolan, D., Richards, G. S., Sunagar, K., Columbus-Shenkar, Y. Y., Moran, Y., & Rentzsch, F. (2020). NvPOU4/Brain3 Functions as a Terminal Selector Gene in the Nervous System of the Cnidarian Nematostella vectensis. Cell Reports, 30(13), 4473-4489.e5. https://doi.org/10.1016/j.celrep.2020.03.031

Vicente, R., Rizzuto, M., Sarica, C., Yamamoto, K., Sadr, M., Khajuria, T., Fatehi, M., Moien-Afshari, F., Haw, C. S., Llinas, R. R., Lozano, A. M., Neimat, J. S., & Zemmar, A. (2022). Enhanced Interplay of Neuronal Coherence and Coupling in the Dying Human Brain. Frontiers in Aging Neuroscience, 14, 813531. https://doi.org/10.3389/fnagi.2022.813531

Voss, U., Holzmann, R., Tuin, I., & Hobson, A. J. (2009). Lucid Dreaming: A State of Consciousness with Features of Both Waking and Non-Lucid Dreaming. Sleep, 32(9), 1191–1200. https://doi.org/10.1093/sleep/32.9.1191

Zhu, Z., Anderson, M. C., & Wang, Y. (2022). Inducing forgetting of unwanted memories through subliminal reactivation. Nature Communications, 13(1), 6496. https://doi.org/10.1038/s41467-022-34091-1

I. CHAPTER 1

Genotyping of sea anemone during early development

Miguel A.P. Silva[1], Nagayasu Nakanishi[1]

[1]Department of Biological Sciences, University of Arkansas, Fayetteville, AR, USA, 72701

Manuscript published in *Journal of Visualized Experiments*, 2019, e59541. doi:10.3791/59541 (2019)

ABSTRACT

Described here is a PCR-based protocol to genotype the gastrula stage embryo of the anthozoan cnidarian *Nematostella vectensis* without sacrificing the life of the animal. Following in vitro fertilization and de-jellying, zygotes are allowed to develop for 24 h at room temperature to reach the early- to mid-gastrula stage. The gastrula embryos are then placed on an agarose gel bed in a Petri dish containing seawater. Under the dissecting microscope, a tungsten needle is used to surgically separate an aboral tissue fragment from each embryo. Post-surgery embryos are then allowed to heal and continue development. Genomic DNA is extracted from the isolated tissue fragment and used as a template for locus-specific PCR. The genotype can be determined based on the size of PCR products or presence/absence of allele-specific PCR products. Post-surgery embryos are then sorted according to the genotype. The duration of the entire genotyping process depends on the number of embryos to be screened, but it minimally requires 4–5 h. This method can be used to identify knockout mutants from a genetically heterogeneous population of embryos and enables analyses of phenotypes during development.

Keywords: genotyping, PCR, CRISPR, Cnidaria, *Nematostella*, embryo

INTRODUCTION

Cnidarians represent a diverse group of animals that include jellyfish, corals, and sea anemones. They are diploblasts, composed of ectoderm and endoderm that are separated by an extracellular matrix (mesoglea). Cnidaria is a sister group to speciose Bilateria, to which traditional animal models such as *Drosophila* and *Mus* belong (1). Additionally, the Cnidaria-Bilateria divergence is thought to have occurred in the pre-Cambrian period (2). As such, comparative studies of cnidarians and bilaterians are essential for gaining insights into the biology of their most recent common ancestor. Recently, comparative genomics has revealed that cnidarians and bilaterians share many developmental toolkit genes such as notch and bHLH, implying that their common ancestor already had these genes (3). However, the role of these developmental toolkit genes in the last common ancestor of Cnidaria and Bilateria is comparably less well understood. To address this problem, it is critical to study how these deeply conserved genes function in cnidarians. One of the emerging cnidarian genetic models is the anthozoan *Nematostella vectensis*. Its genome has been sequenced (3), and a variety of genetic tools, including morpholino-mediated gene knockdown, meganuclease-mediated transgenesis, and CRISPR-Cas9-mediated gene knockins and knockouts, are now available for use in this animal. In addition, *Nematostella* development is relatively well understood. During embryogenesis, gastrulation occurs by invagination (4), and the embryo develops into a free-swimming planula larva. The planula subsequently transforms into a sessile polyp with a mouth and circumoral tentacles. The polyp then grows and reaches sexual maturity. CRISPR-Cas9-mediated targeted mutagenesis is now routinely used to study gene function in *Nematostella vectensis* (5,6,7,8,9). To generate knockout mutants in *Nematostella*, a cocktail containing locus-specific single-guide RNAs and the endonuclease Cas9 protein is first injected into unfertilized or fertilized eggs to produce F0 founder animals that typically show

mosaicism. F0 animals are subsequently raised to sexual maturity and crossed with each other to produce an F1 population, a subset of which may be knockout mutants (6). Alternatively, sexually mature F0 animals can be crossed with wild-type animals to generate F1 heterozygous animals, and F1 heterozygotes that carry a knockout allele in the locus of interest can then be crossed with each other to produce F2 offspring, one-quarter of which are expected to be knockout mutants (5). Both approaches require a method to identify knockout mutants from a genetically heterogeneous population. Polyp tentacles can be used to extract genomic DNA for genotyping (6,7). However, in cases where the developmental function of the gene of interest is being investigated and mutant embryos do not reach the polyp stage (i.e., due to larval lethality associated with the mutation), knockout mutants need to be identified early in ontogeny. Described here is a PCR-based protocol to genotype individual animals at the gastrula stage without sacrificing the animal, which enables identification of knockout mutants from a genetically heterogeneous population of embryos. The duration of the entire genotyping process depends on the number of embryos to be screened, but it minimally requires 4-5 h.

PROTOCOL

1. Induction of spawning, in vitro fertilization, and de-jellying

1. Maintain *Nematostella vectensis* in seawater with a salinity of 12 parts per thousand (ppt) in darkness at 16 °C, feeding Artemia daily.
2. On the day before spawning induction, place animals in a temperature- and light-controlled incubator. Program the incubator so that the animals are exposed to 8 h of light at 25 °C. Optional: Feed a small piece (<1 mm3) of oyster to individual animals before placing them into the incubator to enhance spawning.
3. Leave the animals in the incubator for 1 h at 16 °C.

4. Remove the animals from the incubator and leave them on a benchtop with light at room temperature (RT) to allow spawning. Spawning usually occurs within the next 1.5–2 h.
5. If males and females are in separate containers, place egg packages from the female container into a sperm-containing male container by using a transfer pipette whose tip is cut to enlarge the opening so that the eggs are not damaged by mechanical stress during transfer. Allow eggs to be fertilized by leaving them in the male container for at least 15 min.
6. De-jelly the egg packages in seawater containing 3% cysteine (pH 7.4) on a Petri dish or in a 15 mL tube. Gently agitate on a shaker for 12 min.
7. Use a plastic pipette to break up clumps and continue to agitate for another 2-3 min until completely de-jellied.
8. Remove cysteine by replacing the media with fresh seawater for at least 5x.
9. Keep the fertilized eggs on a glass Petri dish at 16 °C or RT.

2. Surgical removal of an aboral tissue from a gastrula embryo

1. Prepare a DNA extraction buffer consisting of 10 mM Tris-HCl (pH 8), 50 mM KCl, 1 mM EDTA, 0.3% Tween20, 0.3% NP40, and 1 mg/mL proteinase K. Use 20 mL of the extraction buffer per embryo. Mix well by vortexing and aliquot the buffer into PCR tubes.
2. Dissolve 1% agarose in seawater and pour it into a Petri dish to cover the bottom. Cool on a benchtop to make a gel bed. Pour fresh seawater to cover the gel bed in the Petri dish.
3. Transfer 24 h post-fertilization (hpf) embryos (early- to mid-gastrula stage) into the Petri dish containing an agarose gel bed.
4. Insert a tungsten needle into a needle holder and sterilize by dipping the needle tip in alcohol (70% or higher) and placing it in flame to burn off the alcohol.

5. Under a dissecting microscope (at 20x to 40x magnification), use the tungsten needle to make a depression on the agarose bed by removing a piece of surface agarose about the size of an embryo to be manipulated, and place the embryo onto the depression with its lateral side facing down in order to restrict the movement of the embryo for microsurgery.
6. Use the tungsten needle to surgically excise a piece of aboral tissue located opposite to the oral blastoporal opening. An aboral one-third to one-quarter of the embryonic tissue along the oral-aboral axis is usually sufficient.
7. Use a P20 pipette to transfer the isolated aboral tissue (in <2 mL) to a PCR tube containing 20 mL of DNA extraction buffer.
8. Transfer the post-surgery embryo into a well containing at least 500 mL of fresh seawater in a 24- or 96-well plate.
9. Repeat steps 2.4–2.8 for the number of embryos as needed.
10. Place the well plate containing post-surgery embryos in an incubator at 16 °C or RT until genotyping is completed.

3. Genomic DNA extraction and genotyping PCR

1. Briefly spin down the PCR tubes containing the DNA extraction buffer and isolated embryonic tissues using a mini-centrifuge (e.g. at 2,680 x g for 10 s).
2. To extract genomic DNA from single embryos, incubate the PCR tubes at 55 °C for 3 h. Vortex for 30 s every 30 min to ensure breakup of cell clumps and enhance cell lysis.
3. Incubate the PCR tubes at 95 °C for 5 min to inactivate proteinase K.
4. Keep gDNA extracts at 4 °C or on ice, and immediately proceed to PCR. NOTE: The protocol can be paused here by placing gDNA extracts in a -20 °C freezer.

5. Set up a PCR reaction using extracted gDNA as a template to amplify the genomic locus of interest.
    1. If different alleles at the locus of interest differ in size so that the size difference can be detected by agarose gel electrophoresis, design a single set of primers to amplify the entire locus.
    2. Alternatively, use allele-specific primers that generate PCR products only in the presence of the specific allele; for instance, by designing the primer that binds to a region containing insertion/deletion mutations.
    3. Use a typical 20 mL PCR reaction mix as follows: 5 mL of gDNA extracts, 8 mL of nuclease-free water, 4 mL of PCR buffer, 0.2 mL of 10mM dNTPs, 0.6 mL of DMSO, 1 mL of 10 mM forward primer, 1 mL of 10 mM reverse primer, and 0.2 mL of DNA polymerase (see Table of Materials).

        NOTE: Multiple primers can be used in a PCR reaction. For instance, one universal forward primer and two allele-specific reverse primers can be combined, as long as the two reverse primers are designed to generate PCR products of distinct sizes so that the presence/absence of the two alleles can be unambiguously determined by gel electrophoresis (see representative results section).
6. Run agarose gel electrophoresis to determine the size and presence/absence of PCR products. Adjust the condition of agarose gel electrophoresis (e.g., agarose gel percentage, V/cm, and duration) depending on the expected size of PCR products.
7. Use the results from PCR regarding the size and presence/absence of PCR products to assign a genotype to each post-surgery embryo. For instance, if different alleles are expected to generate PCR products of different sizes, use the size information to assign the

genotype for each embryo. If allele-specific primers are used, the data on the presence/absence of PCR products should be used to assign a genotype to each embryo.

8. Sort embryos according to genotype.

REPRESENTATIVE RESULTS

The *Nematostella* genome has a single locus that encodes a precursor protein for the neuropeptide GLWamide. Three knockout mutant alleles at this locus (glw^{-a}, glw^{-b}, and glw^{-c}) have been previously reported (5). Four heterozygous males carrying a wild-type allele (+) and knockout allele glw^{-c} at the GLWamide locus (genotype: $+/glw^{-c}$) were crossed with a heterozygous female carrying a wild-type allele and different knockout allele glw^{-a} at the same locus (genotype: $+/glw^{-a}$) to generate a progeny. There are four possible genotypes in the progeny: glw^{-a}/glw^{-c}, $+/glw^{-c}$, $glw^{-a}/+$, and +/+. Out of all the progeny, eight embryos were randomly selected for this representative genotyping assay. For genotyping PCR, one universal forward primer and two allele-specific reverse primers were designed (5). The reverse primer specific to glw^{-a} binds to a region containing insertion mutations, and the expected size of the PCR product is 151 bp. The reverse primer specific to glw^{-c} binds to a region containing both insertion and deletion mutations, and the expected size of the PCR product is 389 bp. Neither reverse primer can bind to the wild-type sequence, and thus no PCR products will be generated from wild-type embryos. Figure 1 shows a representative result of the PCR assay. Embryos 1 and 2 show a single PCR band consistent with the expected size of glw^{-a}. Embryos 3 and 6 show two PCR bands that correspond to the expected sizes for alleles glw^{-a} and glw^{-c}. Embryos 4, 7, and 8 show a single PCR band consistent with the expected size of glw^{-c}. Embryo 5 shows no bands, suggesting the lack of primer binding. To rule out the possibility of gDNA extraction failure, another PCR was run using a reverse primer that can bind to the wild-type sequence, which showed a PCR product of an

expected size (1290 bp; Figure 2). It should be noted that in Figure 2, one of the samples (indicated by *) showed no PCR products, suggesting a failure in gDNA extraction. Based on the above results, the genotype of each embryo is interpreted to be as follows: embryo 1: +/glw^{-a}, embryo 2: +/glw^{-a}, embryo 3: glw$^{-a/}$glw^{-c}, embryo 4: +/glw^{-c}, embryo 5: +/+, embryo 6: glw$^{-a/}$glw^{-c}, embryo 7: +/glw^{-c}, and embryo 8: +/glw^{-c}.

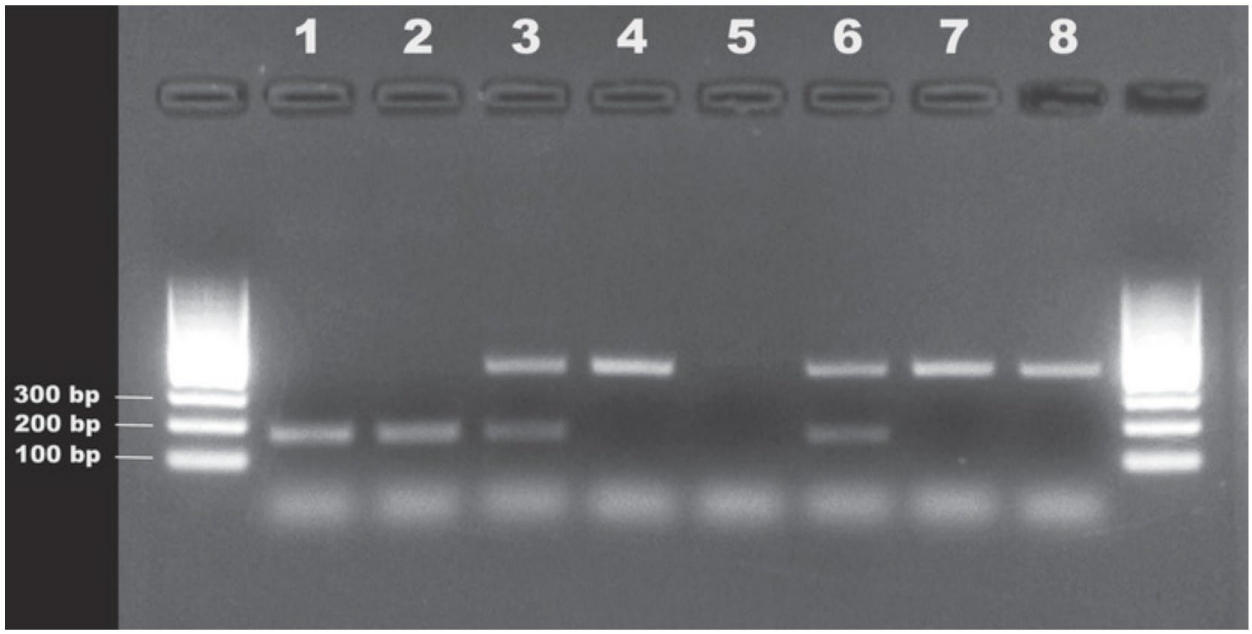

Figure 1: Representative results of a genotyping PCR assay. 1-8 represent genotyping PCR results from randomly sampled embryos among the progeny of an F1 heterozygous mutant cross between one +/glw^{-a} female and +/glw^{-c} males. gDNA was extracted from an embryonic tissue fragment and used as a PCR template. The GLWamide locus was targeted for PCR amplification, and one universal forward primer and two allele-specific reverse primers were used (**Table of Materials**). The reverse primer specific to glw^{-a} generates a 151 bp PCR band (1, 2, 3, 6), while the reverse primer specific to glw^{-c} generates a 389 bp PCR band (3, 4, 6, 7, 8). Neither reverse primer can bind to the wild-type sequence, and thus no PCR products will be generated from wild-type embryos (5). The 1.5% agarose gel was run at 128 V for 25 min. A 100 bp DNA ladder was used. Please click here to view a larger version of this figure.

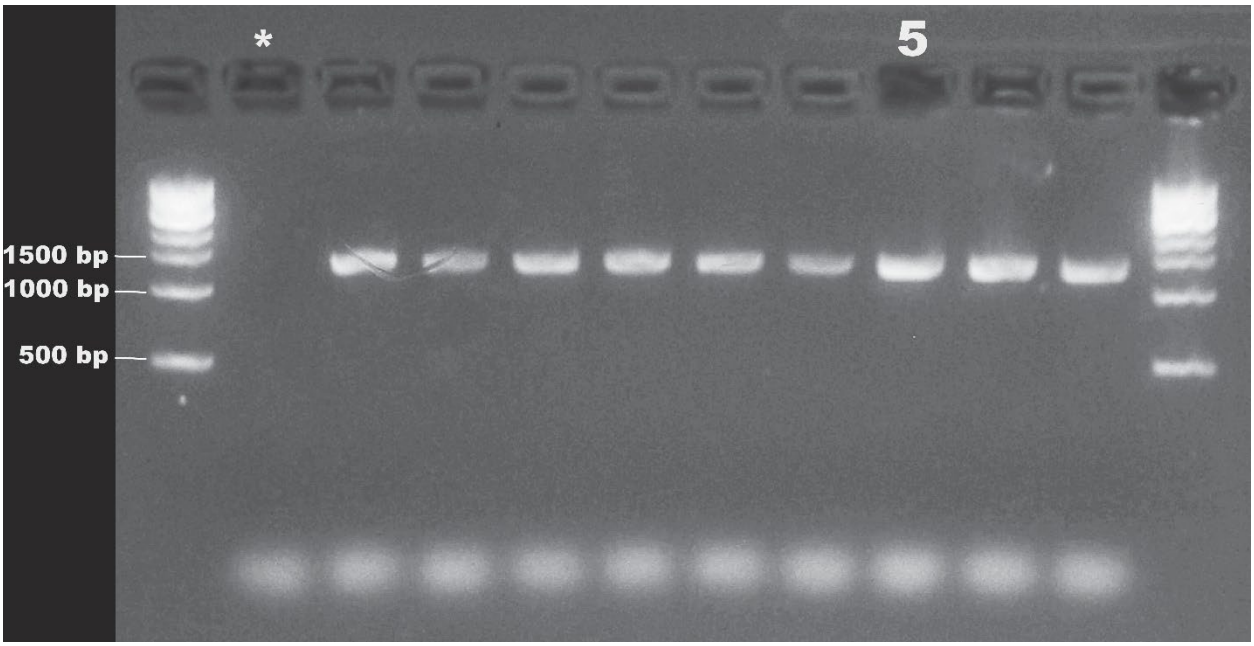

Figure 2: Representative results of locus-specific PCR to confirm the presence of gDNA. Ten gDNA extracts that failed to generate PCR products in glw mutant allele-specific PCR experiments, including embryo 5 from **Figure 1** ('5'), were used as PCR templates for the PCR experiment shown. A universal forward and reverse GLWamide-locus-specific primers were used to generate a 1290 bp PCR product from a wild-type allele. Nine out of ten DNA extracts (except for the one indicated*) showed a PCR band of expected size, including embryo 5 from **Figure 1** ('5'). This suggests that the failure to generate PCR products from the embryo 5 was not due to the lack of a sufficient gDNA template. The 1.5% agarose gel was run at 128 V for 25 min. 1 kb DNA ladder was used. Please click here to view a larger version of this figure.

DISCUSSION

Described here a PCR-based protocol to genotype a single sea anemone embryo without sacrificing the animal. Following spawning and de-jellying, the fertilized eggs are allowed to develop into gastrulae. The aboral region of each gastrula embryo is surgically removed, and the isolated aboral tissue is used for subsequent genomic DNA extraction, while the remaining post-surgery embryos heal and continue development. The gDNA extracts are then used for a PCR assay to determine the genotype of each embryo. This method takes advantage of the ability of the oral halves of the sea anemone embryo to regulate and develop (10,11), and the majority of the embryos (>90%) typically survive the surgery and develop normally under appropriate culture conditions. The tissue amount required for this genotyping assay is less than one-half of an entire gastrula embryo, and

negative results due to gDNA extraction failure are rare (<5%). Given that only a small amount of tissue is necessary, it is likely possible to use pre-gastrula stage embryos for this genotyping assay; although, this has yet to be tested. This method can be performed efficiently as long as the animal has not reached a stage of active swimming (i.e., before the free-swimming planula stage). This genotyping method is particularly advantageous in cases requiring the performance of phenotype analyses during development. One limitation of this protocol is that the number of embryos able to screened may be limited. In particular, surgical removal of an aboral tissue can take one to two minutes per embryo, especially for the uninitiated. An experienced researcher should be able to complete the entire genotyping assay for at least 80 embryos per day, but studies involving hundreds or thousands of embryos are likely too time-consuming to complete in one day. Researchers also need to be mindful that the phenotype observed in post-surgery mutants may be different from that in intact mutants, for instance, due to the effect of gene knockout on healing and/or embryonic regulation in gastrulae. This possibility should be tested by examining whether the phenotype found in post-surgery mutants is indeed observable in intact mutants. There are several alternative approaches to the described method of genotyping. First, immunostaining with an antibody against a protein whose expression is lost in knockout mutants can be performed to identify knockout mutant individuals from a genetically heterogeneous population of developing animals. Second, in situ hybridization can be used for this purpose, if the riboprobe can be designed so that it does not hybridize to mutant mRNAs. For instance, if the mutant alleles of a knockout animal carry large deletion mutations in the same region of the gene, the riboprobe can be designed to hybridize to the region of the gene deleted in the knockout mutants. In both cases, knockout mutants are expected to show no labeling, while heterozygous and wild-type individuals should show labeling. However, the animals will need to be sacrificed due to tissue fixation required for

the staining. Finally, knockout mutants may be raised to sexual maturity and crossed with each other to generate a progeny, all of which should be knockout mutants, and analyses of developmental phenotype can be performed using this progeny (6). This method requires that the knockout animals are viable and capable of reproduction and is thus limited in its application to nonessential genes. Although the described genotyping protocol is designed for sea anemone embryos, it is possible to use this method with other cnidarians in which both genomic information and embryos are accessible (e.g., corals (12) and jellyfish (13)), as long as the embryos are capable of healing and regulation upon surgical removal. Successful CRISPR-mediated gene modification experiments have been already reported in corals (14) as well as hydrozoan jellyfish (15,16). Future applications of this genotyping protocol to non-sea anemone cnidarians will be important for studies of the genetic basis of their development. This, in turn, will be key to gaining mechanistic insights into the evolution of remarkably diverse cnidarian development.

DISCLOSURES

The author has nothing to disclose.

ACKNOWLEDGEMENTS

We thank anonymous reviewers for comments on the earlier version of the manuscript, which improved the manuscript. This work was supported by funds from the University of Arkansas.

REFERENCES

1. Medina, M., Collins, A. G., Silberman, J. D., Sogin, M. L. Evaluating hypotheses of basal animal phylogeny using complete sequences of large and small subunit rRNA. Proceedings of the National Academy of Sciences of the United States of America. 98 (17), 9707-9712 (2001).

2. Erwin, D. H. *et al*. The Cambrian Conundrum: Early Divergence and Later Ecological Success in the Early History of Animals. Science. 334 (6059), 1091-1097 (2011).

3. Putnam, N. H. *et al*. Sea anemone genome reveals ancestral eumetazoan gene repertoire and genomic organization. Science. 317 (5834), 86-94 (2007).

4. Magie, C. R., Daly, M., Martindale, M. Q. Gastrulation in the cnidarian *Nematostella vectensis* occurs via invagination not ingression. Developmental Biology. 305 (2), 483-497 (2007).

5. Nakanishi, N., Martindale, M. Q. CRISPR knockouts reveal an endogenous role for ancient neuropeptides in regulating developmental timing in a sea anemone. eLife. 7, e39742 (2018).

6. He, S. N. *et al*. An axial Hox code controls tissue segmentation and body patterning in *Nematostella vectensis*. Science. 361 (6409), 1377 (2018).

7. Ikmi, A., McKinney, S. A., Delventhal, K. M., Gibson, M. C. TALEN and CRISPR/Cas9-mediated genome editing in the early-branching metazoan *Nematostella vectensis*. Nature Communications. 5, 5486 (2014).

8. Servetnick, M. D. *et al*. Cas9-mediated excision of *Nematostella* brachyury disrupts endoderm development, pharynx formation and oral-aboral patterning. Development. 144 (16), 2951-2960 (2017).

9. Kraus, Y., Aman, A., Technau, U., Genikhovich, G. Pre-bilaterian origin of the blastoporal axial organizer. Nature Communications. 7, 11694 (2016).

10. Fritzenwanker, J. H., Genikhovich, G., Kraus, Y., Technau, U. Early development and axis specification in the sea anemone *Nematostella vectensis*. Developmental Biology. 310 (2), 264-279 (2007).

11. Lee, P. N., Kumburegama, S., Marlow, H. Q., Martindale, M. Q., Wikramanayake, A. H. Asymmetric developmental potential along the animalvegetal axis in the anthozoan cnidarian, *Nematostella vectensis*, is mediated by Dishevelled. Developmental Biology. 310 (1), 169-186 (2007).

12. Shinzato, C. *et al*. Using the *Acropora digitifera* genome to understand coral responses to environmental change. Nature (London). 476 (7360), 320-323 (2011).

13. Gold, D. A. *et al*. The genome of the jellyfish *Aurelia* and the evolution of animal complexity. Nature Ecology & Evolution. 3 (1), 96-104 (2019).

14. Clevesa, P. A., Strader, M. E., Bay, L. K., Pringle, J. R., Matz, M. V. CRISPR/Cas9-mediated genome editing in a reef-building coral. Proceedings of the National Academy of Sciences of the United States of America. 115 (20), 5235-5240 (2018).

15. Momose, T. *et al*. High doses of CRISPR/Cas9 ribonucleoprotein efficiently induce gene knockout with low mosaicism in the hydrozoan *Clytia hemisphaerica* through microhomology-mediated deletion. Scientific Reports. 8, 11734 (2018).

16. Artigas, G. Q. *et al*. A gonad-expressed opsin mediates light-induced spawning in the jellyfish *Clytia*. eLife. 7, e29555 (2018).

II. CHAPTER 2

Gene expression analysis of a pituitary-specific gene, Pit-1, in a pituitary-less sea anemone & possible implications in neuronal development

Miguel A.P. Silva[1], Nagayasu Nakanishi[1]

[1]Department of Biological Sciences, University of Arkansas, Fayetteville, AR, USA, 72701

Manuscript *in preparation*

ABSTRACT

Here I describe the expression pattern of POU-I/Pit1 in *Nematostella vectensis* and lay the foundations for further functional studies of NvPit1 with CRISPR-Cas9 knockout mutants and transgenic reporter lines. NvPit1 was found to be expressed in diverse sensory cells in the tentacular ectoderm of polyps, as well as constituting a complex network of endodermal NvPit1 neurons in larval stages and polyps. The function of POU-I/Pit1 has so far only been described in vertebrates where it acts as a terminal selector in the development of the anterior pituitary gland, as well as a direct regulator of hormone synthesis. Understanding the function of POU-I/Pit1 in Cnidaria is vital to unveil the ancestral function of this transcription factor in the last common ancestor of Bilateria and Cnidaria, and thus gain a better understanding on the origins and evolution of the animal neuroendocrine system.

Keywords: evolution, *POU-I,* cell differentiation, pituitary, sensory, *Nematostella*, Cnidaria,

1) INTRODUCTION

Cnidaria (e.g., jellyfish, corals, sea anemones) occupy a key phylogenetic position to understand the early history of animals and the evolution of nervous and endocrine systems (Boero *et al*., 2007; Tarrant, 2005). Cnidaria and Bilateria (e.g., chordates, arthropods, annelids) are sister groups that diverged around 600 million-years ago before the Cambrian explosion, and share several developmental mechanisms, cell types, tissues, and behaviors (Boero et al., 2007; Galliot, 2000; Gold et al., 2014; Kanaya et al., 2020; Leclère & Röttinger, 2017), including neuronal cell types and neuronal differentiation mechanisms (Marlow *et al*., 2009; Nakanishi *et al*., 2012; Ozment *et al*., 2021; Tournière *et al*., 2020).

In neural organisms, the neuro-endocrine system is the main mediator between the external and internal world, modulating development, sensation, memory, metabolism, and behavior (Ahissar & Assa, 2016; De Marco et al., 2016; Jennings & de Lecea, 2020; Nakanishi & Martindale, 2018a; Seehausen et al., 2008; Soares et al., 2010). To generate a functional neuroendocrine system, several cell types must be differentiated and maintained. Different cell types are generated by the complex activity of specific gene regulatory networks (GRNs), that mediate cell behavior, proliferation, differentiation, and maintenance of cell-specific traits (e.g., neurites) (Fakhry, 2013; Fischer & Smith, 2012; Huang *et al*., 2020; Okawa *et al*., 2016; Scully & Rosenfeld, 2002). Terminal selectors are the final transcription factors of GRNs that directly regulate effector genes, thus terminally differentiating and maintaining cell state (e.g., endocrine cell remains endocrine) (Allan & Thor, 2015; Hobert, 2008; Leyva-Díaz et al., 2020; Leyva-Díaz & Hobert, 2019).

The '*pituitary specific transcription factor 1*' (Pit1), a class I POU-homeodomain transcription factor (Gold et al., 2014; Ingraham et al., 1988), acts as a terminal selector in the anterior pituitary gland of vertebrates maintaining cellular identity of lactotropes, somatotropes and thyrotropes and

directly regulating the transcription of prolactin (PRL), somatotropin (GH) and thyrotropin (TSH) (Cohen et al., 1996; Godfrey, 1993; Ho et al., 2015; Lin, 1993; McNamara et al., 2021; Scully & Rosenfeld, 2002; Shewchuk et al., 2006). Pit1 is an ancient POU gene with orthologs across Metazoa, in Porifera (i.e., sponges), Ctenophores (i.e., comb-jellies), Cnidaria, and Bilateria, with the exception of Echinoderms (e.g., sea-urchin), Mollusks (e.g., oysters, octopus), Ecdysozoa (i.e., nematodes and arthropods), and Placozoa where Pit1 seems to have been lost (Fig. 1; Gold *et al*., 2014).

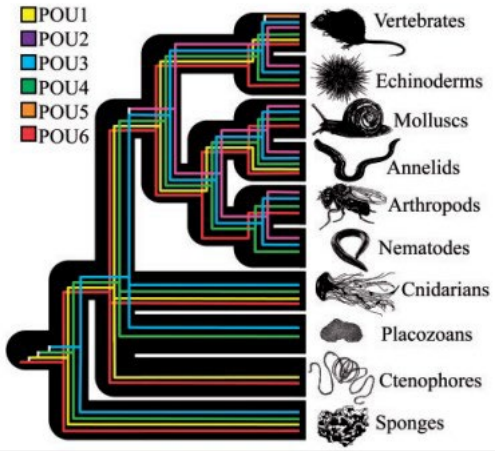

Fig. 1. Phylogeny of POU genes across Metazoa. Note the yellow line denoting POU-I/Pit1. From (Gold et al., 2014).

In vertebrates, mutations in Pit1 result in the loss of cell-state and in hypopituitarism, hypothyroidism, dwarfism, deafness and pituitary cancer (Heaney & Melmed, 2004; S. Li, 1990; Mustapha et al., 2009; Sundaresan et al., 2016).

Non-vertebrate chordates (i.e., ascidians and lancelets) lack pituitary glands (Candiani and Pestarino, 1998). However, studies on the lancelet *Branchiostma floridae* reveal expression of Pit1 in ciliated cells of the external preoral organ/Hatschek's pit, a putative homologous structure to the internalized anterior pituitary gland of vertebrates and, hypothesized to have chemosensory and/or mucous secretory functions (Candiani & Pestarino, 1998, 1999; Candiani *et al*., 2008).

The 'moon jellyfish' *Aurelia*, expresses Pit1 in ectodermal sensory cells of the rhopalia, a sensory organ unique to jellyfish, suggesting that Pit1 mediates cellular differentiation of sensory and/or neurosecretory cells in Cnidaria (Nakanishi et al., 2010).

In the 'starlet sea anemone' *Nematostella vectensis (Nv)*, a powerful cnidarian model organism, single-cell transcriptomic analysis (Sebé-Pedrós et al., 2018) revealed *Nv*Pit1 expression exclusively during polyp stage in a single neuronal cell type, with co-expression of neuronal specific genes (e.g., Elav, Kalirin), several ion channels (e.g., acid-sensing and amiloride-sensitive channels) and neuropeptide receptors (e.g., RYamide receptors). Additionally, it revealed the expression of genes involved in the differentiation of mechanosensory cells and mechanotransduction, such as POU-IV (Brn3) and Pkd1 (Ozment *et al*., 2021), as well as genes involved in endocrine functions, such as TSH receptors and melanocortin receptors (Sebé-Pedrós *et al*., 2018), raising the question if *Nv*Pit1 is involved in cellular differentiation of mechanosensory, neurosecretory, and/or endocrine cells in *Nematostella vectensis*.

Here I describe the expression pattern of *Nv*Pit1 across development of *Nematostella vectensis* using *in-situ* hybridization, immunohistochemistry and a Pit1::Kaede transgenic reporter line. A dynamic expression pattern of *Nv*Pit1, was characterized, with initial expression in the endoderm followed by expression in the ectoderm of tentacles. Additionally, diverse morphologies of *Nv*Pit1^{+} sensory neurons in the tentacles were analyzed and described in detail, and a complex neuronal network of Pit1/Elav endodermal neurons was observed. Furthermore, I laid the foundations for functional studies by generating stable F2 CRISPR-Cas9 knockout lines and F1 Pit1::Kaede transgenic reporter lines.

2) METHODS

2.1) Animal culture and spawning

Nematostella vectensis animals used in this study are descendants of the population collected at Rhode River in Maryland by (Hand and Uhlinger, 1992). Animals were kept in an Aquaneering stand-alone system in 1/3 artificial seawater, pH 7.5-8.0, prepared with artificial sea salt (Instant

Ocean Sea Salt for Aquariums #169526) dissolved in reverse osmosis distilled water. The water temperature was maintained between 16ºC and 18ºC, and animals grew mostly in the dark, except when the aquarium room was in use for feeding or other animal maintenance-related activities. Feeding was done daily, during weekdays, with 2-day old brine shrimp (*Artemia salina*).

To induce spawning of *Nematostella*, sexually mature adults were set in an incubator with light and temperature cycle, of 8h of light at 25ºC and 1h of dark at 16ºC, which triggers gamete production and spawning approximately 1h after being removed from the incubator and brought to the light at room temperature (Fritzenwanker & Technau, 2002; Hand & Uhlinger, 1992). Males and females were screened, separated, and kept in different tanks and bowls to achieve control over the timing of fertilization. A healthy, well-fed, female can lay between 100-600 eggs, thus with a group of females it is possible to regularly obtain large amounts of developmental material. Normally, animals were allowed to rest, feed, and recover at least 2 weeks in between spawning events. To stimulate the first spawning of polyps approaching sexual maturity, to further increase egg yield, or to repeat spawning before the 2-week resting period, pieces of oyster were fed, which acts as a sort of aphrodisiac for the anemones (modified from Hand & Uhlinger, 1992 – where they used mussel ovaries).

2.2) Fertilization and De-jellying

In *Nematostella vectensis* the eggs are delivered in a gelatinous mass ("jelly") – the egg packet. After visually confirming that all the females released their egg packets, these were collected using a clean pipette and transferred into the male bowl with sperm for 15min to be fertilized. After that, the zygotes were transferred to a 4% L-cysteine solution, prepared in 1/3 sea water, and equilibrated to pH 7.4 using 1M NaOH. The egg packets were incubated on a rocker at room temperature for 12min (Keller, 1981) followed by gentle pipetting to further remove jelly and five

washes in 1/3 sea water to remove cysteine. Zygotes then develop at room temperature in a Petri-dish. It is recommended to fertilize before de-jellying since the jelly may be necessary to provide chemotactic cues and/or prevent polyspermy (Fritzenwanker & Technau, 2002).

2.3) Rearing of embryos, larvae, and primary polyps

When not de-jellied, embryos develop in the egg packet until they emerge as swimming larva (planula) at around 2-day-post-fertilization (dpf). One week after fertilization the swimming planulae metamorphose into primary polyps with four tentacles in the oral opening. At this stage, the primary polyps require small 1-day-old *Artemia* brine shrimp to be fed, either by flooding the Petri-dish or by puncturing the brain of *Artemia* with a forceps and putting the live but immobilized shrimp directly in front of the small primary polyp's mouth. It should be noted that for rearing primary polyps, a smaller 35mm Petri-dish is recommended, since it facilitates daily cleaning of dead *Artemia*. Eventually primary polyps grow and feeding becomes less laborious, where bigger 2-day-old *Artemia* can be fed and the polyps can progressively be moved to bigger containers, first a bigger Petri-dish, then a plastic Tupperware bowl, and when grown enough, to the tanks in the system. Feeding diligently, it can take 2 to 3 months to move them to the system tanks.

2.4) Zygote Microinjection

Freshly de-jellied zygotes were injected with either a CRISPR-Cas9 cocktail or a Transgenic Construct with meganuclease cocktail, using freshly pulled capillary needles, a microinjector (FemtoJet® 4i, Eppendorf) and a mechanical needle holder and manipulator. Both cocktails had Dextran568 (Dextran, Alexa Fluor™ 568) which fluoresces orange under green light. This fluorescent dye was used to keep track of injected animals and to sort them after injection, but also to visualize the amount of injected solution. The zygotes should become fully fluorescent, but injection should not inflate the zygote, as this can result in disintegration and death of the injected

animal. Some trial-and-error is required within an injection section to determine the right volume and air pressure, as in every session the breaking point of the needle varies slightly and thus also the needle tip width. Needles should the broken at the most distal point possible, to obtain thin needle tips. It is worth noting that thin needles clog more easily and thus clearing of the needle is often required by pressing the "Clear" setting on the microinjector machine. This shoots a burst of pressurized air in the needle and often unclogs it. If clearing the needle does not solve the issue, the needle tip should be analyzed visually and broken precisely above the obstruction. After injection, animals are let to develop overnight and they can be sorted in the next day, making use of the Dextran 568 fluorescence, into a fresh small 35-mm Petri-dish, where they can then be reared or used directly for experiments.

2.5) RNA extraction, cDNA synthesis and gene cloning

The *in silico* predicted *Nv*Pit1 gene sequence was obtained from the Joint Genome Institute database (N. vectensis v1.0, protein ID 112929), where a single exon is described. To confirm the predicted *in silico* sequence, 5' and 3' RACE PCR was performed. Total RNA was extracted from planulae and primary polyps using TRIzol (Thermo Fisher Scientific) and cDNA was synthesized using the SMARTer RACE cDNA Amplification Kit (Cat. No. 634858; Takara, Mountain View, CA). RACE PCR fragments were ligated into a pCR4-TOPO TA vector, using the TOPO TA Cloning kit (Cat. No. K457501; Thermo Fisher Scientific), and sequenced by (Eurofins, KY).

2.6) Generation and validation of antibodies against *N. vectensis* POU-I

Two antibodies against *N. vectensis* POU-I/Pit1 were generated in rabbit (YenZym Antibodies, LLC). The antibody NvPit1-yz6677 against TIGLAAKEALENHFMKQTKCamide synthetic peptide, corresponding in amino acid sequence to TIGLAAKEALENHFMKQTK in the DNA-Binding Homeodomain region of NvPOU-I/Pit1 and the antibody NvPit1-21-40 against the

CLSHDQRGPPVPPLPLDFGVDamide synthetic peptide, corresponding to the LSHDQRGPPVPPLPLDFGVD amino acid sequence in the N-terminus of the POU domain region of NvPOU-I/Pit1. Both antigen sequences were analyzed with TBLASTN against *N. vectensis* genome (http://metazoa.ensembl.org/Nematostella_vectensis/Info/Index) (Putnam et al., 2007) and both yielded a single hit at the POU-I locus (NEMVEscaffold_114:529,686–530,177), with no matches to other loci. Following immunization, the resulting antisera were affinity purified with the TIGLAAKEALENHFMKQTKCamide and CLSHDQRGPPVPPLPLDFGVDamide peptides. The antibodies were validated using CR-Pit1 F2 animals, where antibody signal was absent in full knockout mutants (-d/-d) and present in wildtype (+/+) siblings (Supplementary Fig. S5 and S6). Additionally, combined *in-situ* and immunohistochemistry data shows Pit1 antibodies colocalizing with Pit1 mRNA, providing further evidence of antibody specificity (Fig. 3 to Fig. 9).

2.7) Generation of Kaede transgenic animals

Kaede is a green fluorescent protein that upon UV excitation undergoes irreversible photoconversion from green fluorescence to red fluorescence (Ando et al., 2002). To design the NvPit1::Kaede construct, the promoter region of NvPit1 (a sequence of 3031bp upstream of the NvPit1 start codon) was extracted and cloned in frame into a Kaede containing vector (Ando *et al*., 2002) using a FastCloning approach (C. Li et al., 2011) (Supplementary Fig. S2 and S3). The plasmid was purified with a Zymo miniprep kit, eluted in water and co-injected with I-SceI meganuclease and Dextran568 into *Nematostella vectensis* zygotes during a 2h time-window before first cell division, as described previously (Renfer et al., 2010).

2.8) CRISPR-Cas9 mediated mutagenesis

Using the gene model of NvPit1, three 20nt-long target sequences were manually selected in Geneious Prime 2022.1.1. The target sequences are as follows: (sgRNA1) 5'-

CAAATGCCTAGCGCCACGCA-3'; (sgRNA2) 5'- CAACGCAGTTCAAACTACGA-3'; (sgRNA3) 5'- CAGTAAGGAATCAGATGCAT-3'. To minimize off-target effects, target sites with a 17bp or higher sequence identity elsewhere in the genome were excluded. sgRNA1 has a single hit in the genome (on NvPit1 locus), and sgRNA2 and sgRNA3 have 2 and 3 hits, respectively, outside of NvPit1 locus, but with 15bp or lower sequence identity, as determined by BLASTN. Target sites were selected and sgRNAs designed to induce the excision of the POU and Homeobox domains of NvPit1 (Fig. 2). The three sgRNAs were synthesized *in vitro* (by Synthego) and combined in equal concentrations. The sgRNAs were co-injected in *Nematostella* zygotes with Cas9 endonuclease and Dextran568 as previously (Ikmi et al., 2014; Nakanishi & Martindale, 2018b; Nakayama et al., 2013). Injected Pit1::Kaede F0 animals were monitored for Kaede expression, isolated, and reared to adulthood to generate F1 transgenic animals (Supplemental Fig. SX).

2.9) DNA Extraction

Genomic DNA was extracted using previously published protocols (Ikmi et al., 2014; Silva & Nakanishi, 2019). Depending on the purpose and needs of the experiment, DNA can be extracted from cutting tentacles of polyps, from sacrificing whole embryos (e.g., to quickly screen CRISPR-Cas9 efficiency), or from the aboral ectoderm of gastrulae excised via microsurgery, without sacrificing the life of the animal (Silva & Nakanishi, 2019). The latter method permits an early screening of mutants and the analysis of phenotypes during embryonic and larval stages.

2.10) Genotyping PCR

The extracted DNA from F1 mutant animals was amplified by nested PCR targeting the NvPit1 genomic locus, using the following set of primers: (1º Forward) 5'-TATTGGTCTT GGATCTGAATGGACGC-3'; (1º Reverse) 5'- AAATGCATAAACTGGCGTGCTGCTGG -3';

(2º Forward 5' – CAACAAGGTCAGCATTATTGTTTGGCCG - 3'; (2º Reverse) 5'- TATCTTT GGCTTCCCCTAATTACGCC -3'. With the expected size of the wildtype fragment for the primary PCR being 1537bp and secondary PCR 1193bp. The amplicons were gel-purified, ligated to pCR4-TOPO TA vectors, and transformed into competent *E. coli* cells (Cat. No. K457501; Thermo Fisher Scientific). Insertion screening was done by colony PCR, and colonies were cultured in liquid LB and incubated overnight (16h at 36ºC shaking at 200rpm). The liquid cultures were miniprepped with ZymoPURE kit (Cat. No. D4211) and sequenced (by Eurofins, KY) in order to characterize the mutant alleles in the F1 population (Fig. 2A).

2.11) Animal Fixation

Animals used for immunohistochemistry were fixed with fresh ice-cold 4% paraformaldehyde (Electron Microscopy Science, 15710) in PBS with 0.5% Triton X-100 (PBSTr) for 1 hour in a rocker at 4ºC. Animals used for *in-situ* hybridization were fixed in fresh ice-cold 4% formaldehyde with 0.25% glutaraldehyde in 1/3 seawater for 90 seconds and post-fixed in a 4% formaldehyde and PBSTr solution and incubated at 4ºC for 1h in a rocker (Nakanishi et al., 2012; Rentzsch et al., 2008). The fixed specimens were washed in PBSTr five times followed by three times in 100% methanol and stored at -20ºC until used (Rentzch *et al*., 2008). After the onset of muscle development, at larval and polyp stages, animals were anesthetized/relaxed in 2.43% $MgCl_2$ in 1/3 seawater for 15 minutes at room temperature (Nakanishi *et al*., 2012).

2.12) Immunohistochemistry and *In-Situ* Hybridization

For immunohistochemistry (IHC), fixed specimens were rehydrated, washed in PBSTr, permeabilized in PBSTr on a rocker for 2h at room temperature and posteriorly blocked in 3% normal goat serum (NGS) in PBSTr for 1h at room temperature in a rocker. Primary antibodies were added, and the specimens incubated overnight at 4ºC in a rocker. The primary antibodies

used in this study were NvPit1yz6677 (rabbit, 1:200), NvPit121-40 (rabbit, 1:200), RPamide (rabbit, 1:200 [Zang and Nakanishi, 2020]), RFamide (rabbit, 1:500, Millipore AB15348), GLWamide (rabbit, 1:200 [Nakanishi *et al*., 2018]), Kaede (rabbit, 1:500, Medical & Biological Laboratories, PM012M), mCherry (mouse, 1:100), acetylated α-tubulin (mouse, 1:500, Sigma T6793?), tyrosinated α-tubulin (mouse, 1:500, Sigma T9028). In the second day of staining specimens were washed in PBSTr and again, permeabilized and blocked in 3% NGS in PBSTr. Secondary antibodies were added; AlexaFluor488 (anti-mouse or anti-rabbit, 1:200), AlexaFluor568 (anti-mouse or rabbit, 1:200) and AlexaFluor647 (anti-mouse or rabbit, 1:200) and samples were incubated overnight on a rocker at 4ºC. Lastly, after PBSTr washes, nuclei were stained using DAPI nuclear label (1:1000, Molecular Probes) and filamentous actin was labeled either with AlexaFluor488-conjugated Phalloidin (1:250, Invitrogen A12379), or SiR-Actin (1:1000, Cytoskeleton CY-SC001, λ_{Em} 674 nm). For *in-situ* hybridization (ISH), sense and antisense digoxigenin-labeled riboprobes were synthesized with the MEGAscript transcription kits (Ambion; T7, AM1333; T3, AM1338) and used at a final concentration of 1ng/ul. *In-situ* was done as described by Nakanishi *et al*. (2012). For DAPI staining of cnidocytes, previously published protocols were followed (Szczepanek *et al*., 2002; Wolenski *et al*., 2013)

2.13) Mounting, Live imaging and Confocal Microscopy

Specimens of immunohistochemistry or *in-situ* hybridization were mounted in ProLong Gold antifade reagent (Invitrogen, P36930) and cured overnight at 4ºC. When analyzing Kaede signal on fixed transgenic animals without Kaede antibody-staining, samples were mounted with Vectashield antifade mounting medium (Cole-Parmer, EW-93952-23), which better preserves Kaede fluorescence. To analyze live Pit1::Kaede transgenics, animals were relaxed in 2.43% $MgCl_2$ and mounted in 1/3 seawater or in 6% methyl cellulose, which is non-toxic and helps

immobilize the animal (Renaud *et al*., 2011; Saina *et al*., 2015). Images of combined *in-situ* hybridization and immunohistochemistry were recorded using a Leica SP5 confocal microscope. All other images were recorded with a Zeiss LSM900. Confocal stacks were analyzed in LAS X (Leica), Zen 3.5 (Zeiss, Blue Edition) and Fiji (just ImageJ). Images were processed in Fiji and Microsoft Publisher.

2.14) Chemosensory behavioral assay

Chemosensation was tested using a shrimp extract of *Artemia* ground with a micropestle (USA Scientific) in 1/3 seawater (Instant Ocean) and gently delivered with a pipette to the tentacle/oral region of primary polyps. The animals were observed for 2 min to examine tentacular retraction and pharyngeal protrusion. Behavioral assays were performed under a Zeiss Stemi 508 dissection-scope with an attached Nikon DSL-4 camera.

3) RESULTS

3.1) NvPit1 Gene model and CRISPR-Cas9 mutant allele characterization

The gene model of NvPit1 in the genomic databases (JGI or Ensembl) predicts a coding region of 492bp. Our cDNA RACE data shows a NvPit1 1679bp long transcript and upon manually searching for the Kozak sequence (Kozak, 1989; Naamati et al., 2009) the translation start site was annotated and an open reading frame of 756bp identified (Supplementary Fig. S1, S2 and S3). The predicted Pit1 protein was 163aa long and our cDNA analysis described a 252aa long protein. Besides the length discrepancy, the single exon architecture prediction of NvPit1 is accurate. The genomic 5' region immediately upstream of the annotated start site was considered a promoter region and was used for transgenic constructs (Supplementary Fig. S4).

The effect of CRISPR-Cas9 activity at the NvPit1 gene locus on F1 CR-NvPit1 animals was addressed by nested PCR (Fig. 2B-C). Upon cloning and sequencing of mutant amplicons, five knockout alleles were detected and characterized (Fig. 1). Mutants with allele *-d* were used in this study, but we also propose the use of allele *-b* mutants for antibody staining of non-functional NvPit1, since the binding site of the antibody αNvPit1 21-40 is preserved (Fig. 1A – Supplementary Fig. S3).

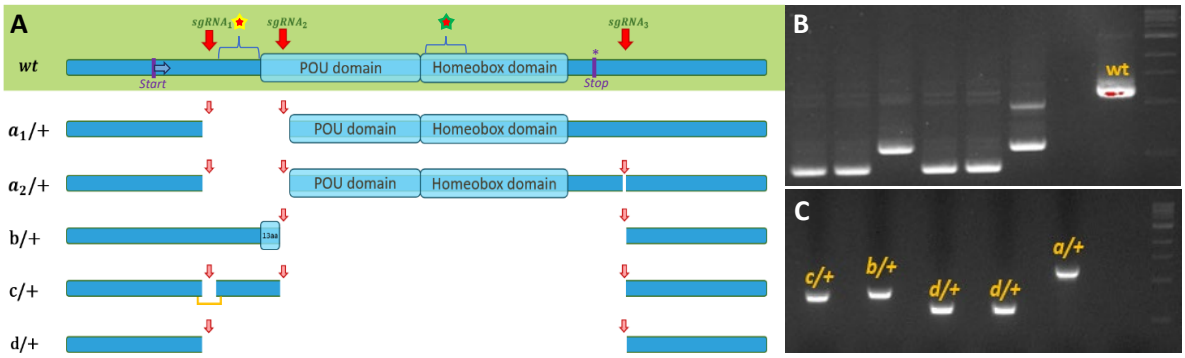

Fig. 2. NvPit1 alleles and genotyping. (**A**) Representation of NvPit-1 genomic locus (blue bar), wildtype (inside green box) and CRISPR-Cas9 mutant alleles a_1/+, a_2/+, b/+, c/+ and d/+. Genomic targets of sgRNAs (red arrows), DNA binding domains, Start and Stop sites indicated by purple bars on wildtype allele. Yellow outlined star represents αNvPIT1-2140 binding site; Green outlined star represents the binding site of αNvPIT1yz6677. **(B)** Secondary PCR of F1 NvPit1 mutants before gel cleanup and positive control (wt). **(C)** Secondary PCR of F1 NvPit1 mutants after gel cleanup.

3.2) Gene Expression Pattern of NvPit1 – Described by combined ISH and IHC

Combined *in-situ* hybridization and immunohistochemistry revealed the expression pattern of NvPit1 during development of *Nematostella vectensis*. At the gastrula stage NvPit1 is not expressed or, if expressed, only at undetectable quantities (Fig. 3A-C) which goes in line with previously published transcriptomic data showing low expression of Pit-1 in early developmental stages (Fig. 3D, Warner *et al*, 2018, Fischer *et al*. 2014, Tulin *et al*. 2013, and Helm *et al*. 2013).

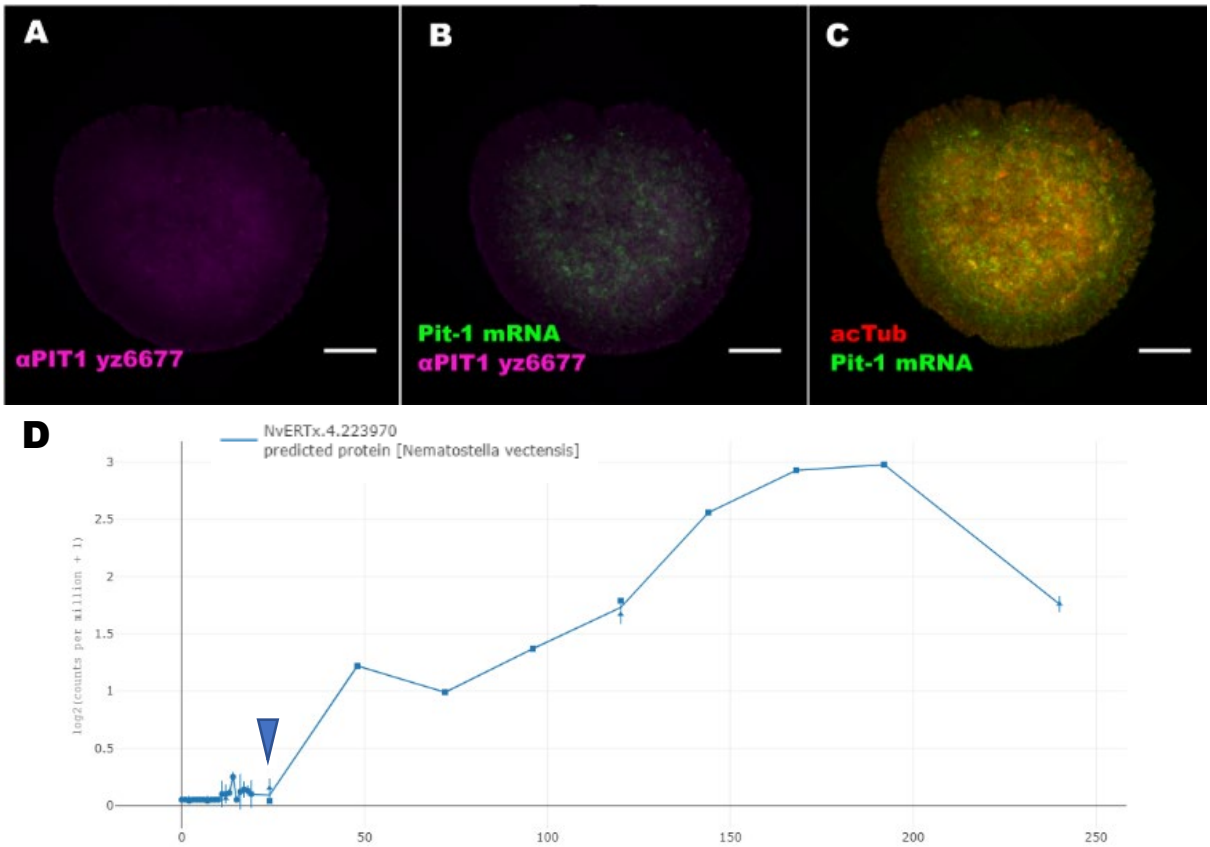

Fig. 3. NvPit1 is not expressed in early embryonic stages. (**A-C**) Confocal section of a gastrula *Nematostella vectensis* stained with antisense riboprobe NvPit1 (Pit-1 mRNA), an antibody against NvPIT1 protein (αPIT1 yz6677) and an antibody against acetylated tubulin (acTub). Oral side is up, aboral side down. Note the absence of NvPIT1 antibody staining and the faint transcript staining (most likely background, compare to figures below) (n=2). (**D**) Graph with expression levels of NvPit1 (ID# 112929), across development of *Nematostella vectensis* based on transcriptomic data, extracted, and modified from http://nvertx.ircan.org/ (Warner et al, 2017, Fischer et al. 2014, Tulin et al. 2013, and Helm et al. 2013). Note the low level of expression during gastrula stage (blue arrowhead). Scale bars: 50 µm in A-C.

At early planula stage, a strong specific signal in the endoderm at the central region of the larva is observed (Fig. 4A-F), where staining reveals neuronal-like processes (Fig. 4g insets). At

mid planula stage, endodermal expression of NvPit1 is detected in the central region of the body column (Fig. 5A-C) in spindle shaped cells with sensory-cell-like morphology (Fig. 5d insets). See additional colorimetric ISH evidence, recapitulating the endodermal expression of NvPit1 at mid planula stage (Supplementary Fig. S7 and S8).

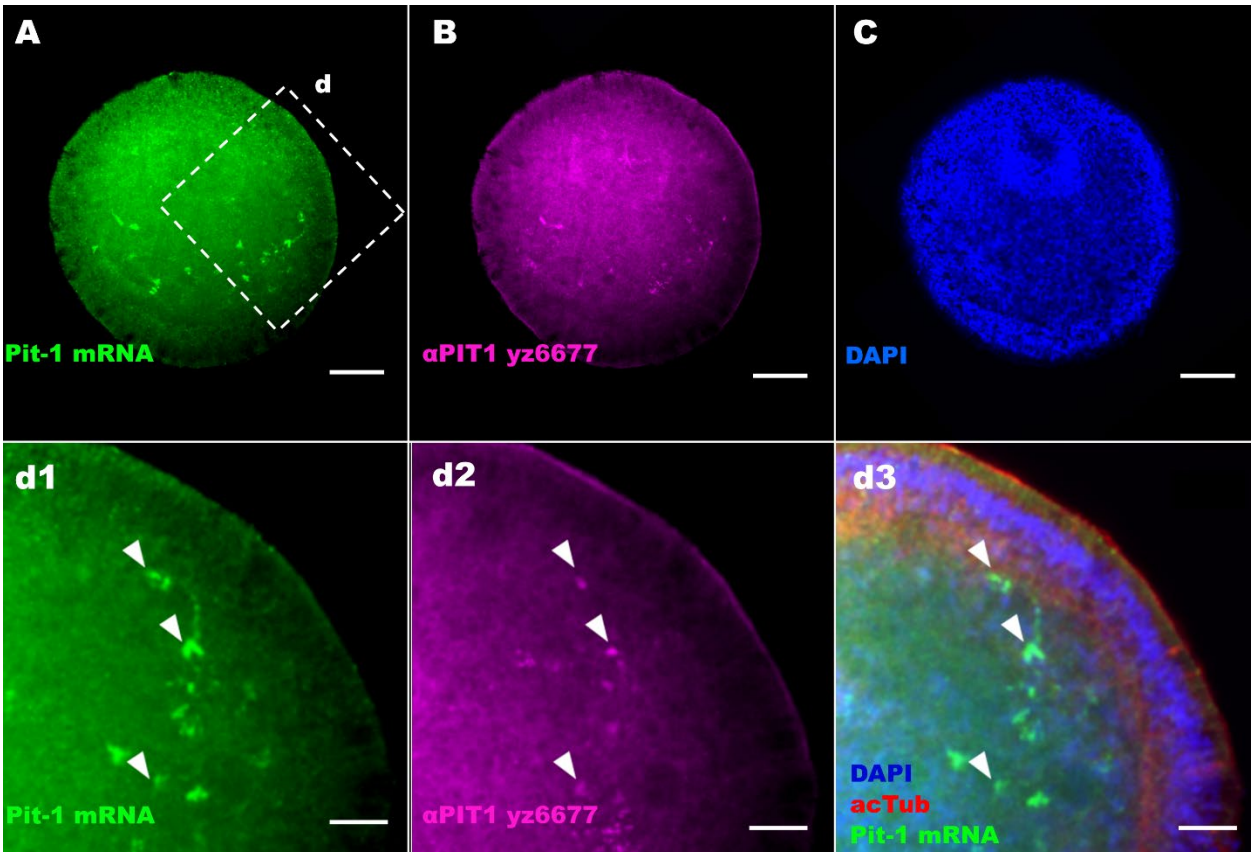

Fig. 4. NvPit1 is expressed in the endoderm of early larval stages. (**A-C**) Confocal section of an early-planula *Nematostella vectensis* stained with antisense riboprobe NvPit1 (Pit-1 mRNA), an antibody against NvPIT1 protein (αPIT1 yz6677), an antibody against acetylated tubulin (acTub) and DAPI, a DNA stain. Oral side is up, aboral side down. Note the expression in specific cells in the endoderm. (**d1-d3**) Insets demonstrate colocalization of NvPit1 transcript and NvPIT1 protein (arrowheads) and reveal staining of neuronal-like processes in the endoderm (n=2). Scale bars: 50µm in D-I, 20µm in j1-j3.

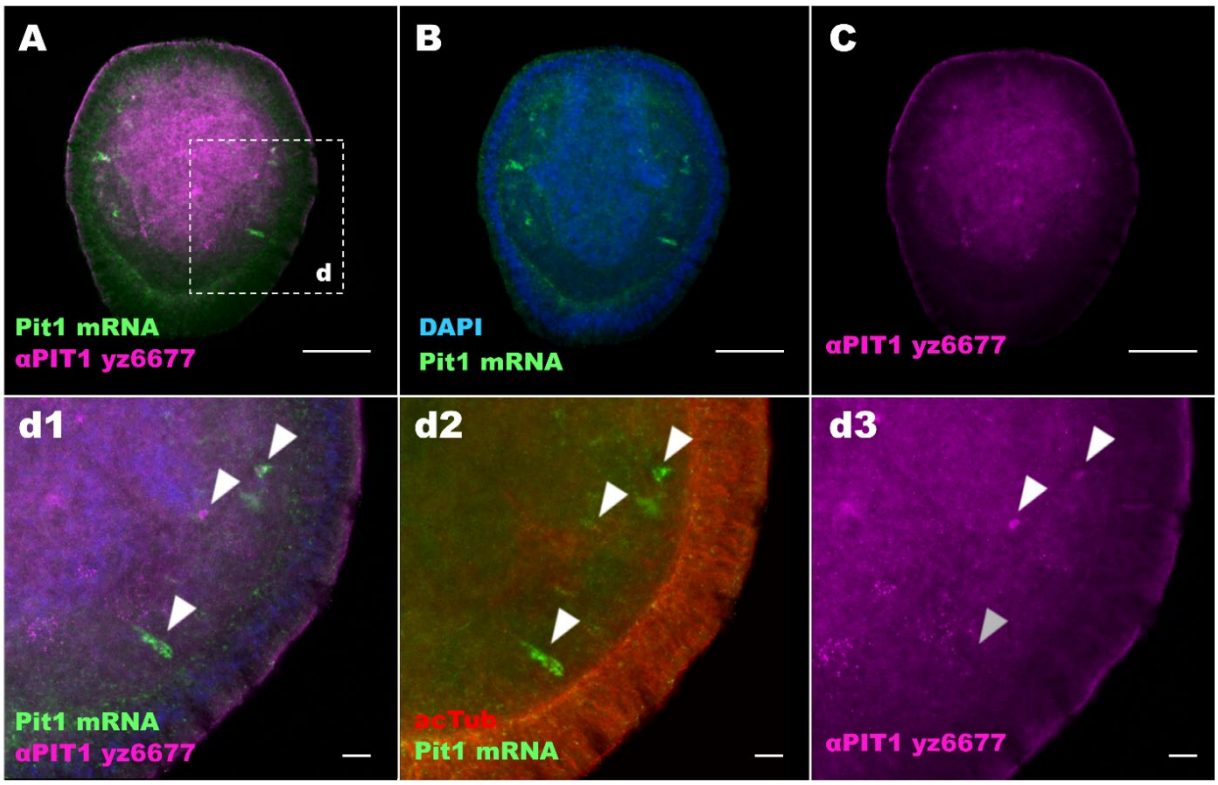

Fig. 5. NvPit1 is expressed in the endoderm of mid-planula stage. (**A-C**) Confocal section of a mid-planula *Nematostella vectensis* stained with antisense riboprobe NvPit1 (Pit1 mRNA), an antibody against NvPIT1 protein (αPIT1 yz6677) and DAPI DNA stain. Oral side is up, aboral side down. Note the expression in specific cells in the endoderm along the central plane of the body column (n=2). (**d1-d3**) Top two arrowheads on insets demonstrate colocalization of NvPit1 transcript and NvPIT1 protein and bottom arrowhead reveals spindle-shaped morphology of endodermal NvPit1^{+} cell, that probably has not yet begun translation, as we can see by the lack of antibody. Scale bars: 50µm in A-C, 10 µm in d1-d3.

At late planula stage, a reduction in NvPit1 expression is observed. The weak expression detected at this stage remains restricted to the endoderm and is more localized in the upper central region (Fig. 6) – see neuropeptide data (Fig. 12 and Fig. 13) for further evidence of the decrease in Pit1 expression at late planula.

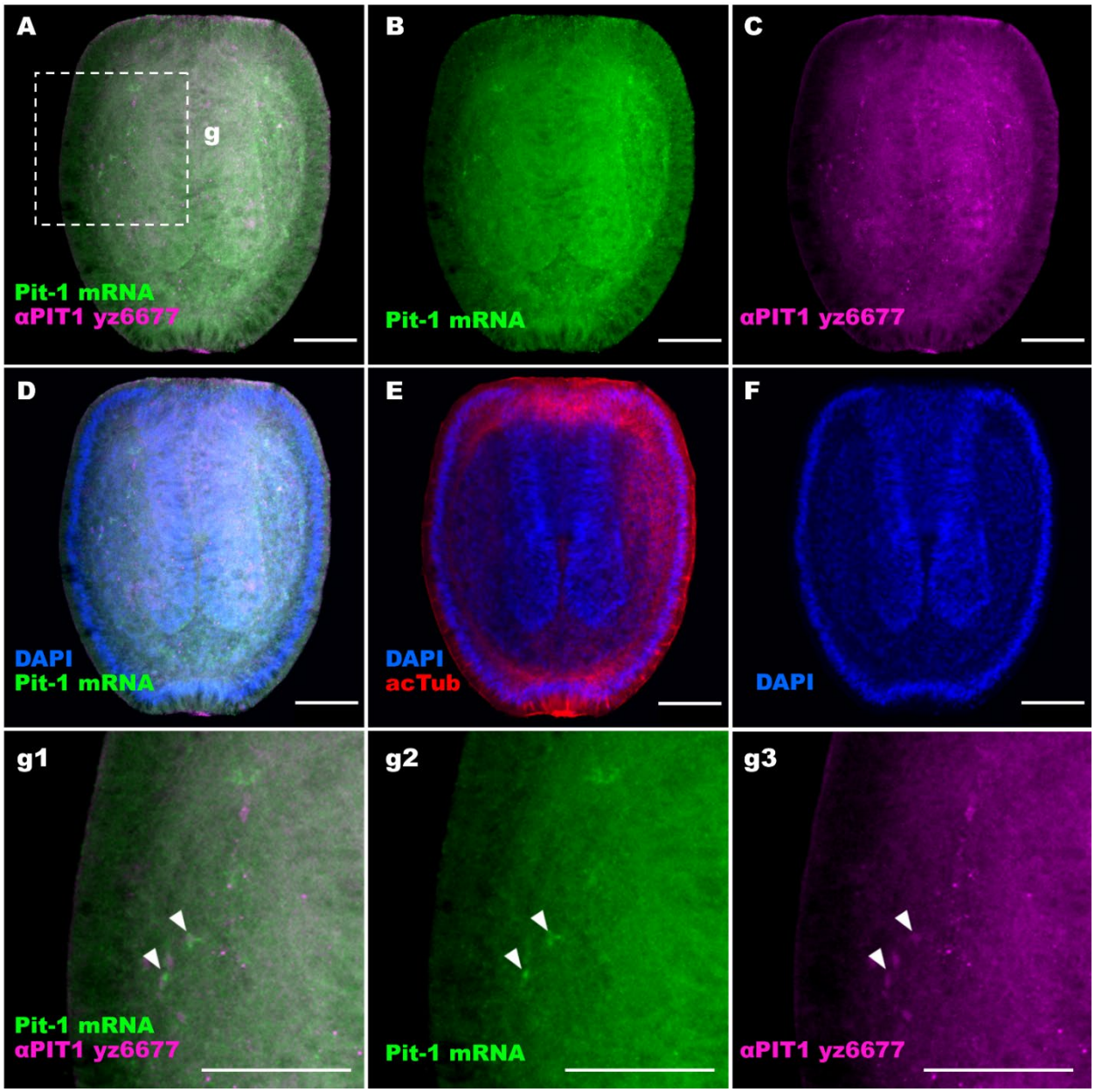

Fig. 6. NvPit1 is weakly expressed in the endoderm of late-planula stage. (**A-F**) Confocal section of a late-planula *Nematostella vectensis* stained with antisense riboprobe NvPit1 (Pit-1 mRNA), an antibody against NvPIT1 protein (αPIT1 yz6677), an antibody against acetylated tubulin (acTub) and DAPI DNA stain. Oral side is up, aboral side down. Note the decrease in stain intensity and number of stained cells compared to mid or early-planula. However, endodermal expression in the center persists and begins expression towards the oral pole of the larva (n=1). (**g1-g3**) Inset on the lateral of the planula shows expression of NvPit1 in the endoderm. The arrowheads point to cells with colocalization of transcript and protein, some other cells have the NvPIT1 protein, but no transcripts, which might mean that transcription halted on those cells, but the protein persisted. Scale bars: 50µm in all.

At the tentacle bud stage, endodermal expression becomes more localized in the oral pole, towards the tentacle primordia region of the animal in higher intensity than in late planula stages (Fig. 7). At a later stage of tentacle bud development, ectodermal expression in the tentacles begins (Fig. 8A-C) and as development progresses, endodermal expression seems to cease completely with expression becoming restricted to the ectoderm of tentacle buds (Fig.8D and insets).

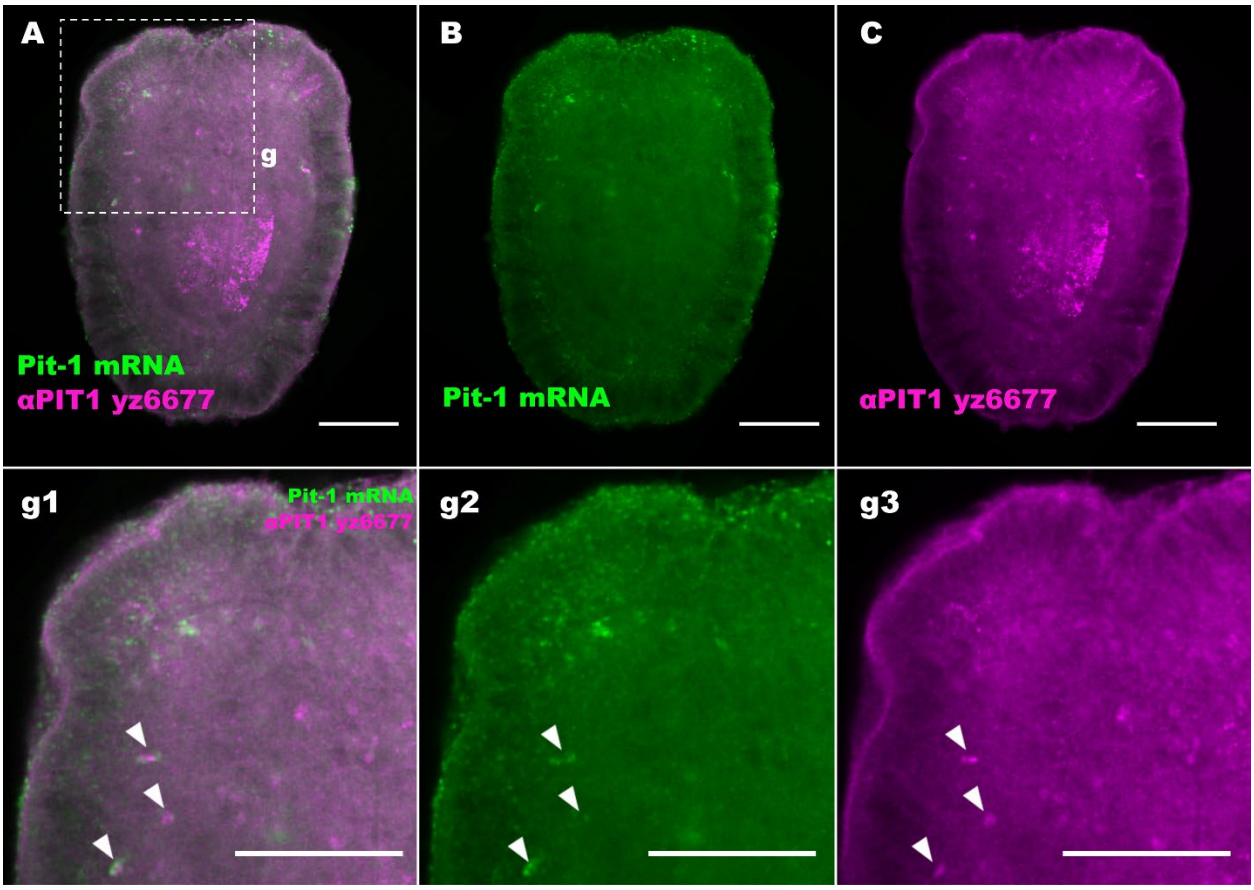

Fig. 7. NvPit1 is expressed in the endoderm of tentacle primordia during early tentacle bud stage. (**A-F**) Confocal section of an early tentacle bud *Nematostella vectensis* stained with antisense riboprobe NvPit1 (Pit-1 mRNA), an antibody against NvPIT1 protein (αPIT1 yz6677), an antibody against acetylated tubulin (acTub) and DAPI DNA stain. Oral side is up, aboral side down. Note the increase in stain intensity and number of stained cells in the endoderm of tentacle primordia and in the top (oral) side of the animal (n=1 this experiment, additional evidence from Pit1 ISH and neuropeptide IHC below). (**g1-g3**) Inset on the tentacle bud shows colocalizing NvPit1^{+} spindle shaped cells in the endoderm of tentacle bud *Nematostella vectensis*. (**g4-g6**) Inset from A in a different confocal section (z17 as opposed to z11) shows a great number of spindle-shaped NvPit1^{+} cells in the endoderm of tentacle primordia. Scale bars: 50µm in all.

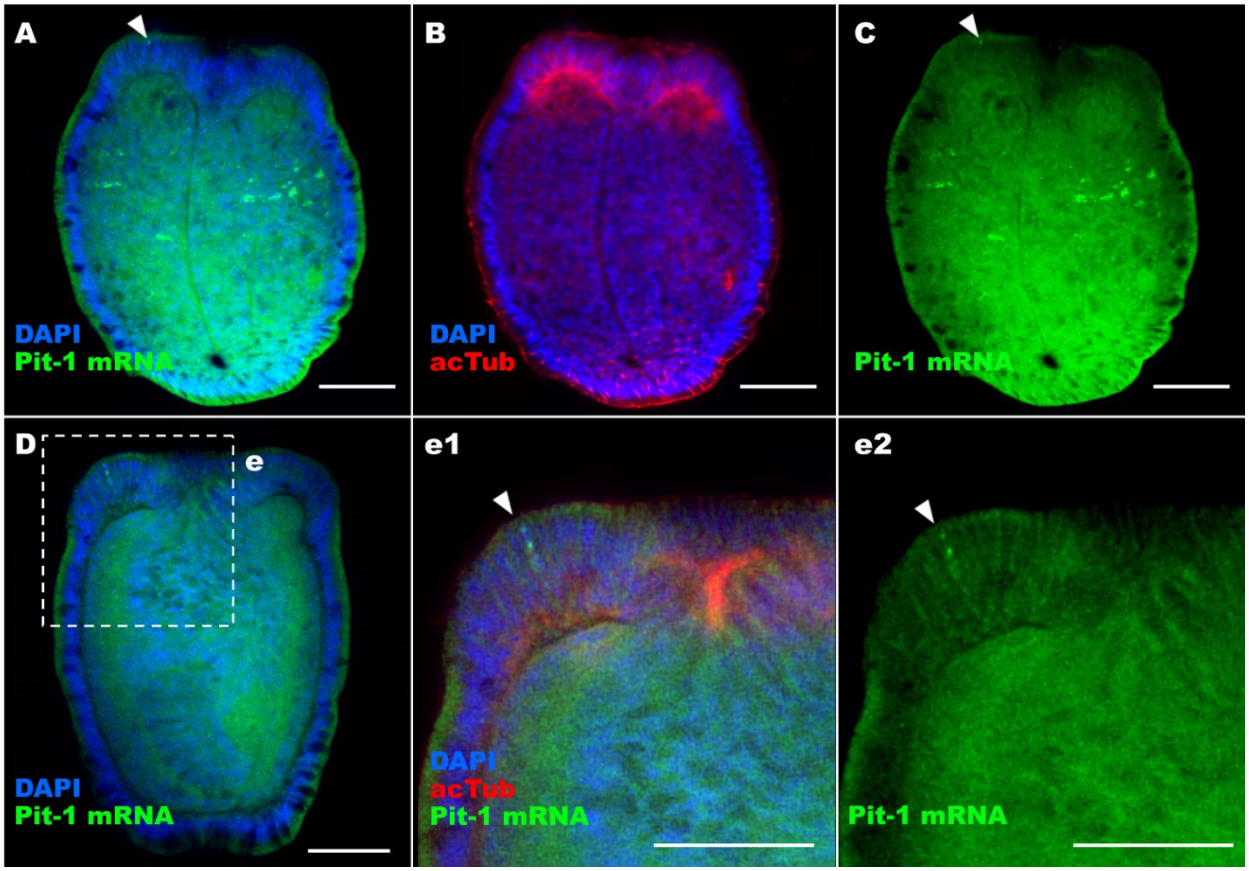

Fig. 8. Late-stage tentacle buds reveal the beginning of ectodermal expression of NvPit1 in the tentacles of *Nematostella vectensis*. Data from Pit1 riboprobe staining combined with GLWamide neuropeptide staining. (**A-C**) Tentacle bud with endodermal expression of NvPit1 begins ectodermal expression in the tentacle primordia (n=1). (**D**) Late tentacle bud lacks endodermal NvPit1 signal and shows single ectodermal NvPit1^{+} spindle-shaped sensory cell (n=1). Scale bars: 50µm in A-E.

At polyp stage, NvPit1 expression becomes very prominent in the ectoderm of the developing tentacles in spindle shaped sensory-like cells and reduced in the endoderm of the body column, where some Pit1 mRNA is detected in endodermal cells (Fig. 9). To summarize the expression pattern, a figure was constructed to depict the NvPit1 transcript expression across all stages (Fig. 10). Two specimens at pre-metamorphosis stages had a single cell with Pit1 mRNA, but no antibody signal, in the ectoderm near the oral end of the planula (Supplementary Fig. S9). This could be an artifact, or fixation could have captured the transcript right before translation.

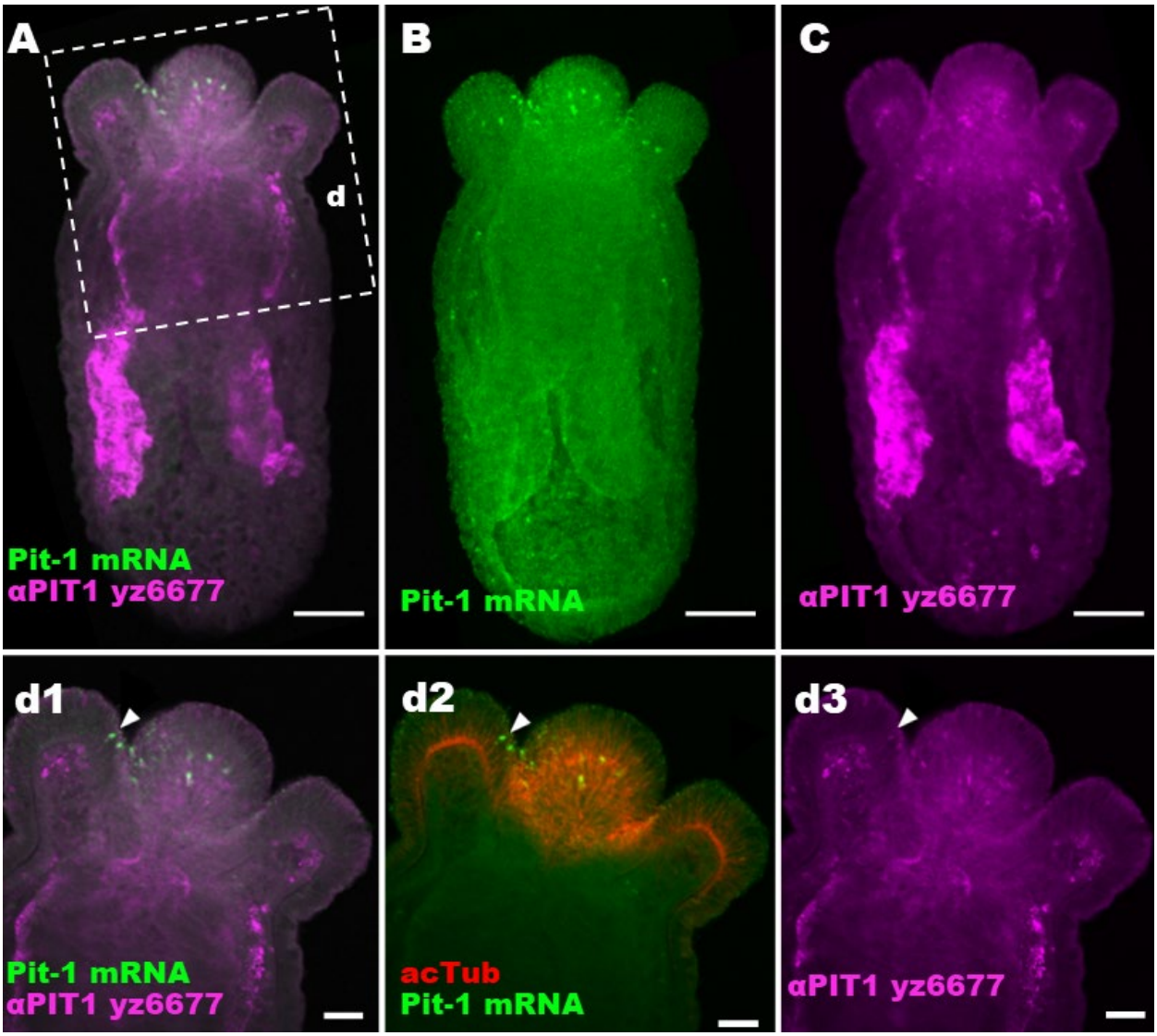

Fig. 9. Primary polyp of *Nematostella vectensis* with ectodermal NvPit1 expression in the tentacles and endodermal expression in body column. (**A-C**) The ectodermal tentacular expression from tentacle bud stage persists to polyp stage where it becomes more localized and numerous. We can see in **A** and **C** "clouds" of NvPIT1 protein, which probably are artefacts and non-specific binding of the antibody in the developing polyp mesenteries. We can see also on **B** some endodermal signal in the body column, meaning that endodermal expression of NvPit1 is not totally lost after metamorphosis. **(d1-d3)** Three tentacles, with the laterally positioned tentacles cross-sectioned and the tentacle in the middle showing a superficial section. On the lateral tentacles we can see the endoderm and ectoderm clearly separated by the mesoglea and on the middle tentacle only ectoderm is visible. The arrowhead points to a spindle shaped sensory cell in the ectoderm with NvPit1 expression. Several other $Pit1^{+}$ cells can be visualized. When looking at **d1** and **d2** it is evident that endodermal transcription is absent. This indicates that $NvPit1^{+}$ activity during polyp stage becomes more prominent in the ectoderm of tentacles, in contrast to the pre-metamorphosis endodermal specific expression of NvPit1 (n=2). Scale bars: 50µm in **A-C** and 20µm in **d1-d3**.

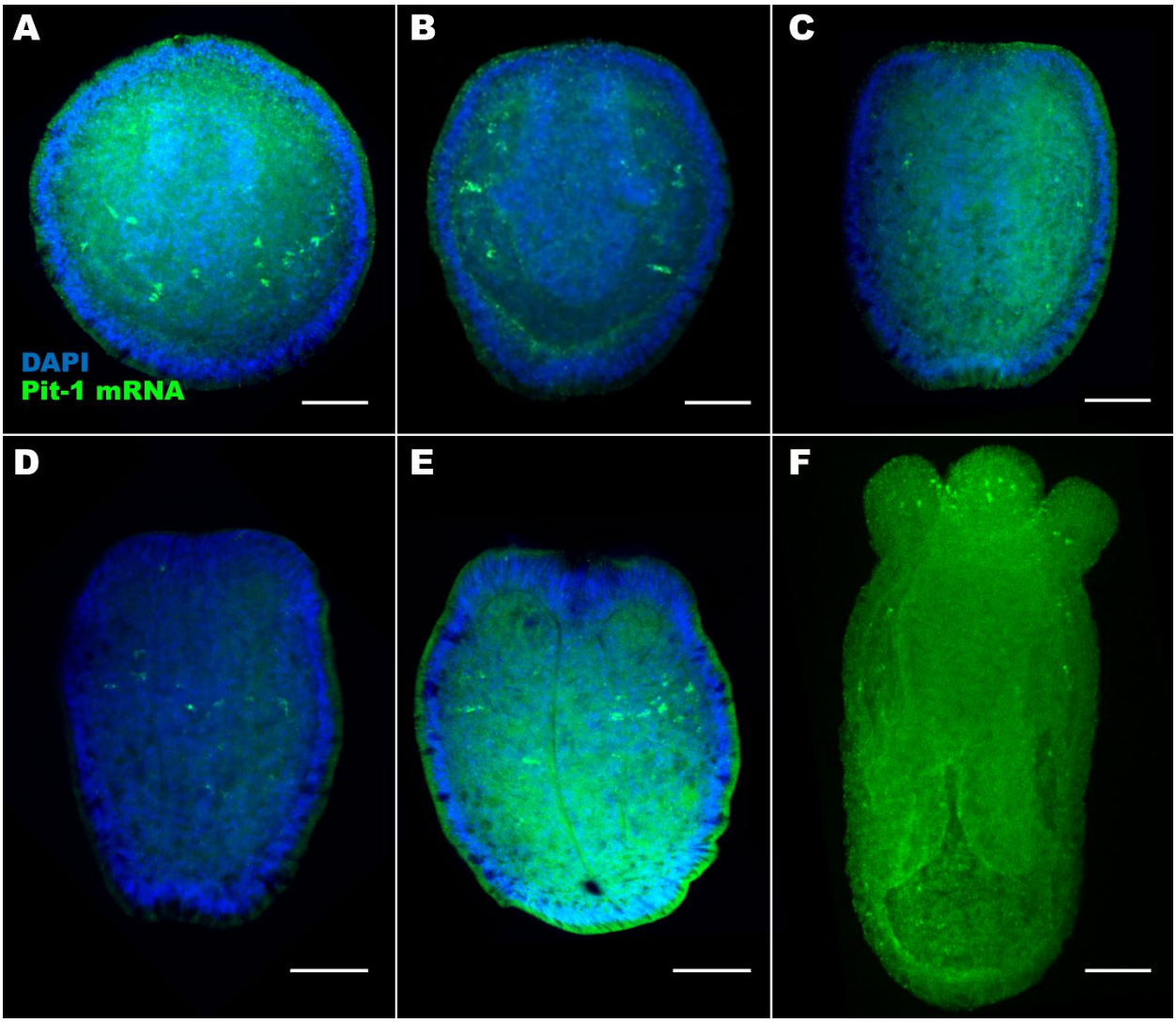

Fig. 10. Expression pattern of NvPit1 across development (**A)** Early planulae have endodermal expression in cells with neuronal processes. (**B**) Mid planulae have endodermal expression in the center of the body column in spindle-shaped cells. (**C**) During late planula there is a decrease in NvPit1 expression in the endoderm. (**D**) NvPit1 increases again in the endoderm during tentacle bud stage more towards the oral side of the animal. (**E**) Later in tentacle bud stage we begin to see ectodermal expression in the tentacles, and at polyp stage (**F**) we see a stark increase in ectodermal signal specific to the tentacles and some endodermal signal in the body column. Scale bars: 50µm.

3.3) Evidence for NvPit1 in Elav endodermal neurons and neuropeptidergic neurons

NvPit1^{+} cells with spindle-shaped morphologies (Fig. 5, 7, 8) and neuronal processes (Fig. 4) were detected across development. Using a pre-established transgenic reporter line (Elav1::mOrange, [Nakanishi *et al*., 2012]) and a validated antibody against NvPit1 (α2140-NvPIT1), NvPit1

expression in Elav endodermal neurons was detected in the central region of planula larva (Fig. 11).

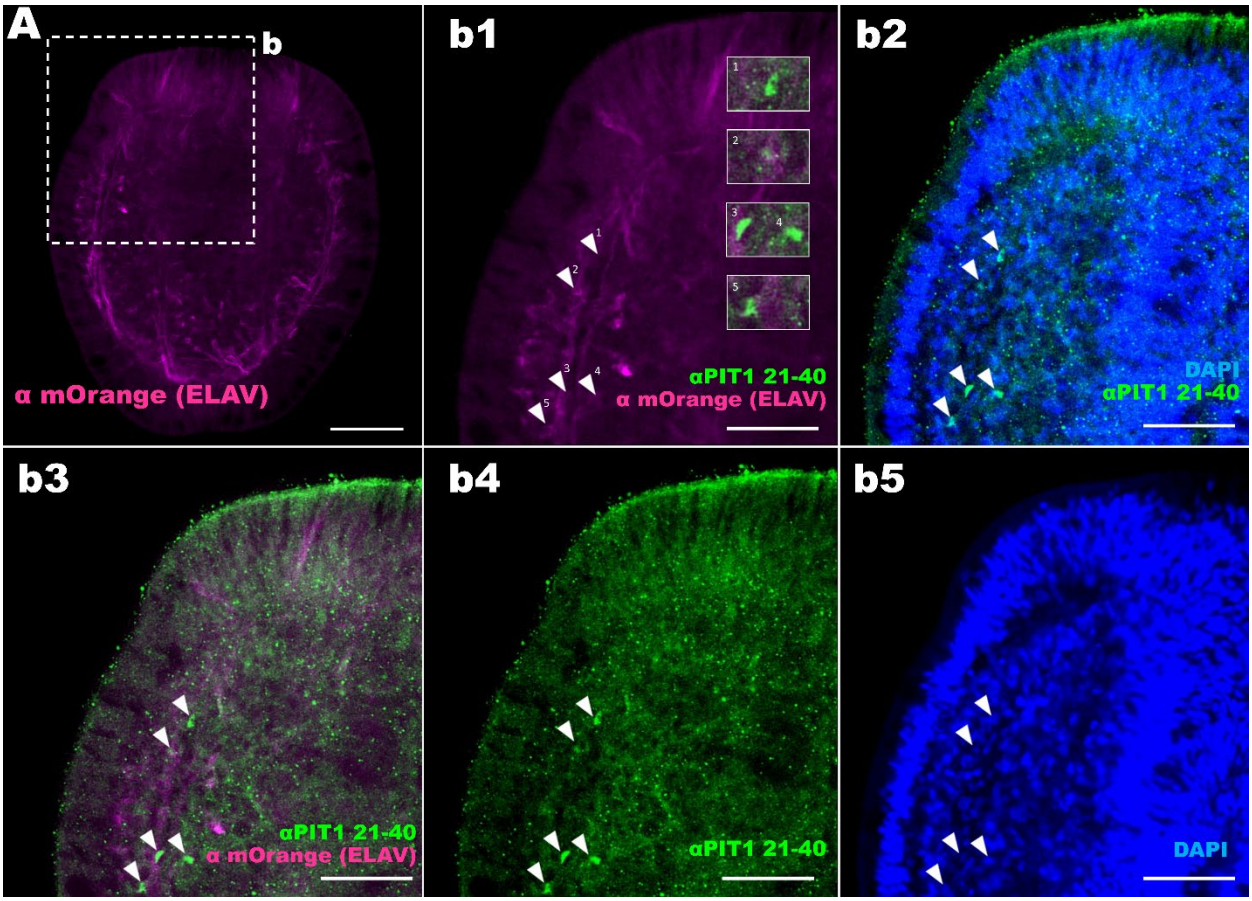

Fig. 11. Colocalization of Pit1 in Elav^{+} Neurons. Figure shows colocalization of Pit1(stained with αPIT1 21-40 antibody) in Elav^{+} neurons and DAPI stained nuclei (n=1, further evidence below). Arrowheads 2, 3 and 5, where we can see Elav neuronal cell morphology and Pit1^{+} nuclei in the soma. Scale bars: 20µm in, 25um in e1-e5.

To address the specific neuronal populations with NvPit1 expression, combined *in-situ* hybridization and immunohistochemistry was performed using a NvPit1 riboprobe and antibodies against neuropeptides such as RPamide (Fig.12, 13), RFamide and GLWamide (Supplementary Fig. S10). During mid planula, NvPit1 expression was observed either in RPamide^{+} cells or in cells synapsing/contacting RPamide cells in the endoderm (Fig. 12A-e3). At this stage no ectodermal Pit1 signal was detected. In the late planula stage, RPamide cells seem to extend neurites towards

a Pit1^{+} cell (Fig. 12F-G). At tentacle bud stage, there is some indication of possible colocalization on the endoderm (Fig. 13 – endodermal arrowheads), but not on the ectoderm, where ectodermal Pit1^{+} cells clearly do not colocalize with RPamide ectodermal neurons (Fig. 13).

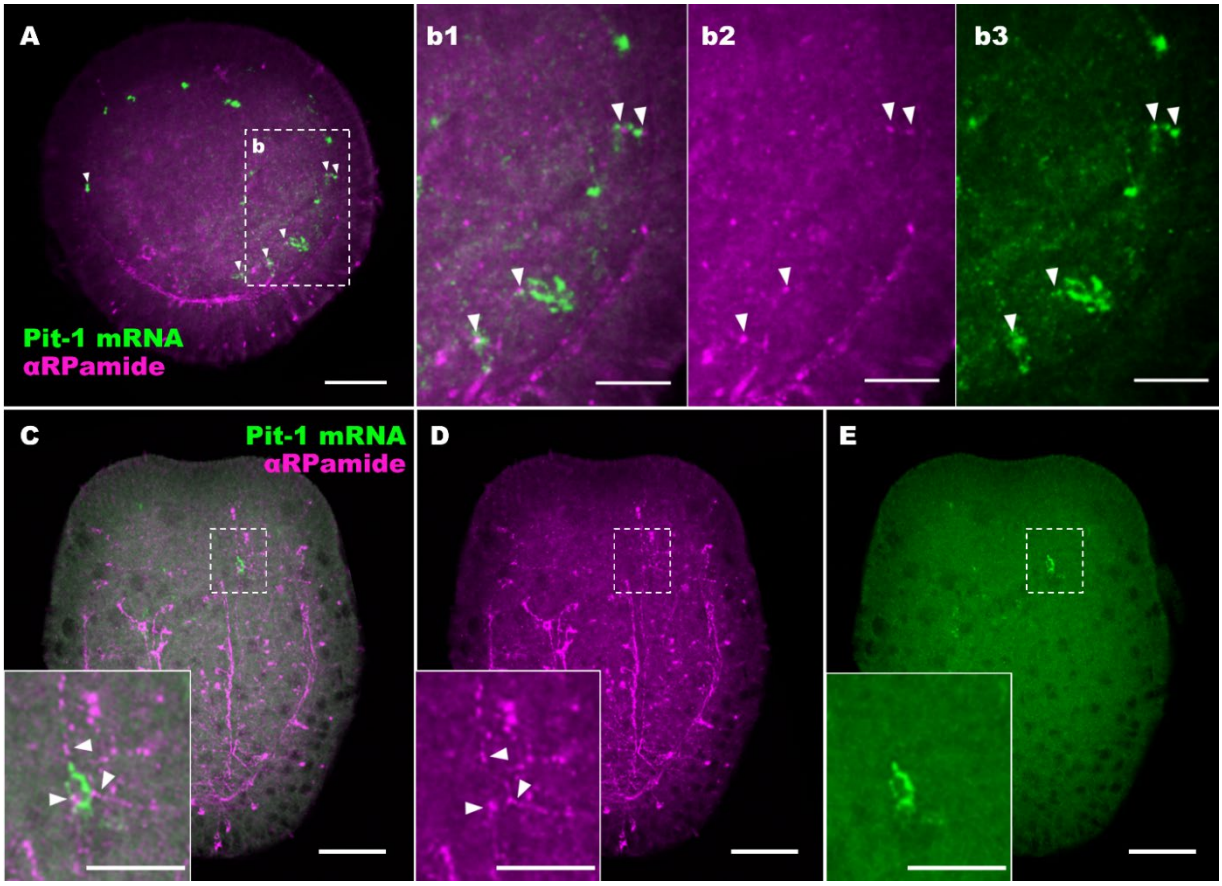

Fig. 12 – RPamide and NvPit1 colocalization in planula. (**A)** Confocal section of early planula stained with antisense riboprobe NvPit1 (Pit-1 mRNA) and an antibody against RPamide (αRPamide) (n=3). **(C-E)** Confocal section of late planula (n=2) with insets show RPamide neurites synapsing a Pit1 mRNA-positive cell. Scale bars: 50µm in A, C-E, 25µm in B and insets of C-E.

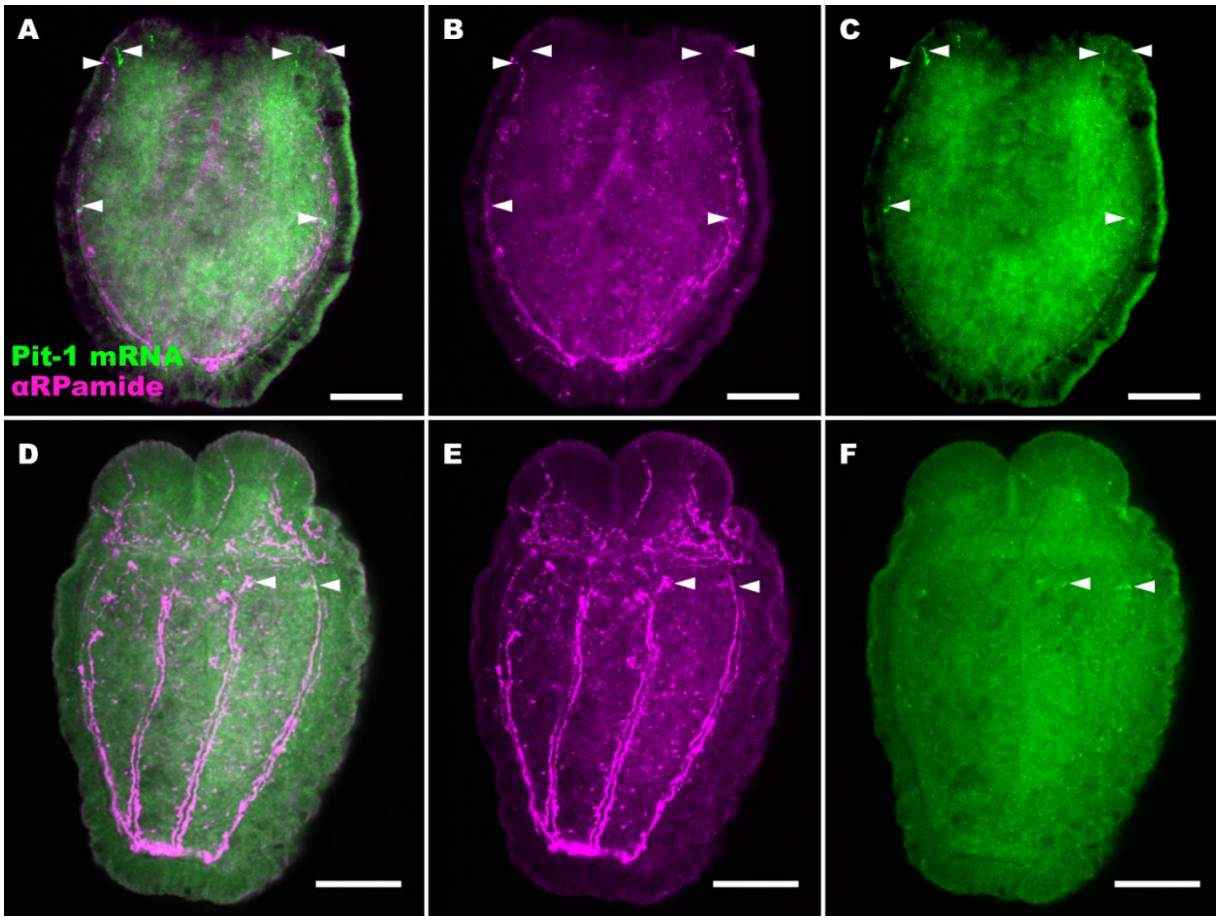

Fig. 13 – RPamide and NvPit1 colocalization. (A-C) Confocal section (z18) of tentacle bud shows colocalization in endodermal RPamide neurons (central/midplane arrowheads) and the absence of colocalization in tentacular ectoderm (apical arrowheads) (n=1). **(D-F)**. Confocal section (z14) of early polyp shows colocalization of Pit1 in endodermal RPamide neurons (arrowheads) and no colocalization in ectodermal cells of the tentacles (n=1). Scale bars: 50um

3.4) Live imaging of Pit1::Kaede F2 polyps

Live imaging of Pit1::Kaede F2 polyps revealed an extensive network of $Pit1^{+}$ endodermal neurons along and across the longitudinal neuronal tracts (Fig. 14D-f) – as well as sensory cells in the tentacles that extend neurites towards the base of the tentacle (Fig. 14C) (addressed in detail below). Imaging animals on a slide resulted in the protrusion of the pharynx which allowed to determine the absence of NvPit1 cells in the pharynx (Fig 14B). Spindle shaped cells are found near the oral region (Fig. 14e').

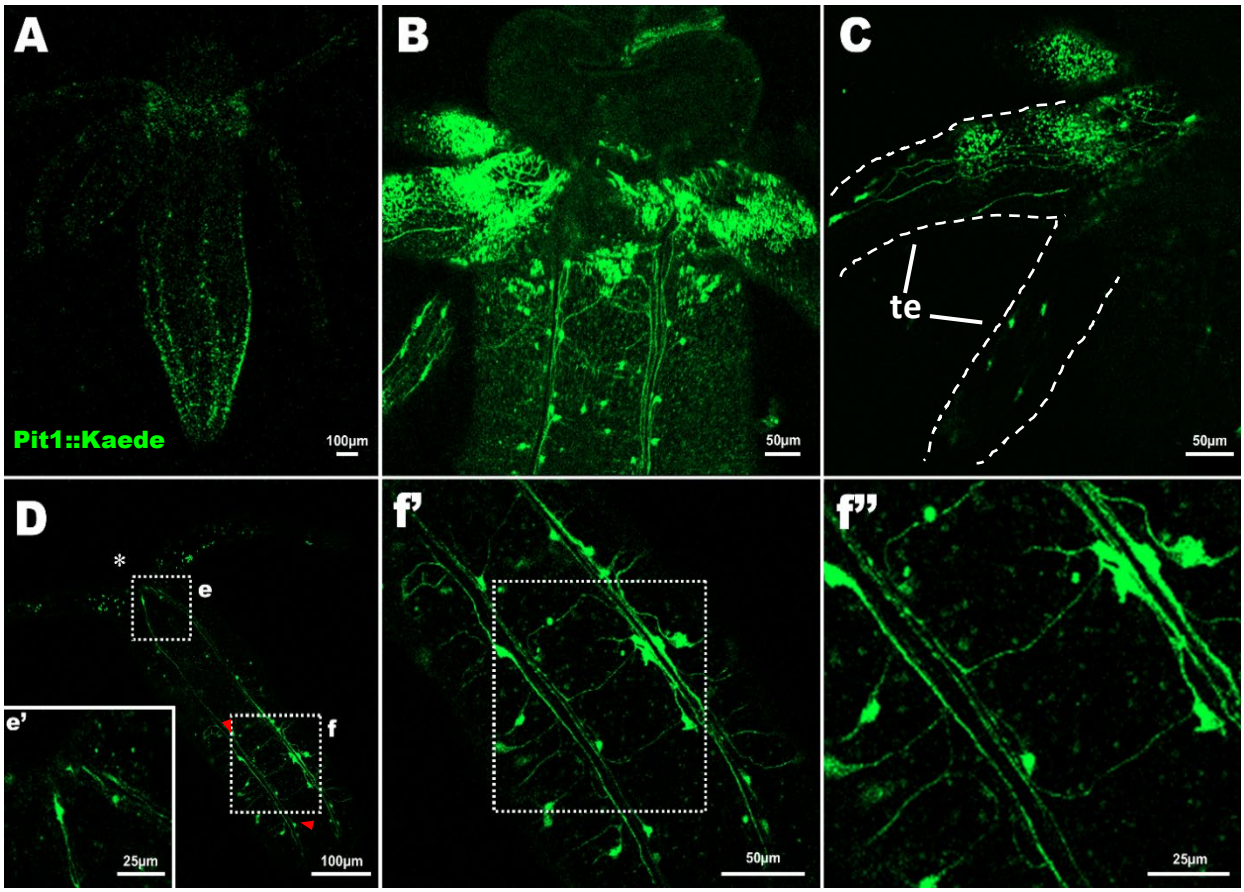

Fig. 14 – Live imaging of Pit1::Kaede F2 polyps. Live imaging of transgenic polyps on Zeiss LSM900 confocal microscope reveals complexes Pit1-positive nerve nets. **(A)** Whole polyp with oral side up, aboral side down. Strong signal of Pit1::Kaede is seen in the aboral end. **(B)** Protrusion of the pharynx reveals absence of Pit1-positive cells in the pharynx. Dense nerve bundles with Pit1 expression are seen along the longitudinal axis and dense networks at the base of the tentacle. Granular signal at the base is most likely an artifact from either endogenous proteins or associated microorganisms. **(C)** Sensory neurons are seen in the tentacles (te) extending neurites towards the base of the tentacle in a distal to proximal direction. It remains unresolved if the ectodermal tentacular network connects with the endodermal net of the body column. **(D)** Whole organism live imaging of a different polyp revealed details of the Pit1-positive endodermal nerve net, mouth (*). **(e')** Shows endodermal sensory neurons that extend long neurites (D) from the oral end of the animal (near the mouth) along the longitudinal axis to the aboral end of the polyp (see red arrowheads in D for possible connecting ganglion neurons – see supplementary figures 11 and 12 for a larger version of panel D). **(f'-f'')** Shows longitudinal Pit1-positive neurons crossing the longitudinal bundle and reveal ganglion neuron morphology. Scale bars: in panels.

Furthermore, live imaging of Pit1::Kaede F2 polyps revealed a complex network of sensory cells in the epidermis of tentacles with apical cilia contacting the external environment and long

neuronal processes extending towards the mouth along the distal-proximal axis. The use of live animal imaging allowed for the observation of these cells in their natural state, revealing a peculiar morphological characteristic of Pit1 sensory cells with an apical region exhibiting a strong Kaede signal with a short cilium and a disk-like structure in the basal region of the soma (Fig. 15).

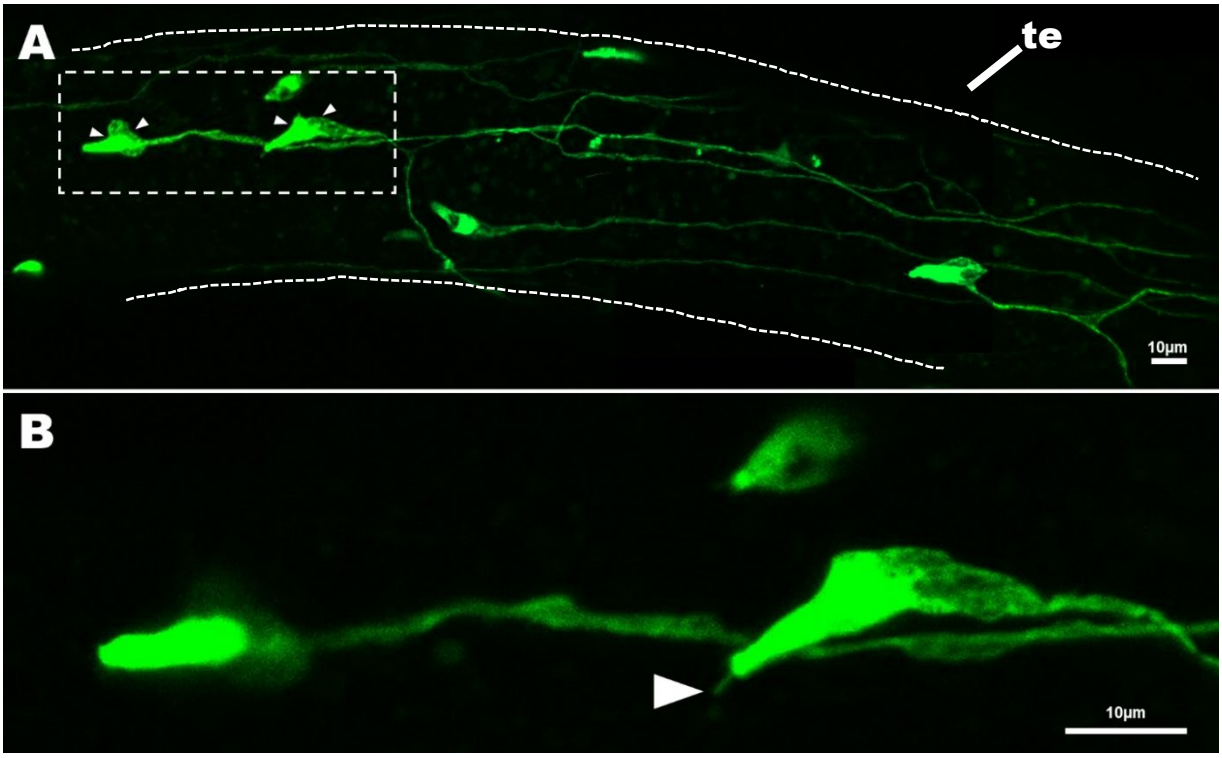

Fig. 15 – Sensory cell neural circuit tracing. – Tentacle of live Pit1::Kaede F2 polyp. **(A)** Collage of several z-stack projections along the tentacle (te) reveal sensory cell morphology and neuronal circuits. The Pit1 cells extend long neurites from distal regions of the tentacle towards the base of the tentacles. Arrowheads point to peculiar morphological characteristic of Pit1 sensory cells, with an apical region with very strong Kaede signal, and the basal region of the soma presenting a disk-like structure. **(B)** Higher magnification images reveal a short cilium (arrowhead) in these Pit1-positive sensory neurons in the epithelium of tentacles. Scale bars: in panels.

3.5) Double transgenics of Pit1::Kaede *x* Elav::mOrange

NvPit1::Kaede F1 animals were crossed with Elav::mOrange F1 to generate a double transgenic line where colocalization of NvPit1 was further confirmed in Elav neurons at high resolution using

antibodies against Kaede and mOrange. In planula and tentacle bud stages, colocalization of NvPit1 in Elav neurons was detected along the longitudinal tracts in the endoderm (Fig. 16A-F) and in endodermal sensory cells towards the oral pole (Fig 16A-C, top arrowhead).

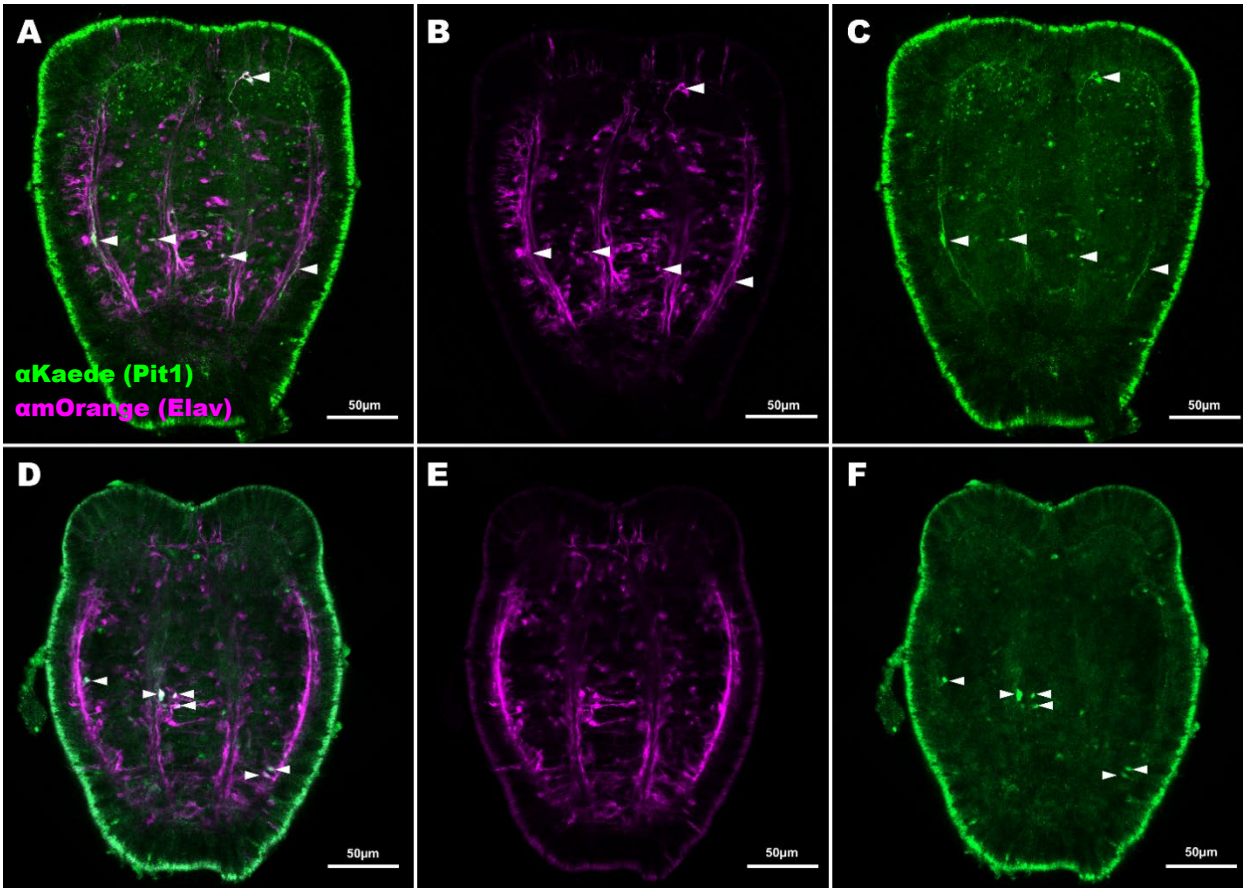

Fig. 16 – Colocalization of Pit1 and Elav in planula and tentacle bud stages of a double transgenic line (*Pit1::KaedeF1 x Elav::mOrangeF1*). Double transgenic F2s were stained with anti-Kaede antibody (αKaede) and anti-mOrange antibody (mCherry). **(A-C)** Confocal section of late planula shows colocalization of Pit1 and Elav expression in longitudinal neurons (central/aboral arrowheads) and in a sensory endodermal cell in the oral pole (see arrowhead). **(D-F)** Section demonstrates colocalization of Pit1 and Elav in endodermal neurons at tentacle bud stage (see arrowheads). Scale bars: in panels.

In early polyp stages, NvPit1/Kaede signal reveals expression of Pit1 in ectodermal sensory-shaped cells (recapitulating the endogenous expression detected by *in-situ* hybridization and immunohistochemistry). An ectodermal sensory neuron co-expressing Elav and Pit1 was

found (Fig. 17A-C, z18). Interestingly, NvPit1^{+} endodermal neurons that do not express Elav (Fig. 17D) were also described, further revealing the complexity of the NvPit1 nerve net.

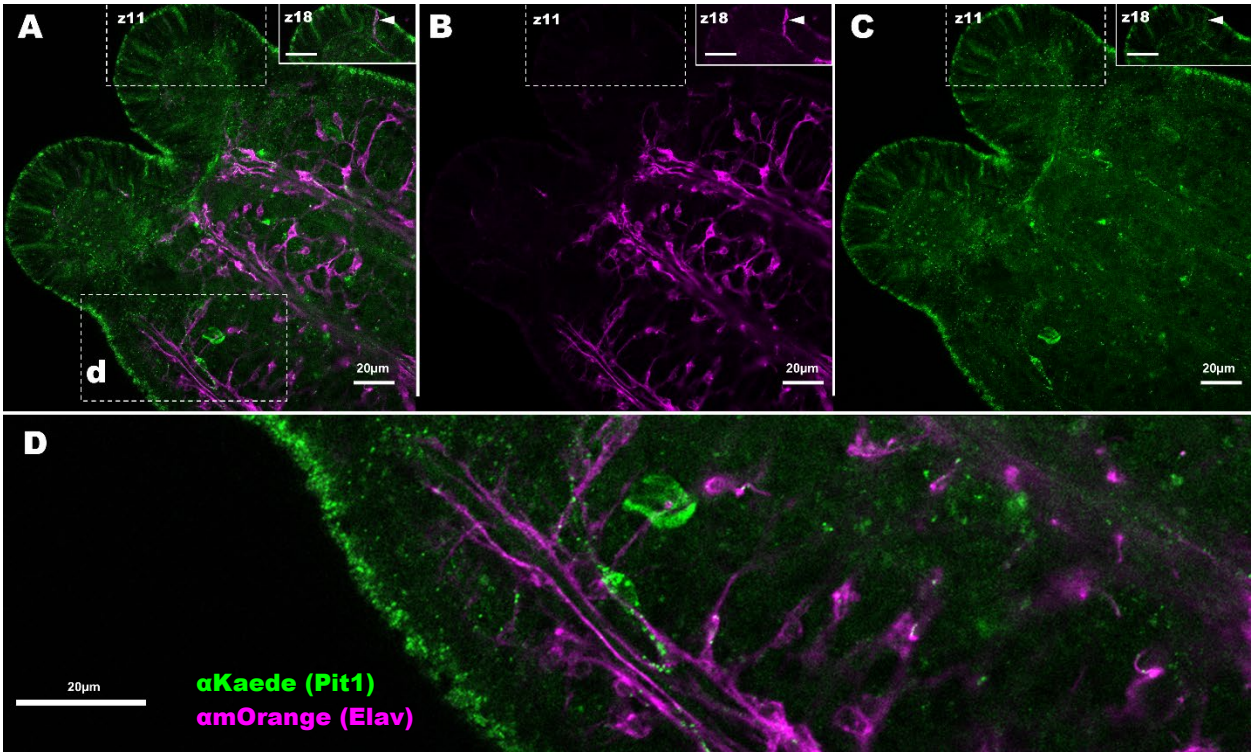

Fig. 17 – Colocalization of Pit1 and Elav in early polyp stage. Double transgenic F2s were stained with anti-Kaede antibody (αKaede) and anti-mOrange antibody (mCherry). **(A-C)** Kaede signal in ectodermal cells of the tentacle become apparent, thus recapitulating the beginning of ectodermal expression described with combined IHC and ISH. Panels A-D are at a specific confocal plane (z11). Looking at a different medial-plane section (z18), we found an ectodermal Elav-positive sensory neuron with Pit1expression (arrowhead on insets of A-C). **(D)** Confocal section of oral pole of primary polyp reveals Pit1-positive/Elav-negative neurons Scale bars: in panels and 20um in insets of A-C.

At polyp stage, colocalization of Kaede and Elav in endodermal neurons was still observed (Fig. 18A-C), as well as in ectodermal sensory cells in the tentacles (Fig. 18A'-C').

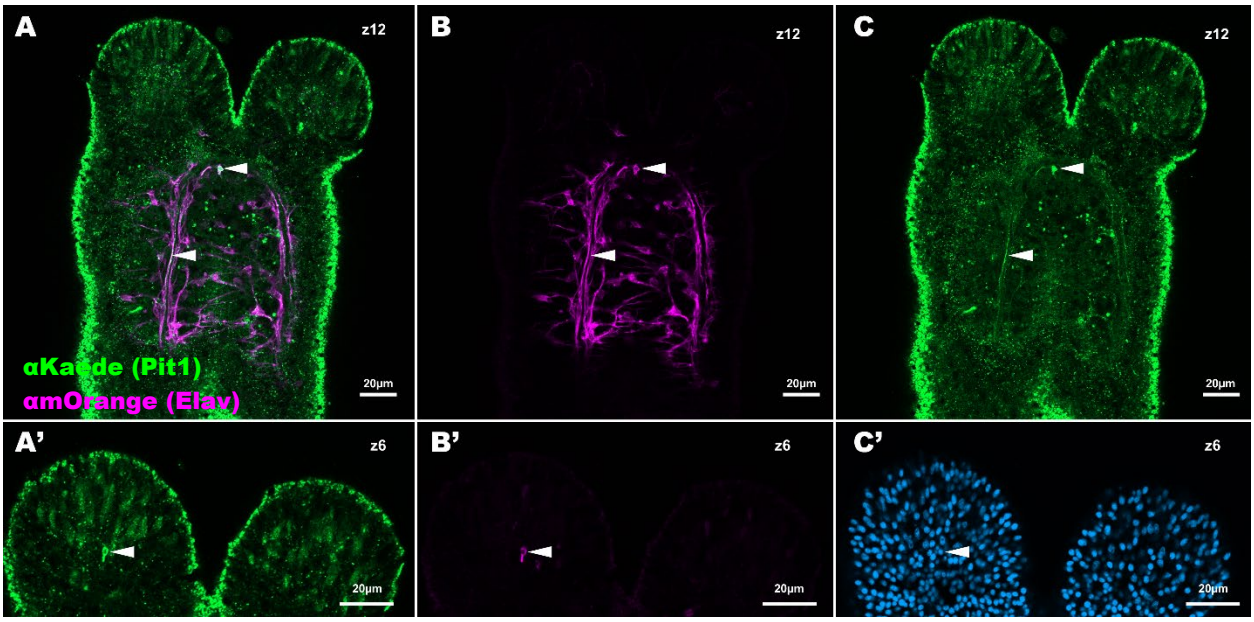

Fig. 18 – Colocalization of Pit1 and Elav at polyp stage. Double transgenic F2s were stained with anti-Kaede antibody (αKaede) and anti-mOrange antibody (mCherry). **(A-C)** Medial confocal section shows endodermal colocalization of Elav and Pit1 (arrowheads). **(A'-C')** Superficial section shows ectodermal Pit1-positive/Elav-positive spindle-shaped sensory cell (arrowhead). Scale bars: in panels.

3.6) Characterizing Pit1 sensory cell types

In an effort to unveil the nature of the Pit1-positive tentacular sensory cells, NvPit1::Kaede F2 animals were fixed and stained with SiR-actin to stain stereovilli and stereovillar rootlets characteristic of hair cells (Ozment *et al*., 2021) (Fig. 19).

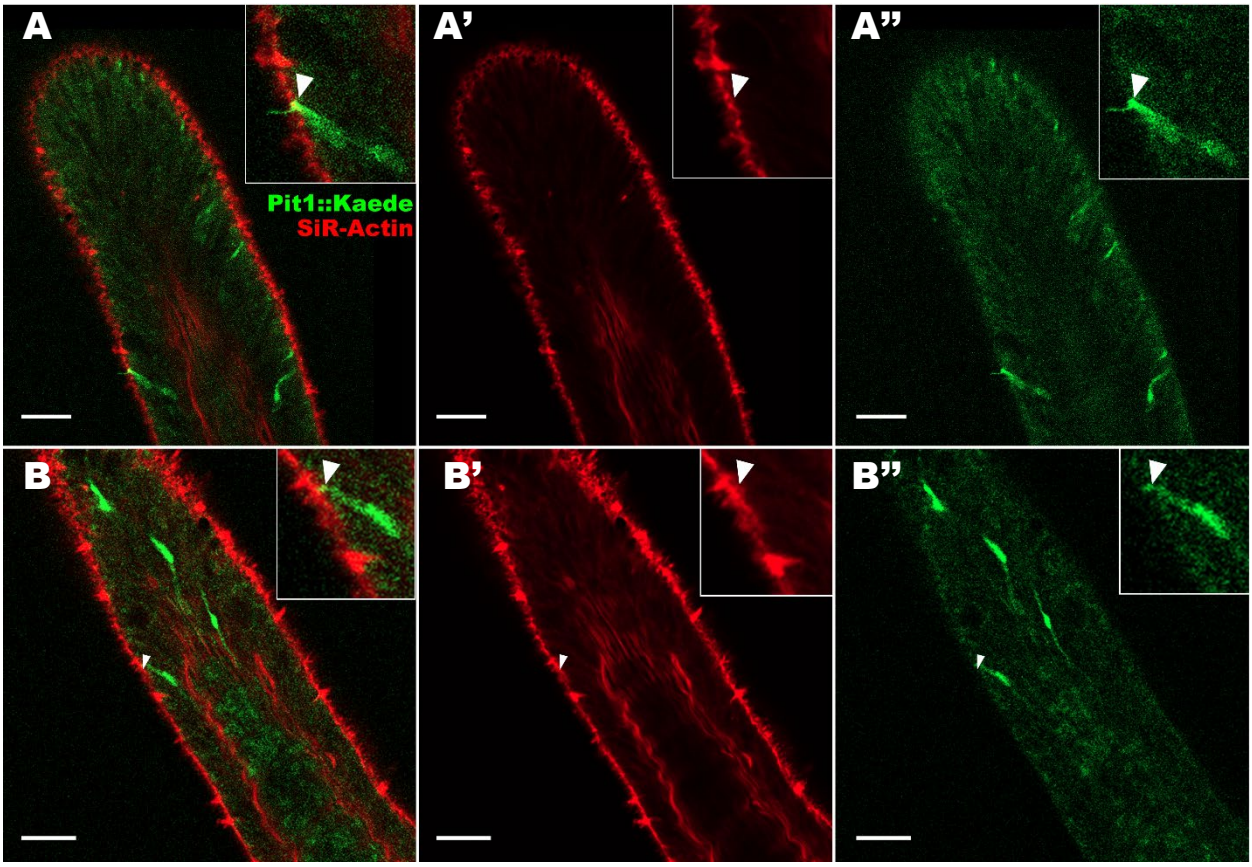

Fig. 19 – Actin stain analysis on Pit1::Kaede F2 polyp tentacles. SiR-actin staining combined with Kaede intrinsic fluorescence found in **(A-A'')** a Pit1^{+} sensory cell with a distinguishable cilium but without actin rootlets (see arrowheads). **(B-B'')** Shows one Pit1^{+} cell with short actin rootlets (arrowhead) and short actin rich stereocilia, next to a cell towards the distal end with more prominent actin stereocilia and another cell towards the proximal end of the tentacle with prominent rootlets. Scale bars: 20um.

To further characterize these Pit1-positive sensory cells, Pit1::Kaede F2 animals were stained with anti-Kaede antibody and Phalloidin actin stain. Diverse cells with diverse morphologies were described, and only two cells displayed hair cell-like structures (Fig. 20E and Fig. 21A). and found that most NvPit1^{+} cells do not appear to be hair cells, lacking prominent stereocilia or rootlets (Fig. 20A, Supplementary Fig. S13), and displaying diverse morphologies (Fig. 21-22). However, two cells with clear stereovillar rootlets and stereovilli were found (Fig. 20E, Fig. 21A).

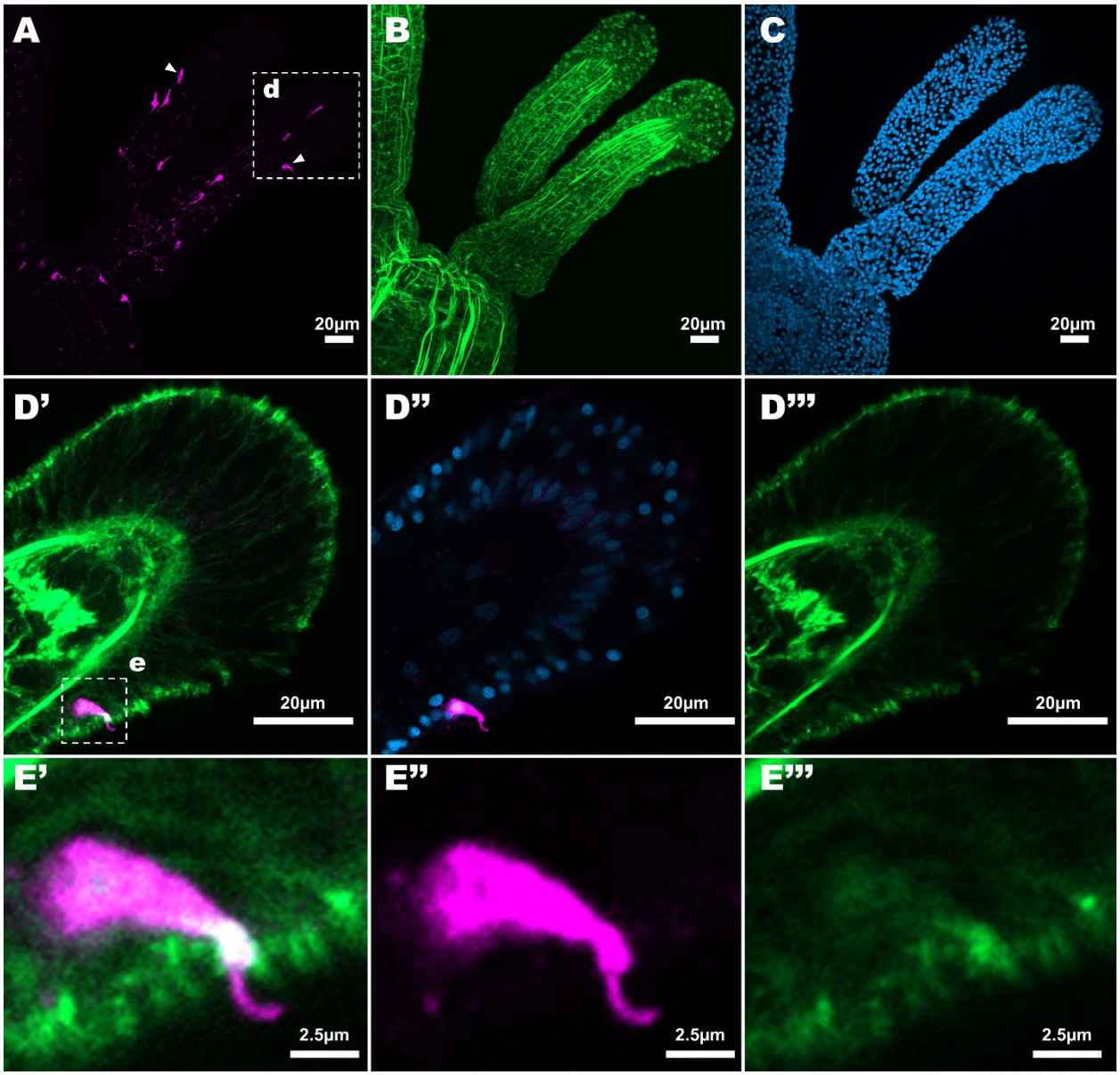

Fig. 20 – Actin and Kaede stain on F2 Pit1::Kaede Transgenic polyps. (A-C) Confocal Z-projection of stained Pit1::Kaede F2 polyp reveals eleven sensory ectodermal cells with diverse morphologies. 2 out 11 (~18%) have hair cell-like structures such as actin rootlets and stereocilia (see arrowheads in A; inset **E** and Fig. 21**A**). Furthermore, ganglion neurons were detected at the base of the tentacle (see supplemental material for larger image). **(D-D'')** Confocal section shows a Pit1+ sensory cell near the tentacle tip. **(E)** Confocal section reveals putative $Pit1^{+}$ hair cell. Scale bars: in panels.

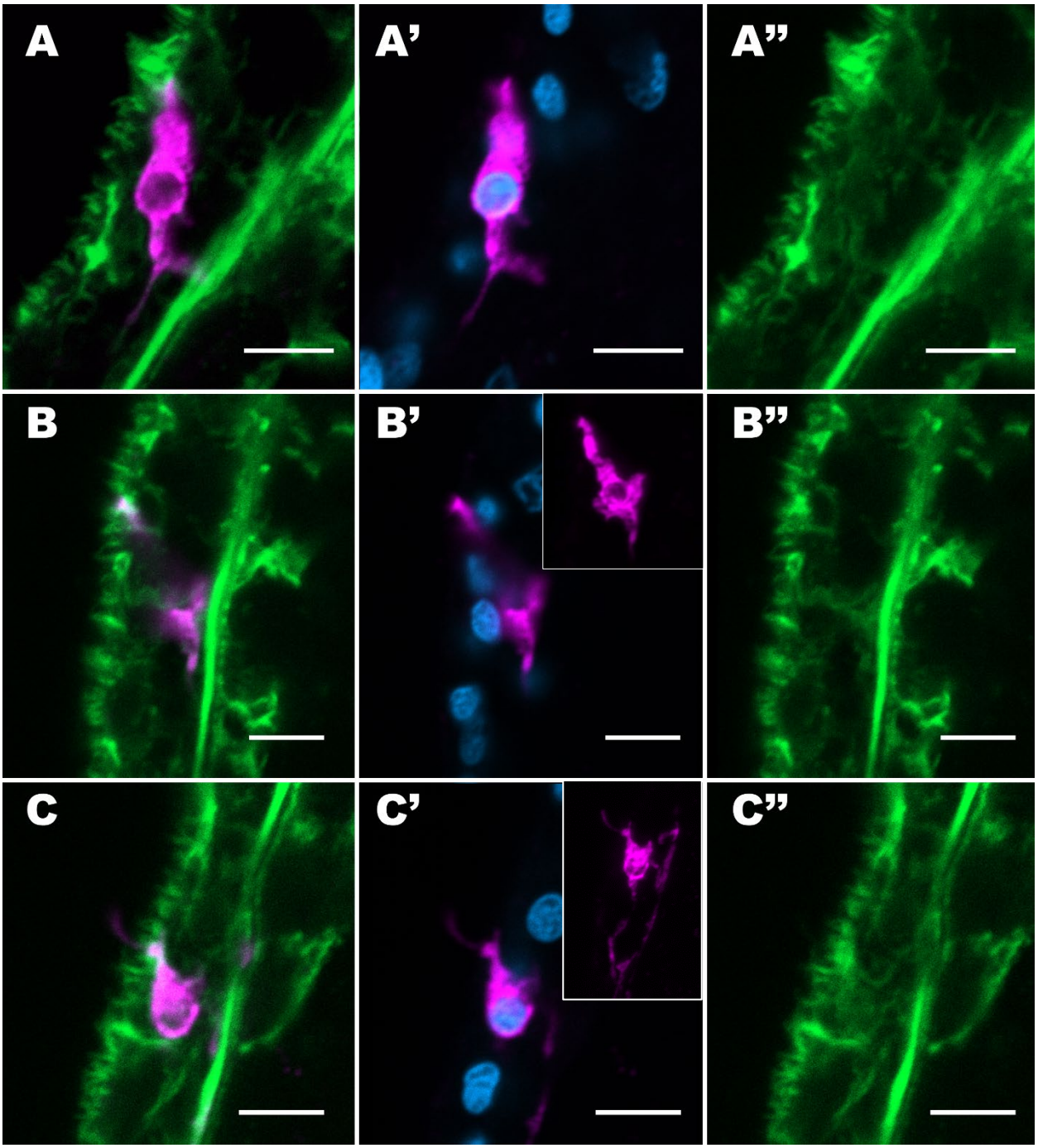

Fig. 21 – Cellular resolution of Pit1$^+$ sensory cells (A). Confocal section shows putative Pit1$^+$ hair cell, with the apical tip of the cell rich in (or surrounded by) actin stereocilia. A different confocal section (z7) of the same cell better resolves this (see supplementary figure 14). **(B)** Confocal section reveals a Pit1 cell with a very thin apical tip contacting the exterior of the animal, with no noticeable cilium or stereocilia and no prominent rootlets. **(B' inset)** A confocal Z-projection of this cell reveals a unique morphology, not previously seen in this study, and to the best of my knowledge, not described in the literature (of *Nematostella*). **(C)** Confocal section of Pit1 cell further expands on our knowledge of the diverse morphologies of Pit1 cell types. Here, a cilium is detected (arrowhead) but no stereocilia or acting rootlets. Z-projection in **C' inset** reveals a complex neuronal network associated with this cell. Scale bars: All 5um.

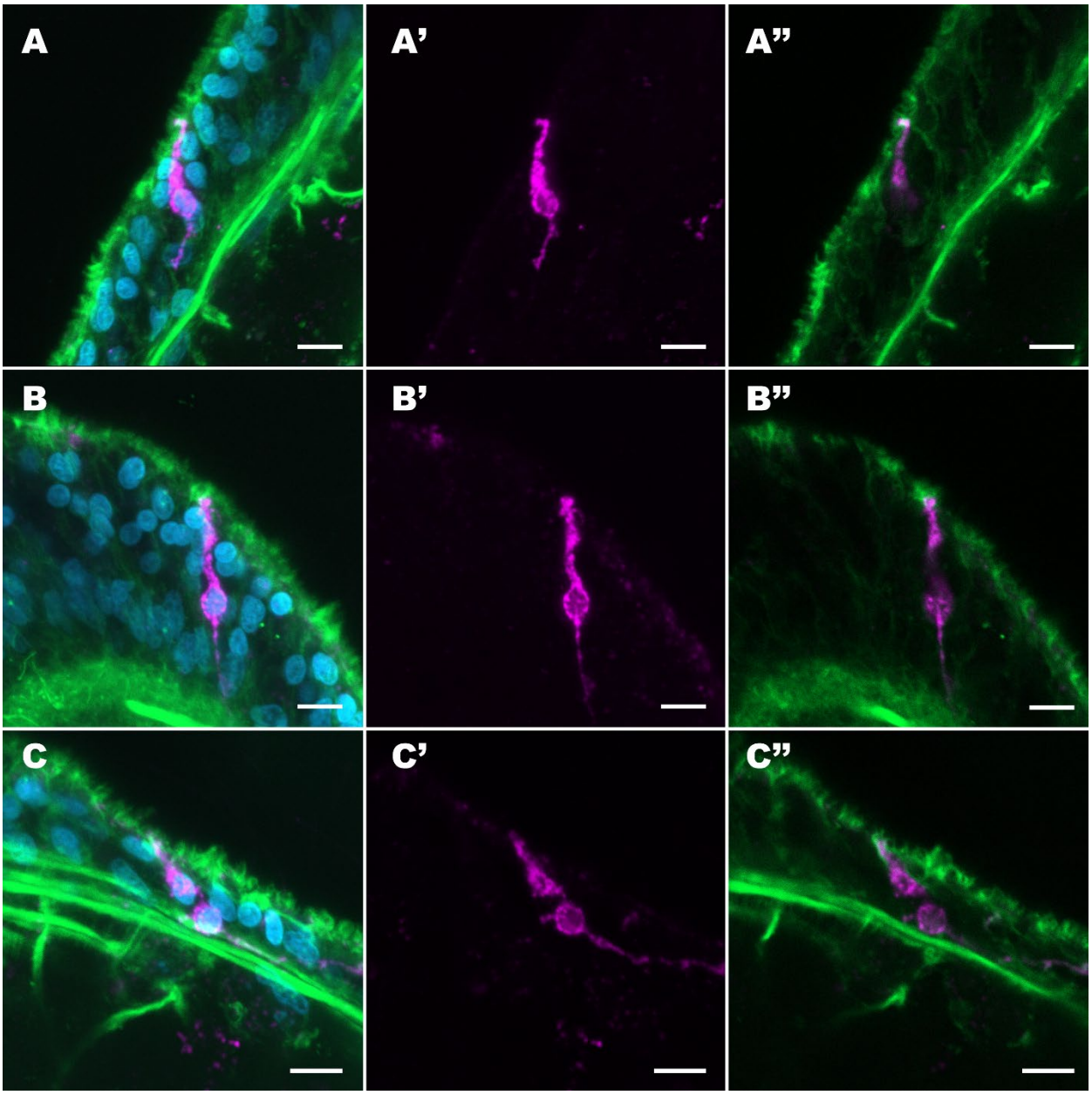

Fig. 22 – Spindle-shaped Pit1^{+} sensory cells. (A-B) Confocal Z-projection reveals a typical spindle-shaped morphology with basal processes. No cilia, stereocilia or actin rootlets were identified. **(C)** Confocal Z-projection reveals a interestingly shaped cell, with the apical structure of the cell connected to the soma by a thin process (see supplementary figure 15). No prominent actin structures were found. Scale bars: all 5um.

To address expression of Pit1 in cnidocytes, Pit1::Kaede F1s were stained with anti-Kaede antibody, Phalloidin, acTub and a cnidocyte-DAPI-staining (see methods) and no Pit1 expression in cnidocytes was detected (Supplementary Fig. S16).

3.7) Addressing the function of Pit1 in *Nematostella*

To analyze the function of Pit1 in *Nematostella*, I generated CR-Pit1 KO mutants and isolated animals carrying different alleles (Fig. 2). For functional studies, animals with allele d/+ with a complete deletion of the functional domain of Pit1 were selected. These animals were reared and F2 stable lines were generated.

3.7.1) Addressing Pit1 *role in RPamide neural development*

Based on the colocalization results that showed expression of NvPit1 transcript in, or in adjacent cells to, RPamide neurons, we hypothesized that NvPit1 could be involved in differentiation or maintenance of RPamide endodermal neurons. As such, CR-Pit1 F3 KO and WT animals were stained using an RPamide antibody. No noticeable differences in the RPamide nerve net were detected between KO and WT (Supplementary Fig. S17); however, further investigation is needed.

3.7.2) Addressing Pit1 *role in chemosensation*

Following up on the diverse cell morphologies described with the Pit1::Kaede transgenics (Fig. 20-22), and on the raised hypothesis of chemosensory Pit1 cells in the lancelet, I aimed to determine if Pit1 could be involved in chemosensation. For that, a food-cue chemosensitivity assay was performed on *Nematostella* F3 knockout polyps, which resulted in an immediate response to shrimp juice with body contractions followed by the protrusion of the pharynx, as the previously described response seen in wildtypes (Ozment et al., 2021). Thus, even though I lack wildtype data for this particular assay, I infer that chemosensation (at least to food cues) is not affected, however, other chemosensorial capabilities in *Nematostella* could be affected and remain undiscovered and undescribed (see Discussion).

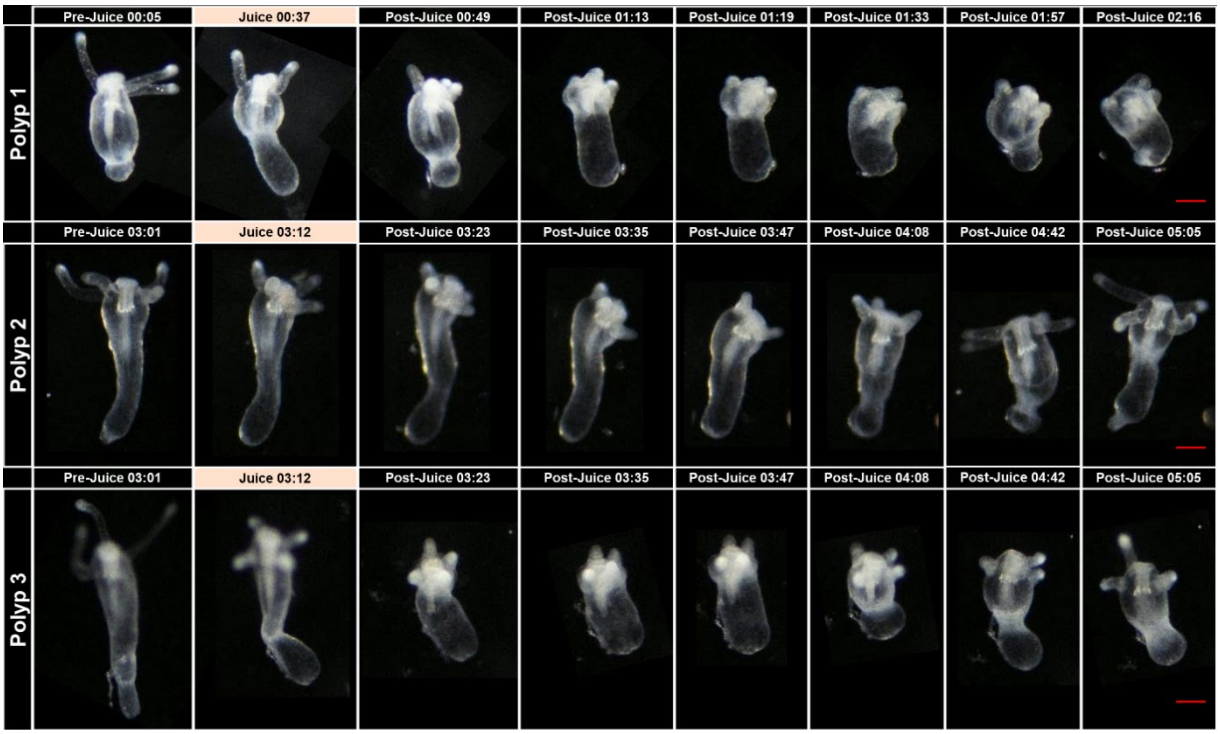

Fig. 23 – Chemosensory behavioral assay. Behavior of mutant (F2 CR-Pit1$^{-/-}$) *Nematostella vectensis* polyps in response to exposure to *Artemia* extract. Mutant animals contracted tentacles and protruded the pharynx within 1 min of exposure to the extract (F2 CR-Pit1$^{-/-}$, 100%, n = 3), which recapitulates the previously described response in Ozment et al., 2021. Scale bar: 1 mm.

4) DISCUSSION

This is the first description of the POU-I/Pit1 gene expression patterns, and of the morphology of Pit1-positive cells in *Nematostella vectensis*. Our gene expression analysis indicates a dynamic expression of NvPit1, with expression first being detected in the endoderm during planula stage, when the endodermal neurons begin development (Nakanishi *et al*., 2012), and later beginning in the ectoderm of tentacular primordia during tentacle bud stage. At polyp stage simultaneous endodermal and ectodermal expression is observed, in the body column and in the tentacles, respectively. In vertebrates, Pit1 is mostly expressed in the anterior pituitary, which develops from the ectoderm (Scully & Rosenfeld, 2002). In lancelets, Pit1 is expressed in the Hatschek's pit, also of ectodermal nature (Candiani *et al*., 2008). In *Nematostella*, in addition to

the ectodermal expression of Pit1 in the tentacles, endodermal expression was here described, thus suggesting that either Pit1 endodermal expression was lost in the Bilaterian lineage, or it is a Cnidarian specific innovation related to the fact that *Nematostella* has endodermal neurons.

The majority of endodermal cells with Pit1 expression described here were $Elav^{+}$ neurons, with the exception of one detected Pit1 neuron that did not colocalize with Elav (Fig. 17D). Elav are conserved RNA-binding proteins, shared across Metazoa, that play a crucial role in post-transcriptional regulation of gene expression in neurons and are necessary for normal neuronal differentiation (Akamatsu et al., 1999; Campos et al., 1985; Denes et al., 2007; Marlow et al., 2009; Nomaksteinsky et al., 2009; Satoh et al., 2001). The discovery of Pit1 expression in $Elav^{+}$ neurons suggests that Pit1 may play a role in the development and function of the nervous system of *Nematostella*. Future directions should aim to compare the Elav-positive nerve net between wildtype and knockout Pit1 animals, using a knockout transgenic reporter line (i.e., CR-$Pit1^{-/-}$/Elav::mO) (see methods and Supplementary Table S1).

In vertebrates, the neurons of the hypothalamus regulate the activity of $Pit1^{+}$ cells of the adenohypophysis (i.e., thyrotropes, somatotropes, lactotropes), via neuropeptidergic signals (Freeman *et al*., 2000; Murray *et al*., 2015). Neuropeptides are small, cleaved peptides, that are often synthesized in neurons and neuroendocrine cells found in nervous systems of Metazoa and hypothesized to be the primordial means of neuronal communication in the early evolution of nervous systems (Grimmelikhuijzen & Hauser, 2012). RPamide is a neuropeptide that is found exclusively in cnidarians (Carstensen et al., 1993; Hayakawa et al., 2019; Zang & Nakanishi, 2020). RPamide function is currently unknown but ongoing research efforts aim to uncover its role in *Nematostella* (Baranyk and Nakanishi, *in preparation*). Our results in *Nematostella* suggest that neuropeptidergic RPamide neurons either synapse to $Pit1^{+}$ endodermal cells (Fig. 11C-E) or

express Pit1 (Fig. 11A-B). Clarifying the relationship between RPamide and Pit1 in *Nematostella* will elucidate the possibility of structural and physiological homologies (i.e., neurons synapsing to $Pit1^{+}$ cells and neuropeptides regulating activity of $Pit1^{+}$ cells) across Cnidaria and Bilateria. Preliminary data collected from CRISPR-Cas9 full knockout mutants of Pit1 indicates that mutations in Pit1 do not affect the RPamide network. However, further evidence is needed to confirm this observation and to address the putative synapsis between RPamide neurons and Pit1 cells using higher resolution imaging.

There has been an increasing amount of evidence suggesting a crucial role of Pit1, Prop1 (Prophet of Pit1) and thyroid hormones in the normal development of the vertebrate inner ear hair cells, with $Pit1^{dw}$ mutations resulting in hypothyroidism and completely deaf mice (Fang et al., 2012; Mustapha et al., 2009; Sundaresan et al., 2016). In the Cnidarian 'moon jellyfish' *Aurelia*, Pit1 was detected in cells with sensory-cell-like morphology in a separate domain adjacent to $Brn3^{+}$ cells (Nakanishi et al., 2010), but the specific cell type was not defined. In *Nematostella* we see abundant $Pit1^{+}$ sensory cells in the tentacles with diverse morphologies. Tentacles constitute the primary sensorial apparatus of sea anemones, rich in Brn3/Pkd1 mechanosensory hair-cell bundles (Ozment et al., 2021; Westfall et al., 1998), mechanosensory stinging cnidocytes (Babonis & Martindale, 2017) and, feasibly, additional unknown/undescribed sensory cells, such as photoreceptors and chemoreceptors.

Some of the ectodermal $Pit1^{+}$ sensory neurons observed in this study have hair-cell like features, such as an apical cilia surrounded by stereocilia and actin rootlets, previously described in detail in *Nematostella* (Ozment et al., 2021). The single-cell study (Sebé-Pedrós et al., 2018) indicated expression of Brn3 and Pkd1 in Pit1 cells. Thus, future work should aim to address this.

If this is verified in *Nematostella*, it raises the question of how the Pit1 cells became segregated from the Brn3 cell population in the 'moon jellyfish' *Aurelia*. Furthermore, if the role of Pit1 in Brn3^{+} hair cells is proven, it would indicate that the function of Pit1 in hair cell differentiation and maintenance is conserved across Cnidaria and Bilateria.

To address this, we can 1) stain Pit1::Kaede F2 animals with Brn3 antibodies and analyze them with Kaede intrinsic fluorescence; 2) cross CR-Pit1F2$^{-/-}$ with Brn3::Kaede and Pkd::Kaede and examine Brn3 and Pkd cellular phenotypes; 3) perform touch assay on CR-Pit1F2$^{-/-}$ animals. Additionally, I here propose the development of an auditory threshold assay, to address sound sensitivity in *Nematostella* (see Jézéquel et al., 2021; Lapshin & Vorontsov, 2019; Solé et al., 2016, 2023, for conceptual and experimental frameworks).

In the lancelet *Branchiostma floridae,* Pit1 is expressed exclusively in the Hatschek's pit, which is rich in ciliated cells and is hypothesized to function as a chemosensory organ (Candiani *et al*., 2008; Schlosser *et al*., 2014; Uchida *et al*., 2003). Based on that hypothesis and on the diverse morphologies of Pit1^{+} sensory cells in the tentacles of *Nematostella*, we aimed to address the chemosensorial potential of Pit1 sensory cells. The chemosensory assay in Pit1 knockout mutants revealed a normal response to shrimp juice extract (based on Ozment *et al*., 2021). This could indicate that if indeed a subset of Pit1^{+} sensory cells are chemoreceptors, this cell population is not entirely responsible for the detection of food chemical cues. Additionally, other modalities of chemosensation, besides food detection, must be considered and tested, such as alarm communication, which is undescribed in *Nematostella* but is well documented in the 'aggregating anemone' *Anthopleura elegantissima* (Harris & Howe, 1979; Howe & Sheikh, 1975; Musich & Rapoport, 1978) and the ability to detect population density and modulate asexual reproduction accordingly (Al-Shaer *et al*., 2023).

In line with our findings, the whole-organism single-cell analysis from Sebé-Pedrós and colleagues (2018), detected co-expression of Elav in the Pit1^{+} metacell (see cell #79 in Table S2 – Sebé-Pedrós *et al*., 2018). However, the co-expression of Brn3, Pkd1 and neuropeptide receptors (RYamide receptor) needs to be further validated. Although extremely useful, our results indicate that the single-cell data might be incomplete, since we here demonstrate expression of Pit1 in larval stages, and in the single-cell study Pit1 is presented as exclusively expressed in the polyp stage.

Furthermore, other homologs of genes involved in the development of the vertebrate pituitary gland are found in *Nematostella*, such as Lhx3, Prop-1 and Gata. Thus, the pituitary GRN could be tested in *Nematostella,* by systematically perturbing putatively upstream genes and addressing Pit1^{+} cell phenotypes, with the use of the established transgenic lines.

During our work we did not find any noticeable abnormalities in the Pit1 mutant animals, which grew, ate, and reproduced well. But to further address the role of Pit1 as an endocrine regulator in *Nematostella*, assays such as growth rate, regeneration rate, developmental timing and sexual maturity timing can be performed comparing WT and KO animals. Furthermore, the expression of melanocortin and thyrotropin receptors in the Pit1 metacell (Sebé-Pedrós *et al*., 2018) could be validated by *in-situ* hybridization or immunohistochemistry in Pit1::Kaede transgenics.

In conclusion, here I considerably expanded the knowledge of Pit1 outside of Bilateria, further demonstrated the expression of Pit1 in sensory and ganglion cells in Cnidaria and laid the foundations for functional studies by generating stable CRISPR-Cas9 and Kaede reporter lines of Pit1, which will allow to address the function of Pit1 in *Nematostella*. EdU labeling must be performed to characterize the mitotic potential of Pit1 cells and further validate its function as a terminal selector in Cnidaria. FACS technology and the Pit1::Kaede lines will allow to dissect the

molecular profile of specific Pit1^{+} cells, which can be isolated from tentacles or body columns. Moreover, individual Pit1::Kaede cells of interest can be photoconverted, isolated and analyzed as specific subpopulations. Furthermore, ChIP-seq can be performed using the validated antibodies in combination with KO (-b) and WT animals to identify the target genes of Pit1 in *Nematostella.* The discovery of a conserved function of Pit1 between Cnidaria and Bilateria would shed light on the origins and evolution of pituitary cell types and contribute to the understanding and the reconstruction of the neuroendocrine system of the last common ancestor of Bilateria and Cnidaria.

5) REFERENCES

Ahissar, E., & Assa, E. (2016). Perception as a closed-loop convergence process. *ELife*, *5*, e12830. https://doi.org/10.7554/eLife.12830

Akamatsu, W., Okano, H. J., Osumi, N., Inoue, T., Nakamura, S., Sakakibara, S.-I., Miura, M., Matsuo, N., Darnell, R. B., & Okano, H. (1999). Mammalian ELAV-like neuronal RNA-binding proteins HuB and HuC promote neuronal development in both the central and the peripheral nervous systems. *Proceedings of the National Academy of Sciences*, *96*(17), 9885–9890. https://doi.org/10.1073/pnas.96.17.9885

Allan, D. W., & Thor, S. (2015). Transcriptional selectors, masters, and combinatorial codes: Regulatory principles of neural subtype specification: Regulation of neural subtype generation. *Wiley Interdisciplinary Reviews: Developmental Biology*, *4*(5), 505–528. https://doi.org/10.1002/wdev.191

Al-Shaer, L., Leach, W., Baban, N., Yagodich, M., Gibson, M. C., & Layden, M. J. (2023). *Environmental and molecular regulation of asexual reproduction in the sea anemone Nematostella vectensis* [Preprint]. Animal Behavior and Cognition. https://doi.org/10.1101/2023.01.27.525773

Ando, R., Hama, H., Yamamoto-Hino, M., Mizuno, H., & Miyawaki, A. (2002). An optical marker based on the UV-induced green-to-red photoconversion of a fluorescent protein. *Proceedings of the National Academy of Sciences*, *99*(20), 12651–12656. https://doi.org/10.1073/pnas.202320599

Babonis, L. S., & Martindale, M. Q. (2017). PaxA, but not PaxC, is required for cnidocyte development in the sea anemone *Nematostella vectensis. EvoDevo*, *8*(1), 14. https://doi.org/10.1186/s13227-017-0077-7

Boero, F., Schierwater, B., & Piraino, S. (2007). Cnidarian milestones in metazoan evolution. *Integrative and Comparative Biology*, *47*(5), 693–700. https://doi.org/10.1093/icb/icm041

Campos, A. R., And, D. G., & White, K. (1985). Mutant Alleles at the Locus elav in Drosophila melanogaster lead to Nervous System Defects. A Developmental-Genetic Analysis. *Journal of Neurogenetics*, *2*(3), 197–218. https://doi.org/10.3109/01677068509100150

Candiani, S., Holland, N. D., Oliveri, D., Parodi, M., & Pestarino, M. (2008). Expression of the amphioxus Pit-1 gene (AmphiPOU1F1/Pit-1) exclusively in the developing preoral organ, a putative homolog of the vertebrate adenohypophysis. *Brain Research Bulletin*, *75*(2–4), 324–330. https://doi.org/10.1016/j.brainresbull.2007.10.023

Candiani, S., & Pestarino, M. (1998). Evidence for the presence of the tissue-specific transcription factor Pit-1 in lancelet larvae. *The Journal of Comparative Neurology*, *400*(3), 310–316. https://doi.org/10.1002/(SICI)1096-9861(19981026)400:3<310::AID-CNE2>3.0.CO;2-B

Candiani, S., & Pestarino, M. (1999). The tissue-specific transcription factor Pit-1 is expressed in the spinal cord of the lancelet, *Branchiostoma lanceolatum*. *Neuroscience Letters*, *260*(1), 25–28. https://doi.org/10.1016/S0304-3940(98)00933-1

Carstensen, K., McFarlane, I. D., Rinehart, K. L., Hudman, D., Sun, F., & Grimmelikhuijzen, C. J. P. (1993). Isolation of <Glu-Asn-Phe-His-Leu-Arg-Pro-NH2 (Antho-RPamide II), a novel, biologically active neuropeptide from sea anemones. *Peptides*, *14*(2), 131–135. https://doi.org/10.1016/0196-9781(93)90020-H

Cohen, L. E., Wondisford, F. E., & Radovick, S. (1996). ROLE OF PIT-1 IN THE GENE EXPRESSION OF GROWTH HORMONE, PROLACTIN, AND THYROTROPIN. *Endocrinology and Metabolism Clinics of North America*, *25*(3), 523–540. https://doi.org/10.1016/S0889-8529(05)70339-X

De Marco, R. J., Thiemann, T., Groneberg, A. H., Herget, U., & Ryu, S. (2016). Optogenetically enhanced pituitary corticotroph cell activity post-stress onset causes rapid organizing effects on behaviour. *Nature Communications*, *7*(1), 12620. https://doi.org/10.1038/ncomms12620

Denes, A. S., Jékely, G., Steinmetz, P. R. H., Raible, F., Snyman, H., Prud'homme, B., Ferrier, D. E. K., Balavoine, G., & Arendt, D. (2007). Molecular Architecture of Annelid Nerve Cord Supports Common Origin of Nervous System Centralization in Bilateria. *Cell*, *129*(2), 277–288. https://doi.org/10.1016/j.cell.2007.02.040

Fakhry, M. (2013). Molecular mechanisms of mesenchymal stem cell differentiation towards osteoblasts. *World Journal of Stem Cells*, *5*(4), 136. https://doi.org/10.4252/wjsc.v5.i4.136

Fang, Q., Giordimaina, A. M., Dolan, D. F., Camper, S. A., & Mustapha, M. (2012). Genetic Background of Prop1 df Mutants Provides Remarkable Protection Against Hypothyroidism-Induced Hearing Impairment. *Journal of the Association for Research in Otolaryngology*, *13*(2), 173–184. https://doi.org/10.1007/s10162-011-0302-3

Fischer, A. H. L., Mozzherin, D., Eren, A. M., Lans, K. D., Wilson, N., Cosentino, C., & Smith, J. (2014). SeaBase: A Multispecies Transcriptomic Resource and Platform for Gene Network Inference. *Integrative and Comparative Biology*, *54*(2), 250–263. https://doi.org/10.1093/icb/icu065

Fischer, A. H. L., & Smith, J. (2012). Evo-Devo in the Era of Gene Regulatory Networks. *Integrative and Comparative Biology*, *52*(6), 842–849. https://doi.org/10.1093/icb/ics112

Freeman, M. E., Kanyicska, B., Lerant, A., & Nagy, G. (2000). *Prolactin: Structure, Function, and Regulation of Secretion*. *80*.

Fritzenwanker, J. H., & Technau, U. (2002). Induction of gametogenesis in the basal cnidarian *Nematostella vectensis* (Anthozoa). *Development Genes and Evolution*, *212*(2), 99–103. https://doi.org/10.1007/s00427-002-0214-7

Galliot, B. (2000). Conserved and divergent genes in apex and axis development of cnidarians. *Current Opinion in Genetics & Development*, *10*(6), 629–637. https://doi.org/10.1016/S0959-437X(00)00141-6

Godfrey, P. (1993). GHRH receptor of little mice contains a missense mutation in the extracellular domain that disrupts receptor function. *Nature Genetics*, *4*(3), 227–232. https://doi.org/10.1038/ng0793-227

Gold, D. A., Gates, R. D., & Jacobs, D. K. (2014). The Early Expansion and Evolutionary Dynamics of POU Class Genes. *Molecular Biology and Evolution*, *31*(12), 3136–3147. https://doi.org/10.1093/molbev/msu243

Grimmelikhuijzen, C. J. P., & Hauser, F. (2012). Mini-review: The evolution of neuropeptide signaling. *Regulatory Peptides*, *177*, S6–S9. https://doi.org/10.1016/j.regpep.2012.05.001

Hand, C., & Uhlinger, K. R. (1992). The Culture, Sexual and Asexual Reproduction, and Growth of the Sea Anemone *Nematostella vectensis*. *The Biological Bulletin*, *182*(2), 169–176. https://doi.org/10.2307/1542110

Harris, L. G., & Howe, N. R. (1979). AN ANALYSIS OF THE DEFENSIVE MECHANISMS OBSERVED IN THE ANEMONE *ANTHOPLEURA ELEGANTISSIMA* IN RESPONSE TO ITS NUDIBRANCH PREDATOR *AEOLIDIA PAPILLOSA*. *The Biological Bulletin*, *157*(1), 138–152. https://doi.org/10.2307/1541083

Hayakawa, E., Watanabe, H., Menschaert, G., Holstein, T. W., Baggerman, G., & Schoofs, L. (2019). A combined strategy of neuropeptide prediction and tandem mass spectrometry identifies evolutionarily conserved ancient neuropeptides in the sea anemone *Nematostella vectensis*. *PLOS ONE*, *14*(9), e0215185. https://doi.org/10.1371/journal.pone.0215185

Heaney, A. P., & Melmed, S. (2004). Molecular targets in pituitary tumours. *Nature Reviews Cancer*, *4*(4), 285–295. https://doi.org/10.1038/nrc1320

Helm, R., Siebert, S., Tulin, S., Smith, J., & Dunn, C. (2013). Characterization of differential transcript abundance through time during *Nematostella vectensis* development. *BMC Genomics*, *14*(1), 266. https://doi.org/10.1186/1471-2164-14-266

Ho, Y., Cooke, N. E., & Liebhaber, S. A. (2015). An Autoregulatory Pathway Establishes the Definitive Chromatin Conformation at the *Pit-1* Locus. *Molecular and Cellular Biology*, *35*(9), 1523–1532. https://doi.org/10.1128/MCB.01283-14

Hobert, O. (2008). Regulatory logic of neuronal diversity: Terminal selector genes and selector motifs. *Proceedings of the National Academy of Sciences*, *105*(51), 20067–20071. https://doi.org/10.1073/pnas.0806070105

Howe, N. R., & Sheikh, Y. M. (1975). Anthopleurine: A Sea Anemone Alarm Pheromone. *Science*, *189*(4200), 386–388. https://doi.org/10.1126/science.238286

Huang, B., Lu, M., Galbraith, M., Levine, H., Onuchic, J. N., & Jia, D. (2020). Decoding the mechanisms underlying cell-fate decision-making during stem cell differentiation by random circuit perturbation. *Journal of The Royal Society Interface*, *17*(169), 20200500. https://doi.org/10.1098/rsif.2020.0500

Ikmi, A., McKinney, S. A., Delventhal, K. M., & Gibson, M. C. (2014). TALEN and CRISPR/Cas9-mediated genome editing in the early-branching metazoan Nematostella vectensis. *Nature Communications*, *5*(1), 5486. https://doi.org/10.1038/ncomms6486

Ingraham, H. A., Albert, V. R., Chen, R., & Crenshaw, E. B. (1988). *A Family of Pou-Domain and Pit-1 Tissue-Specific Transcription Factors in Pituitary and Neuroendocrine Development*.

Jen, H.-I., Singh, S., Tao, L., Maunsell, H. R., Segil, N., & Groves, A. K. (2022). GFI1 regulates hair cell differentiation by acting as an off-DNA transcriptional co-activator of ATOH1, and a DNA-binding repressor. *Scientific Reports*, *12*(1), 7793. https://doi.org/10.1038/s41598-022-11931-0

Jennings, K. J., & de Lecea, L. (2020). Neural and Hormonal Control of Sexual Behavior. *Endocrinology*, *161*(10), bqaa150. https://doi.org/10.1210/endocr/bqaa150

Jézéquel, Y., Jones, I. T., Bonnel, J., Chauvaud, L., Atema, J., & Mooney, T. A. (2021). Sound detection by the American lobster (*Homarus americanus*). *Journal of Experimental Biology*, *224*(6), jeb240747. https://doi.org/10.1242/jeb.240747

Kanaya, H. J., Park, S., Kim, J., Kusumi, J., Krenenou, S., Sawatari, E., Sato, A., Lee, J., Bang, H., Kobayakawa, Y., Lim, C., & Itoh, T. Q. (2020). A sleep-like state in *Hydra* unravels conserved sleep mechanisms during the evolutionary development of the central nervous system. *Science Advances*, *6*(41), eabb9415. https://doi.org/10.1126/sciadv.abb9415

Keller, R. E. (1981). An experimental analysis of the role of bottle cells and the deep marginal zone in gastrulation ofXenopus laevis. *Journal of Experimental Zoology*, *216*(1), 81–101. https://doi.org/10.1002/jez.1402160109

Kozak, M. (1989). The scanning model for translation: An update. *Journal of Cell Biology*, *108*(2), 229–241. https://doi.org/10.1083/jcb.108.2.229

Lacalli, T. (2007). Mucus secretion and transport in amphioxus larvae: Organization and ultrastructure of the food trapping system, and implications for head evolution: Mucus secretion and transport in amphioxus larvae. *Acta Zoologica*, *89*(3), 219–230. https://doi.org/10.1111/j.1463-6395.2007.00310.x

Lapshin, D. N., & Vorontsov, D. D. (2019). Directional and frequency characteristics of auditory neurons in Culex male mosquitoes. *Journal of Experimental Biology*, jeb.208785. https://doi.org/10.1242/jeb.208785

Leclère, L., & Röttinger, E. (2017). Diversity of Cnidarian Muscles: Function, Anatomy, Development and Regeneration. *Frontiers in Cell and Developmental Biology*, *4*. https://doi.org/10.3389/fcell.2016.00157

Leyva-Díaz, E., & Hobert, O. (2019). Transcription factor autoregulation is required for acquisition and maintenance of neuronal identity. *Development*, *146*(13), dev177378. https://doi.org/10.1242/dev.177378

Leyva-Díaz, E., Masoudi, N., Serrano-Saiz, E., Glenwinkel, L., & Hobert, O. (2020). Brn3/POU-IV-type POU homeobox genes—Paradigmatic regulators of neuronal identity across phylogeny. *WIREs Developmental Biology*, *9*(4). https://doi.org/10.1002/wdev.374

Li, C., Wen, A., Shen, B., Lu, J., Huang, Y., & Chang, Y. (2011). FastCloning: A highly simplified, purification-free, sequence- and ligation-independent PCR cloning method. *BMC Biotechnology*, *11*(1), 92. https://doi.org/10.1186/1472-6750-11-92

Li, S. (1990). Dwarf locus mutants lacking three pituitary cell types result from mutations in the POU-domain gene pit-1. *Nature*, *19*(6293), 528–533. https://doi.org/doi: 10.1038/347528a0

Lin, S. C. (1993). Molecular basis of the little mouse phenotype and implications for cell type-specific growth. *Nature*, *364*(6434), 208–213. https://doi.org/doi: 10.1038/364208a0

Marlow, H. Q., Srivastava, M., Matus, D. Q., Rokhsar, D., & Martindale, M. Q. (2009). Anatomy and development of the nervous system of *Nematostella vectensis* , an anthozoan cnidarian. *Developmental Neurobiology*, *69*(4), 235–254. https://doi.org/10.1002/dneu.20698

McNamara, A. V., Awais, R., Momiji, H., Dunham, L., Featherstone, K., Harper, C. V., Adamson, A. A., Semprini, S., Jones, N. A., Spiller, D. G., Mullins, J. J., Finkenstädt, B. F., Rand, D., White, M. R. H., & Davis, J. R. E. (2021). Transcription Factor Pit-1 Affects Transcriptional Timing in the Dual-Promoter Human Prolactin Gene. *Endocrinology*, *162*(4), bqaa249. https://doi.org/10.1210/endocr/bqaa249

Murray, P. G., Higham, C. E., & Clayton, P. E. (2015). 60 YEARS OF NEUROENDOCRINOLOGY: The hypothalamo-GH axis: the past 60 years. *Journal of Endocrinology*, *226*(2), T123–T140. https://doi.org/10.1530/JOE-15-0120

Musich, J. A., & Rapoport, H. (1978). Synthesis of anthopleurine, the alarm pheromone from Anthopleura elegantissima. *Journal of the American Chemical Society*, *100*(15), 4865–4872. https://doi.org/10.1021/ja00483a037

Mustapha, M., Fang, Q., Gong, T.-W., Dolan, D. F., Raphael, Y., Camper, S. A., & Duncan, R. K. (2009). Deafness and Permanently Reduced Potassium Channel Gene Expression and Function in Hypothyroid *Pit1* ^{dw} Mutants. *The Journal of Neuroscience*, *29*(4), 1212–1223. https://doi.org/10.1523/JNEUROSCI.4957-08.2009

Naamati, G., Fromer, M., & Linial, M. (2009). Expansion of tandem repeats in sea anemone Nematostella vectensis proteome: A source for gene novelty? *BMC Genomics*, *10*(1), 593. https://doi.org/10.1186/1471-2164-10-593

Nakanishi, N., & Martindale, M. Q. (2018a). CRISPR knockouts reveal an endogenous role for ancient neuropeptides in regulating developmental timing in a sea anemone. *ELife*, *7*, e39742. https://doi.org/10.7554/eLife.39742

Nakanishi, N., Renfer, E., Technau, U., & Rentzsch, F. (2012). Nervous systems of the sea anemone *Nematostella vectensis* are generated by ectoderm and endoderm and shaped by distinct mechanisms. *Development*, *139*(2), 347–357. https://doi.org/10.1242/dev.071902

Nakanishi, N., Yuan, D., Hartenstein, V., & Jacobs, D. K. (2010). Evolutionary origin of rhopalia: Insights from cellular-level analyses of Otx and POU expression patterns in the developing rhopalial nervous system: Otx and POU expression patterns in *Aurelia*. *Evolution & Development*, *12*(4), 404–415. https://doi.org/10.1111/j.1525-142X.2010.00427.x

Nakayama, T., Fish, M. B., Fisher, M., Oomen-Hajagos, J., Thomsen, G. H., & Grainger, R. M. (2013). Simple and efficient CRISPR/Cas9-mediated targeted mutagenesis in *Xenopus tropicalis*: CRISPR-Cas Genome Editing in *Xenopus*. *Genesis*, *51*(12), 835–843. https://doi.org/10.1002/dvg.22720

Nomaksteinsky, M., Röttinger, E., Dufour, H. D., Chettouh, Z., Lowe, C. J., Martindale, M. Q., & Brunet, J.-F. (2009). Centralization of the Deuterostome Nervous System Predates Chordates. *Current Biology*, *19*(15), 1264–1269. https://doi.org/10.1016/j.cub.2009.05.063

Okawa, S., Nicklas, S., Zickenrott, S., Schwamborn, J. C., & del Sol, A. (2016). A Generalized Gene-Regulatory Network Model of Stem Cell Differentiation for Predicting Lineage Specifiers. *Stem Cell Reports*, *7*(3), 307–315. https://doi.org/10.1016/j.stemcr.2016.07.014

Ozment, E., Tamvacakis, A. N., Zhou, J., Rosiles-Loeza, P. Y., Escobar-Hernandez, E. E., Fernandez-Valverde, S. L., & Nakanishi, N. (2021). Cnidarian hair cell development illuminates an ancient role for the class IV POU transcription factor in defining mechanoreceptor identity. *ELife*, *10*, e74336. https://doi.org/10.7554/eLife.74336

Renaud, O., Herbomel, P., & Kissa, K. (2011). Studying cell behavior in whole zebrafish embryos by confocal live imaging: Application to hematopoietic stem cells. *Nature Protocols*, *6*(12), 1897–1904. https://doi.org/10.1038/nprot.2011.408

Renfer, E., Amon-Hassenzahl, A., Steinmetz, P. R. H., & Technau, U. (2010). A muscle-specific transgenic reporter line of the sea anemone, *Nematostella vectensis*. *Proceedings of the National Academy of Sciences*, *107*(1), 104–108. https://doi.org/10.1073/pnas.0909148107

Rentzsch, F., Fritzenwanker, J. H., Scholz, C. B., & Technau, U. (2008). FGF signalling controls formation of the apical sensory organ in the cnidarian *Nematostella vectensis*. *Development*, *135*(10), 1761–1769. https://doi.org/10.1242/dev.020784

Saina, M., Busengdal, H., Sinigaglia, C., Petrone, L., Oliveri, P., Rentzsch, F., & Benton, R. (2015). A cnidarian homologue of an insect gustatory receptor functions in developmental body patterning. *Nature Communications*, *6*(1), 6243. https://doi.org/10.1038/ncomms7243

Satoh, G., Wang, Y., Zhang, P., & Satoh, N. (2001). Early development of amphioxus nervous system with special reference to segmental cell organization and putative sensory cell precursors: A study based on the expression of pan-neuronal marker geneHu/elav. *Journal of Experimental Zoology*, *291*(4), 354–364. https://doi.org/10.1002/jez.1134

Schlosser, G., Patthey, C., & Shimeld, S. M. (2014). The evolutionary history of vertebrate cranial placodes II. Evolution of ectodermal patterning. *Developmental Biology*, *389*(1), 98–119. https://doi.org/10.1016/j.ydbio.2014.01.019

Scully, K. M., & Rosenfeld, M. G. (2002). Pituitary Development: Regulatory Codes in Mammalian Organogenesis. *Science*, *295*(5563), 2231–2235. https://doi.org/10.1126/science.1062736

Sebé-Pedrós, A., Saudemont, B., Chomsky, E., Plessier, F., Mailhé, M.-P., Renno, J., Loe-Mie, Y., Lifshitz, A., Mukamel, Z., Schmutz, S., Novault, S., Steinmetz, P. R. H., Spitz, F., Tanay, A., & Marlow, H. (2018). Cnidarian Cell Type Diversity and Regulation Revealed by Whole-Organism Single-Cell RNA-Seq. *Cell*, *173*(6), 1520-1534.e20. https://doi.org/10.1016/j.cell.2018.05.019

Seehausen, O., Terai, Y., Magalhaes, I. S., Carleton, K. L., Mrosso, H. D. J., Miyagi, R., van der Sluijs, I., Schneider, M. V., Maan, M. E., Tachida, H., Imai, H., & Okada, N. (2008). Speciation through sensory drive in cichlid fish. *Nature*, *455*(7213), 620–626. https://doi.org/10.1038/nature07285

Shewchuk, B. M., Ho, Y., Liebhaber, S. A., & Cooke, N. E. (2006). A Single Base Difference between Pit-1 Binding Sites at the *hGH* Promoter and Locus Control Region Specifies Distinct Pit-1 Conformations and Functions. *Molecular and Cellular Biology*, *26*(17), 6535–6546. https://doi.org/10.1128/MCB.00267-06

Silva, M. A. P., & Nakanishi, N. (2019). Genotyping of Sea Anemone during Early Development. *Journal of Visualized Experiments*, *147*, 59541. https://doi.org/10.3791/59541

Soares, M. C., Bshary, R., Fusani, L., Goymann, W., Hau, M., Hirschenhauser, K., & Oliveira, R. F. (2010). Hormonal mechanisms of cooperative behaviour. *Philosophical Transactions of the Royal Society B: Biological Sciences*, *365*(1553), 2737–2750. https://doi.org/10.1098/rstb.2010.0151

Solé, M., Kaifu, K., Mooney, T. A., Nedelec, S. L., Olivier, F., Radford, A. N., Vazzana, M., Wale, M. A., Semmens, J. M., Simpson, S. D., Buscaino, G., Hawkins, A., Aguilar de Soto, N., Akamatsu, T., Chauvaud, L., Day, R. D., Fitzgibbon, Q., McCauley, R. D., & André, M. (2023). Marine invertebrates and noise. *Frontiers in Marine Science*, *10*, 1129057. https://doi.org/10.3389/fmars.2023.1129057

Solé, M., Lenoir, M., Fontuño, J. M., Durfort, M., van der Schaar, M., & André, M. (2016). Evidence of Cnidarians sensitivity to sound after exposure to low frequency noise underwater sources. *Scientific Reports*, *6*(1), 37979. https://doi.org/10.1038/srep37979

Sundaresan, S., Balasubbu, S., & Mustapha, M. (2016). Thyroid hormone is required for the pruning of afferent type II spiral ganglion neurons in the mouse cochlea. *Neuroscience*, *312*, 165–178. https://doi.org/10.1016/j.neuroscience.2015.11.020

Szczepanek, S., Cikala, M., & David, C. N. (2002). Poly-γ-glutamate synthesis during formation of nematocyst capsules in *Hydra*. *Journal of Cell Science*, *115*(4), 745–751. https://doi.org/10.1242/jcs.115.4.745

Tarrant, A. M. (2005). Endocrine-like Signaling in Cnidarians: Current Understanding and Implications for Ecophysiology. *Integrative and Comparative Biology*, *45*(1), 201–214. https://doi.org/10.1093/icb/45.1.201

Tournière, O., Dolan, D., Richards, G. S., Sunagar, K., Columbus-Shenkar, Y. Y., Moran, Y., & Rentzsch, F. (2020). NvPOU4/Brain3 Functions as a Terminal Selector Gene in the Nervous System of the Cnidarian *Nematostella vectensis*. *Cell Reports*, *30*(13), 4473-4489.e5. https://doi.org/10.1016/j.celrep.2020.03.031

Tulin, S., Aguiar, D., Istrail, S., & Smith, J. (2013). A quantitative reference transcriptome for *Nematostella vectensis* earlyembryonic development: A pipeline for de novo assembly in emergingmodel systems. *EvoDevo*, *4*(1), 16. https://doi.org/10.1186/2041-9139-4-16

Uchida, K., Murakami, Y., Kuraku, S., Hirano, S., & Kuratani, S. (2003). Development of the adenohypophysis in the lamprey: Evolution of epigenetic patterning programs in organogenesis. *Journal of Experimental Zoology*, *300B*(1), 32–47. https://doi.org/10.1002/jez.b.44

Warner, J. F., Guerlais, V., Amiel, A. R., Johnston, H., Nedoncelle, K., & Röttinger, E. (2018). NvERTx: A gene expression database to compare embryogenesis and regeneration in the sea anemone *Nematostella vectensis*. *Development*, dev.162867. https://doi.org/10.1242/dev.162867

Westfall, J. A., Sayyar, K. L., & Elliott, C. F. (1998). Cellular Origins of Kinocilia, Stereocilia, and Microvilli on Tentacles of Sea Anemones of the Genus Calliactis (Cnidaria: Anthozoa). *Invertebrate Biology*, *117*(3), 186. https://doi.org/10.2307/3226984

Wolenski, F. S., Bradham, C. A., Finnerty, J. R., & Gilmore, T. D. (2013). NF-κB is required for cnidocyte development in the sea anemone *Nematostella vectensis*. *Developmental Biology*, *373*(1), 205–215. https://doi.org/10.1016/j.ydbio.2012.10.004

Zang, H., & Nakanishi, N. (2020). Expression Analysis of Cnidarian-Specific Neuropeptides in a Sea Anemone Unveils an Apical-Organ-Associated Nerve Net That Disintegrates at Metamorphosis. *Frontiers in Endocrinology*, *11*, 63. https://doi.org/10.3389/fendo.2020.00063

6) SUPPLEMENTARY MATERIAL

Supplementary Table 1. Key resources generated in this study.

Reagent type (species) or resource	Designation	Source or reference	Additional information
Antibody	Anti-Pit1 21-40 (rabbit)	this paper	(1:200) See the Methods section of the paper for a description of the antibody.
Antibody	Anti-Pit1 yz6677 (rabbit)	this paper	(1:200) See the Methods section of the paper for a description of the antibody.
Plasmid	Pit1::Kaede	this paper	See the Methods and Supplementary Material section of the paper for a description of the plasmid.
Biological sample	Pit1::Kaede F1	this paper	See the Methods and Supplementary Material section of the paper for a description of the plasmid.
Biological sample	F2 Pit1$^{-d/+}$ x Elav::mO	this paper	See the Discussion section of the paper.
Biological sample	F1 CR-Pit1$^{-a/-a}$	this paper	See the Results section of the paper for a description of the biological sample.
Biological sample	F1 CR-Pit1$^{-b/-b}$	this paper	See the Results section of the paper for a description of the biological sample.
Biological sample	F1 CR-Pit1$^{-c/-c}$	this paper	See the Results section of the paper for a description of the biological sample.
Biological sample	F2 CR-Pit1$^{-d/-d}$	this paper	See the Results section of the paper for a description of the biological sample.

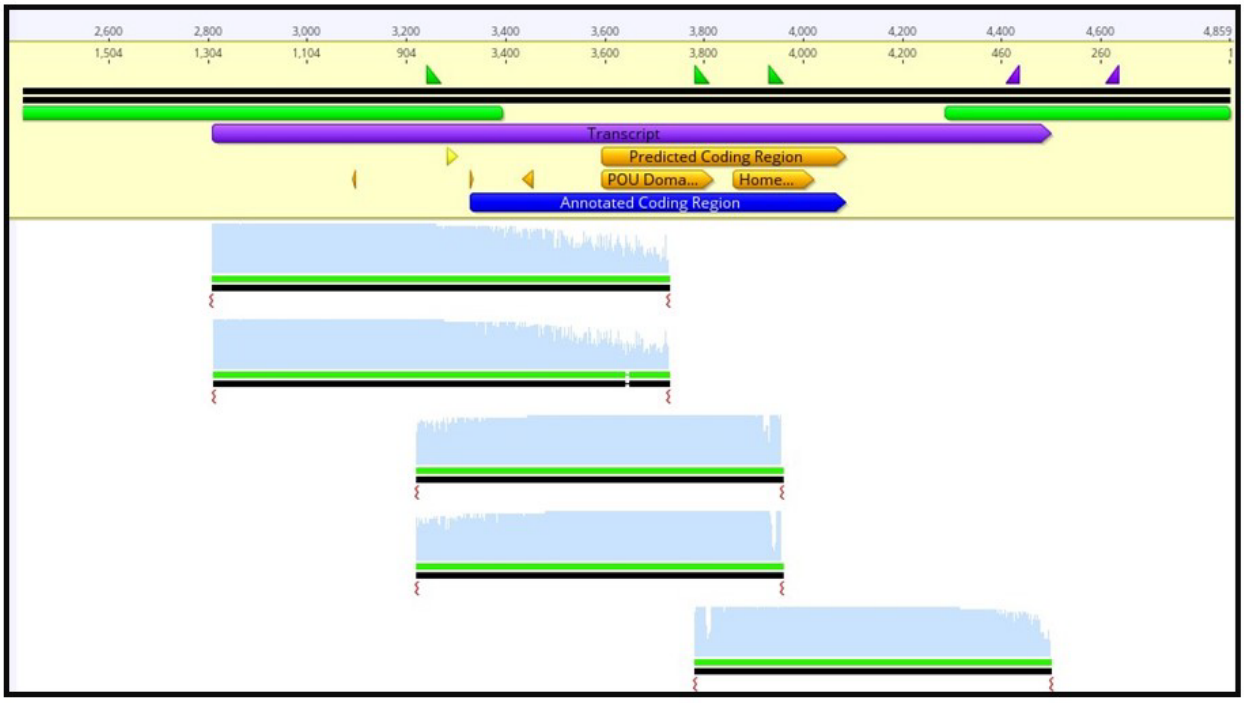

Supplementary Figure 1. RACE cDNA results confirm a single exon of Pit1, and analysis of Start site indicated a longer coding region (blue annotation) than previously predicted by EST data (yellow annotation).

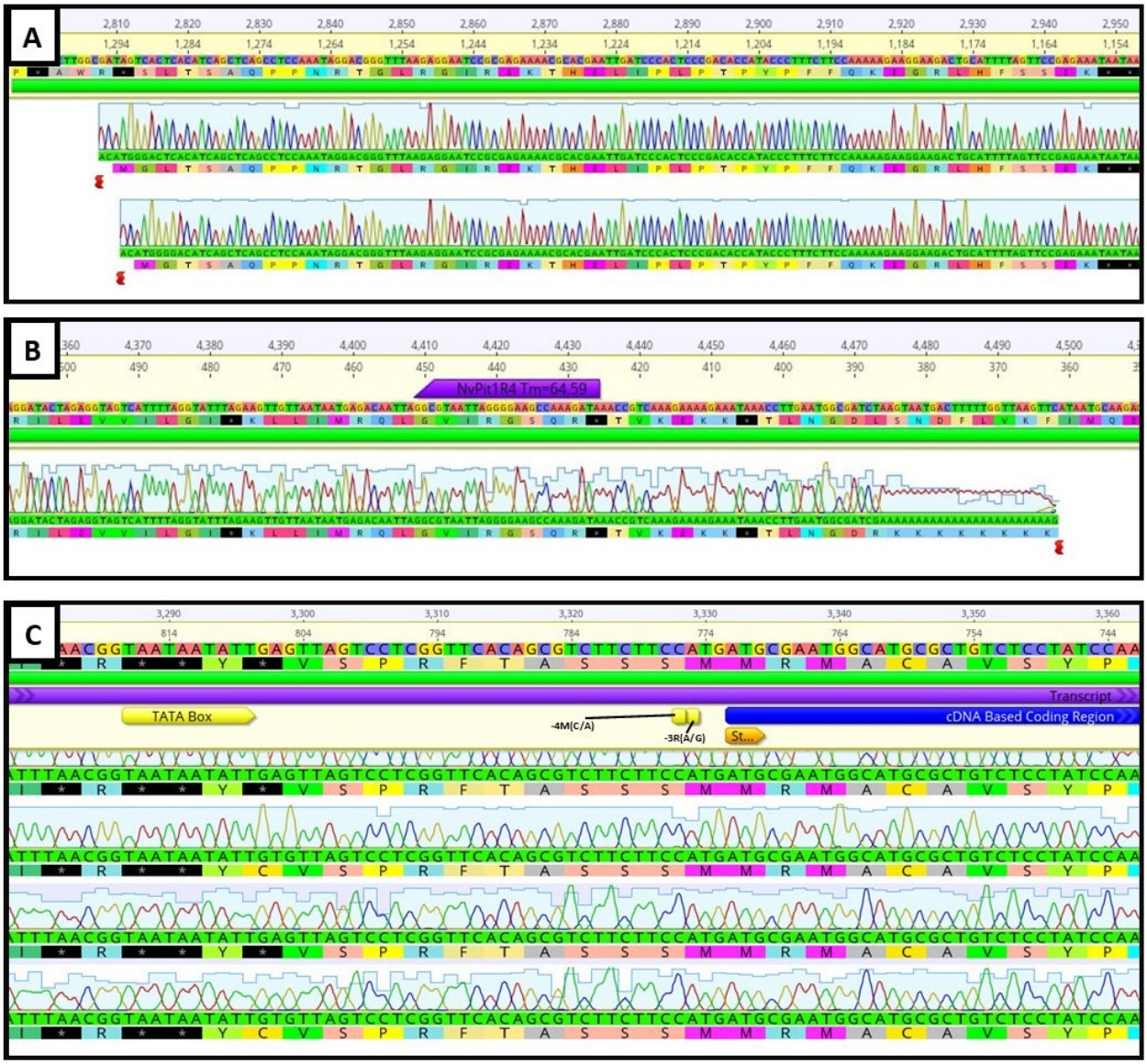

Supplementary Figure 2. Detailed analysis of cDNA. (**A**) UTR region of Pit1 transcript. (**B**) Poly-A tail of Pit1 transcript. (**C**) Annotation of Start site, Kozak sequence (-3R, -4M) and TATA box region of the characterized Pit1 promoter. 3031bp of genomic sequence upstream of the annotated Start site was extracted, amplified, and used for the Pit1::Kaede transgenic construct.

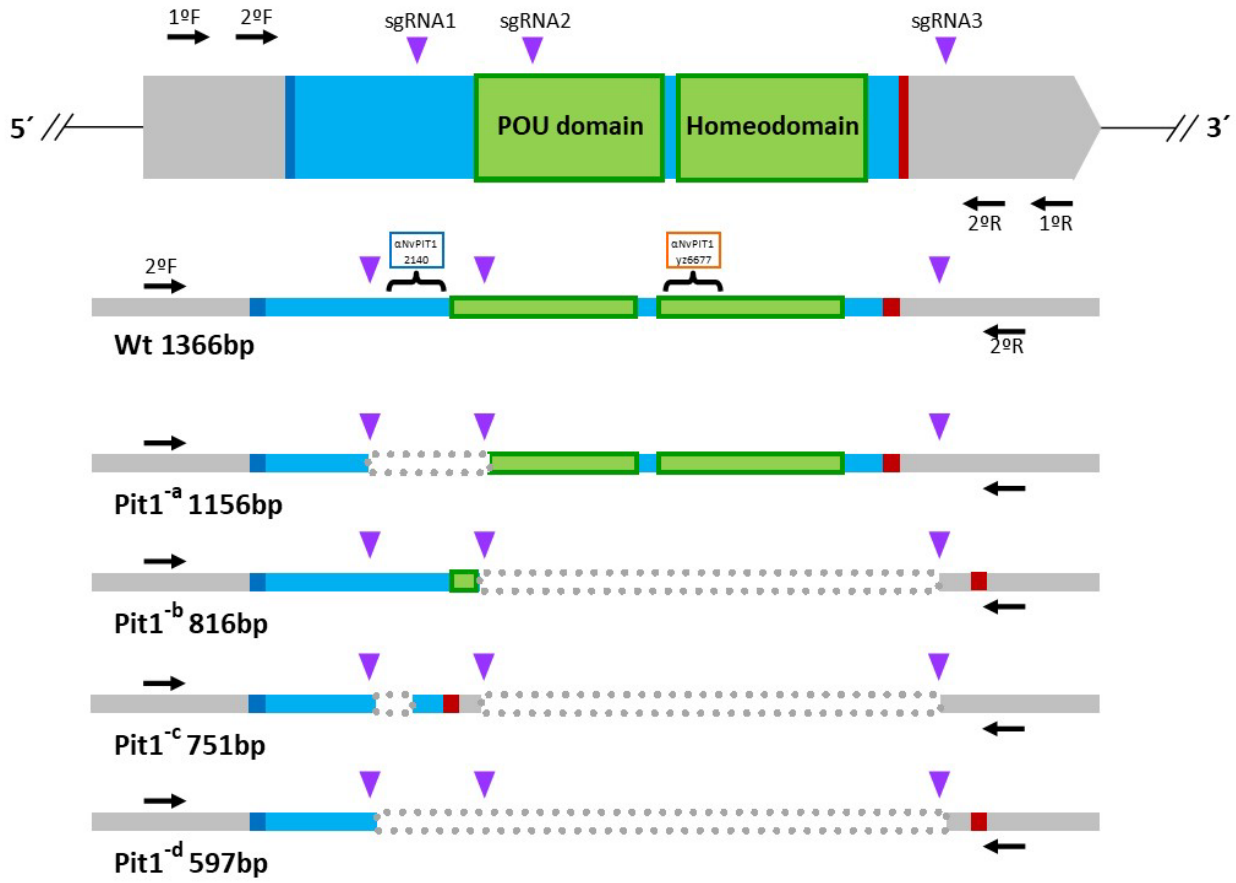

Supplementary Figure 3. Single exon Pit1 gene confirmed by RACE PCR and mutant alleles generated by CRISPR-Cas9 mediated mutagenesis. (**A**) Gene model of Pit1 as confirmed by RACE cDNA data, sgRNAs were designed to knockout the entire functional domains, POU domain and Homeodomain. Dark blue indicates Start site, light blue the coding region, green indicates functional domains, red the Stop codon. Target sites of sgRNAs are in purple and primer binding sites denoted as black arrows. (**B**) In the WT allele, antibody binding sites are represented by brackets and labeled. Different patterns of CRISPR-Cas9 activity. Allele -a does not result in a frameshift mutation or an early stop codon, 543bp coding region for a 181aa protein. Allele -b has the binding site of anti-NvPit1 21-40 intact, which can be exploited for functional studies, it results in a non-functional truncated protein as the functional POU and Homeodomains are knocked out. The STOP codon is deleted, and a further downstream STOP codon terminates translation, 402bp, 134aa. Allele -c knockout results in a frameshift and an early stop codon, 153bp, 51aa. Allele -d has the longest deletion, from sgRNA target site 1 to sgRNA target site 3, 192bp, 64aa truncated protein.

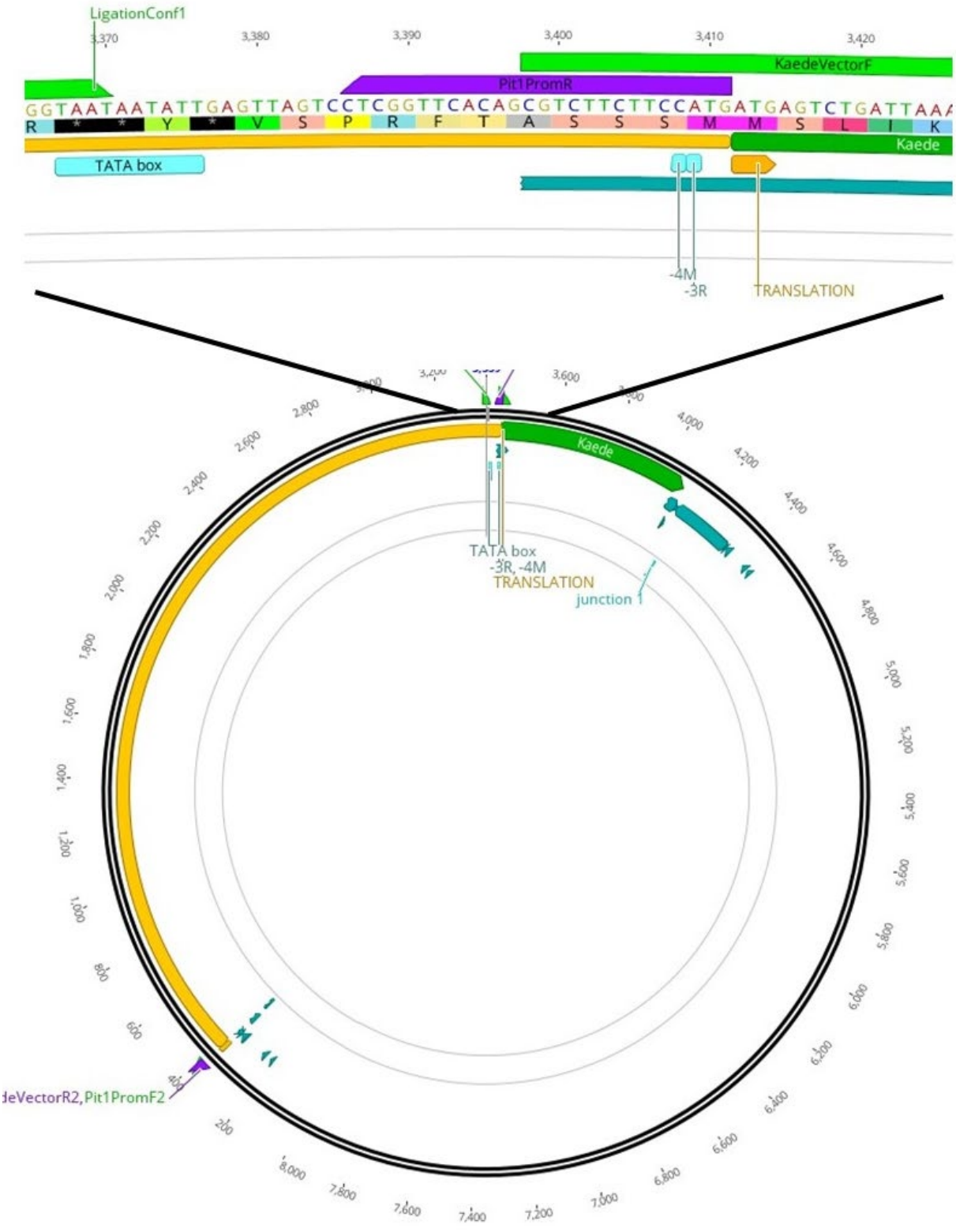

Supplementary Figure 4. Pit1::Kaede plasmid.

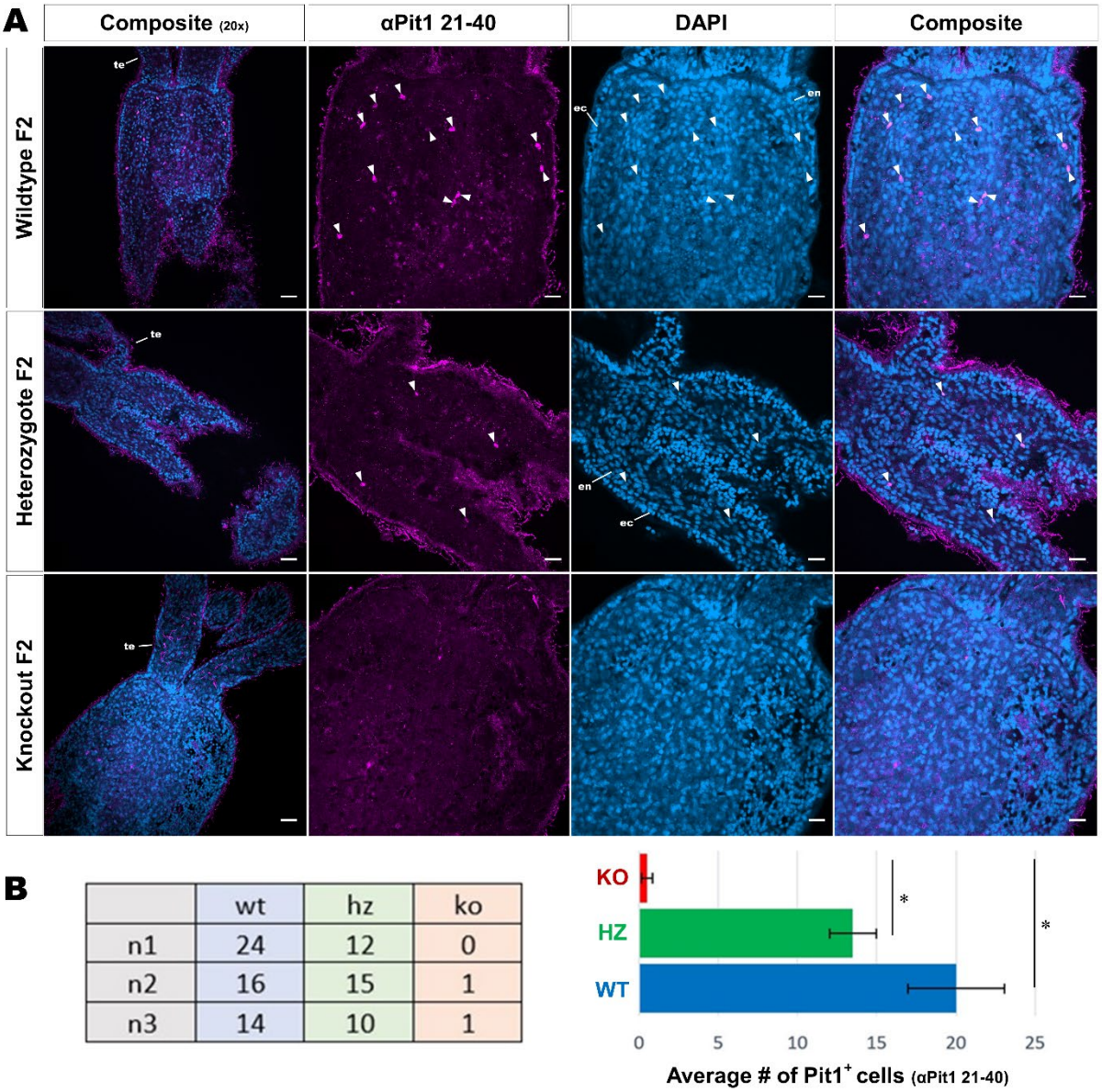

	wt	hz	ko
n1	24	12	0
n2	16	15	1
n3	14	10	1

Supplementary Figure 5. To validate the newly made NvPit1 antibodies, immunohistochemistry experiments were performed on F2 CR-NvPit1 animals. Gastrula genotyping (Silva & Nakanishi, 2019) allowed to sort the F2s by genotype (i.e., Wildtype$^{+/+}$, Heterozygotes$^{-d/+}$, Knockout$^{-d/-d}$) and stain the separate populations. Staining was performed at the same time and using the same protocol for all. Stained Pit1^{+} nuclei were manually counted and annotated in Fiji using the plug-in "Colocalization Object Counter" (Lunde & Glover, 2020). Counted samples were all at the same developmental stage and imaged at 40x magnification and 1x zoom, with all the confocal parameters equal (e.g., gain, pinhole, laser power). Scanning and counting was done in the oral region of the polyp, from epidermal superficial layers, down to the pharyngeal sections (along the directive axis). One-way ANOVA and Tukey Test were used for statistical analysis (see supplemental material). NvPit1-2140 antibodies showed a significant decrease of Pit1 staining between wildtype and knockout animals (Fig. 3), with wildtype having in average 25 cells (n=3), heterozygotes 12 cells (n=3), and knockout animals <1 cell (n=3) ($P < 0.05$; $P=0.002$).

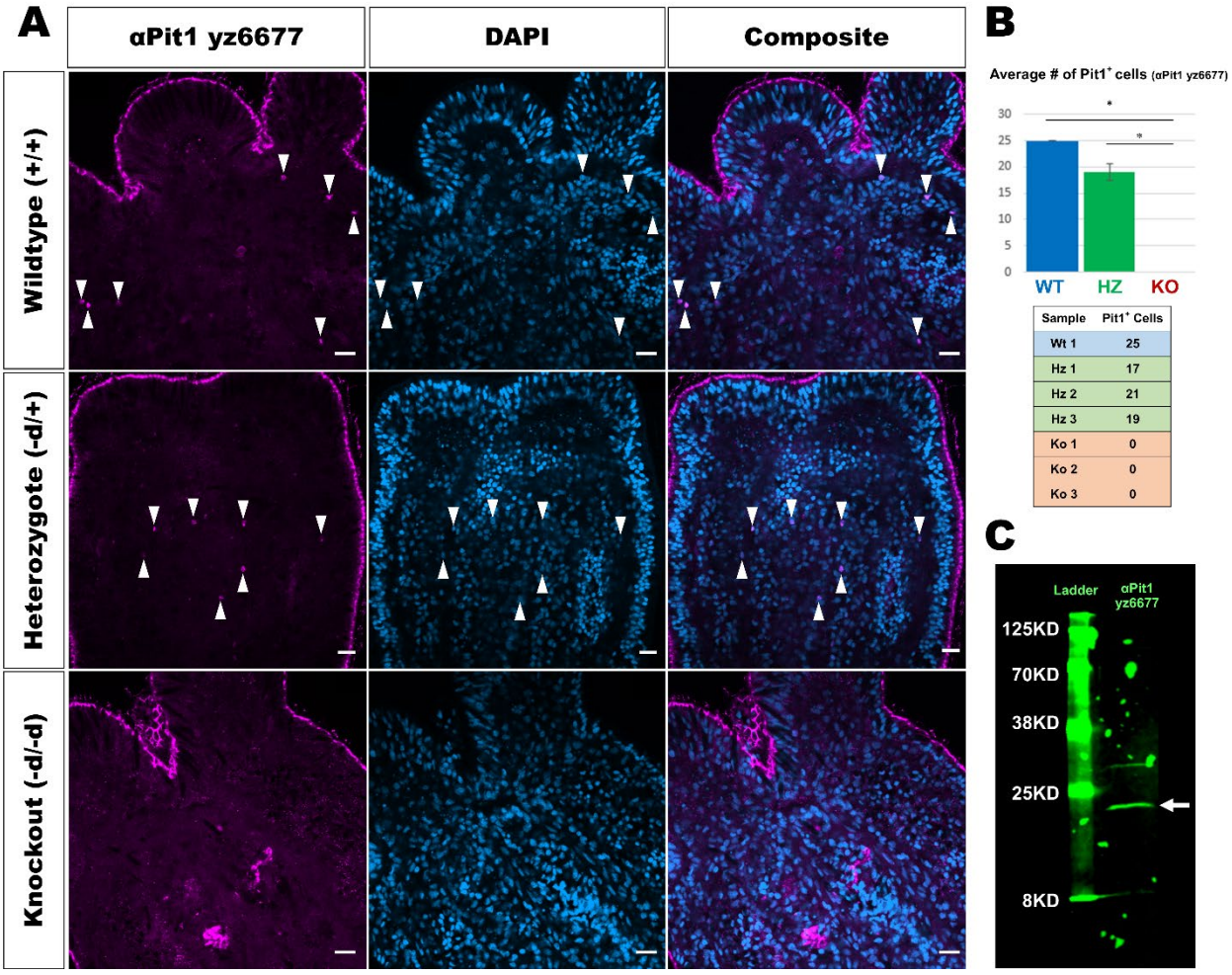

Supplemental Figure 6. (A-B) The NvPit1-yz6677 antibody shows absence of staining in knockout animals (n=3), with wildtype having 25 stained cells (n=1) and heterozygotes with 19 stained cells in average (n=3). (**C**) Western blot was done for both antibodies, with NvPit1-yz6677 showing a specific band of 24KD. Combined in-situ and immunohistochemistry experiments done with NvPit1-yz6677 using wildtype animals further demonstrate the specificity of the antibody by the colocalization of Pit1 transcripts with the antibody.

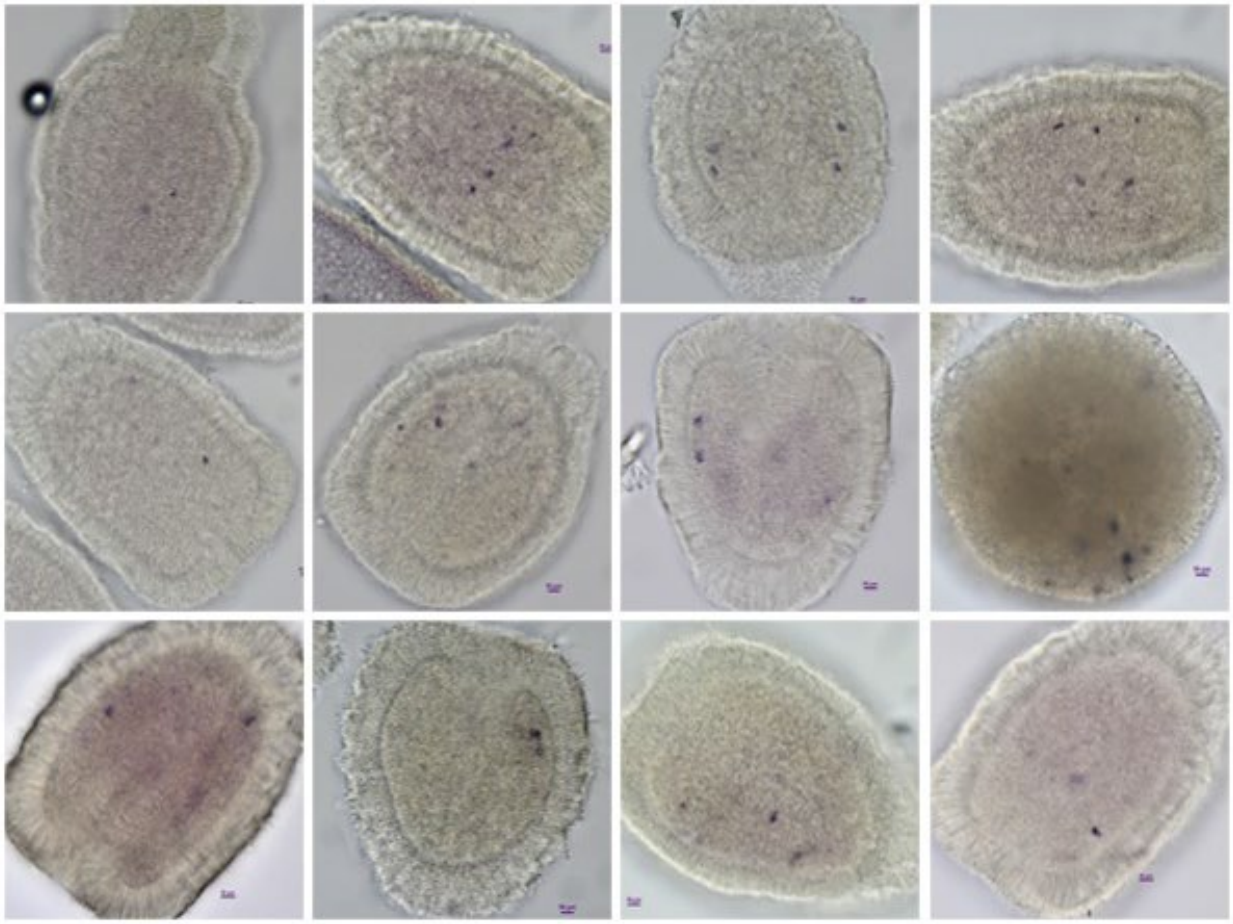

Supplemental Figure 7. Colorimetric in-situ of wildtype animals at several stages with Pit1 anti-sense riboprobe recapitulates the pattern seen with fluorescent in-situ hybridization.

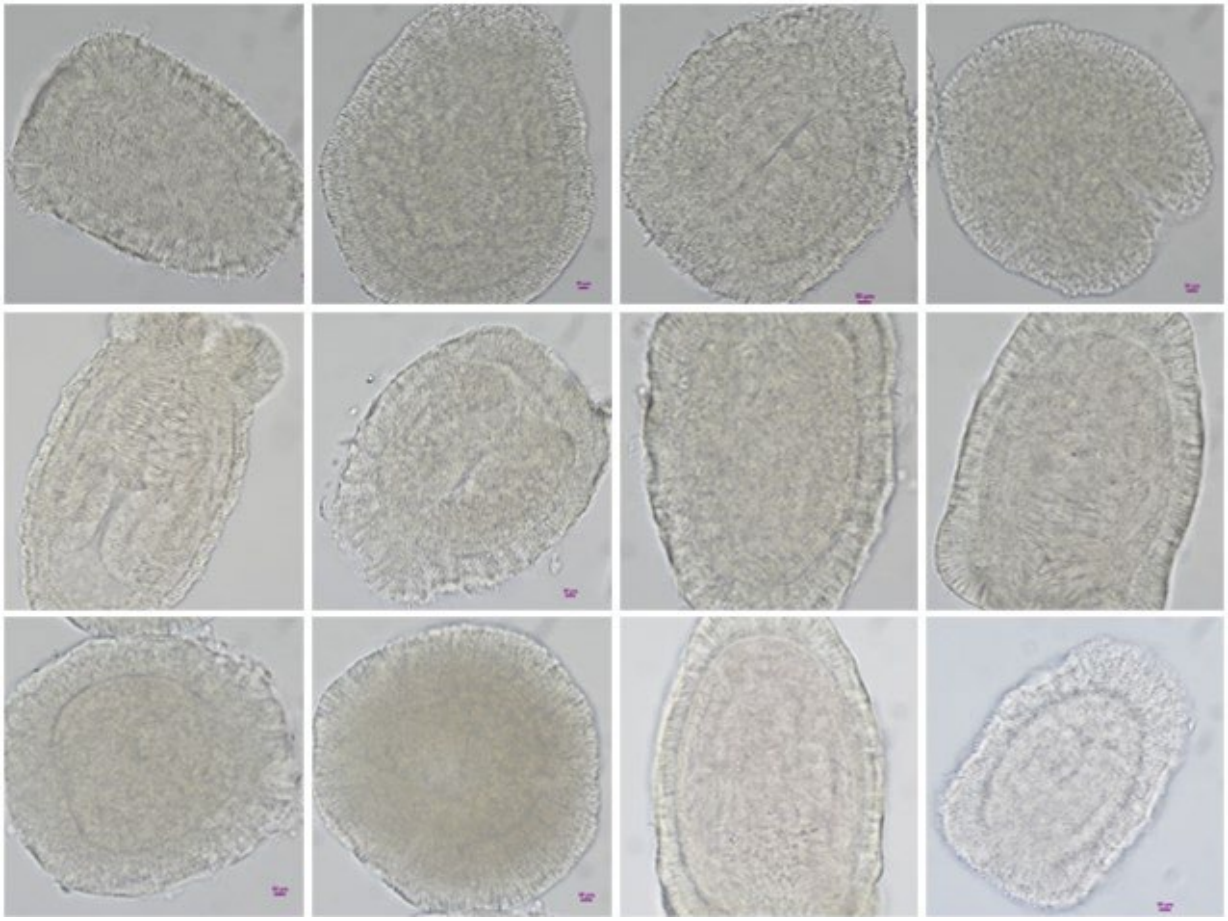

Supplemental Figure 8. Positive control for colorimetric in-situ using a sense Pit1 riboprobe.

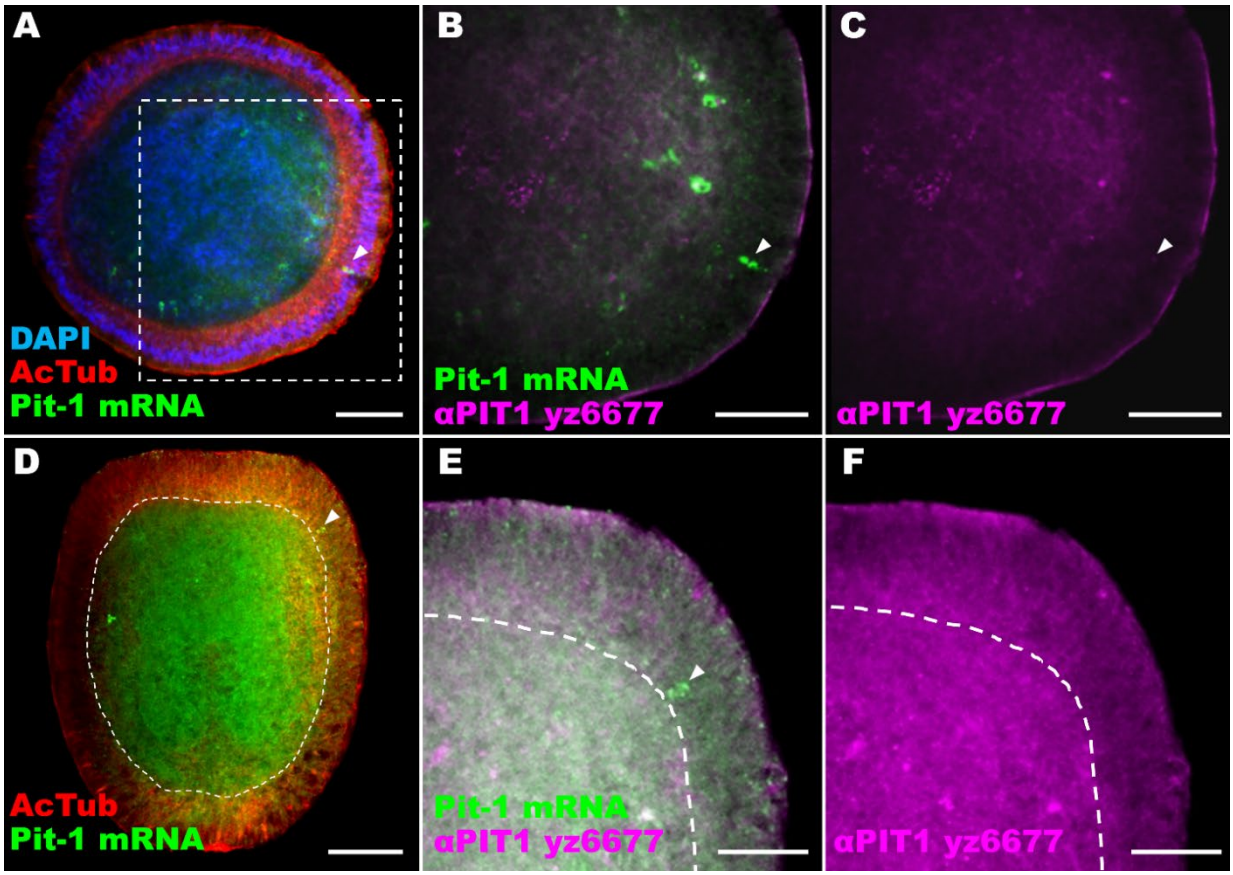

Supplementary Figure 9. Single cell ectodermal expression during larval development. (A-C) Early planula showing expression of Pit1 in a single cell in the ectoderm. The arrowed in (A) and (B) points to a spindle-shaped sensory cell in the ectoderm, stained with a riboprobe bound to Pit1 transcripts in the cytoplasm; arrowed in (C) points to a nucleus faintly stained with αPIT1 yz6677 antibody, bound to the PIT1 transcription factor. **(D-F)** Late planula showing expression of Pit1 in a single ectodermal cell, arrowheads in (D) and (E) showing Pit1 transcript, but no PIT1 translation (F) at this developmental time point. Scale bars, 50um A-D, 25um E and F.

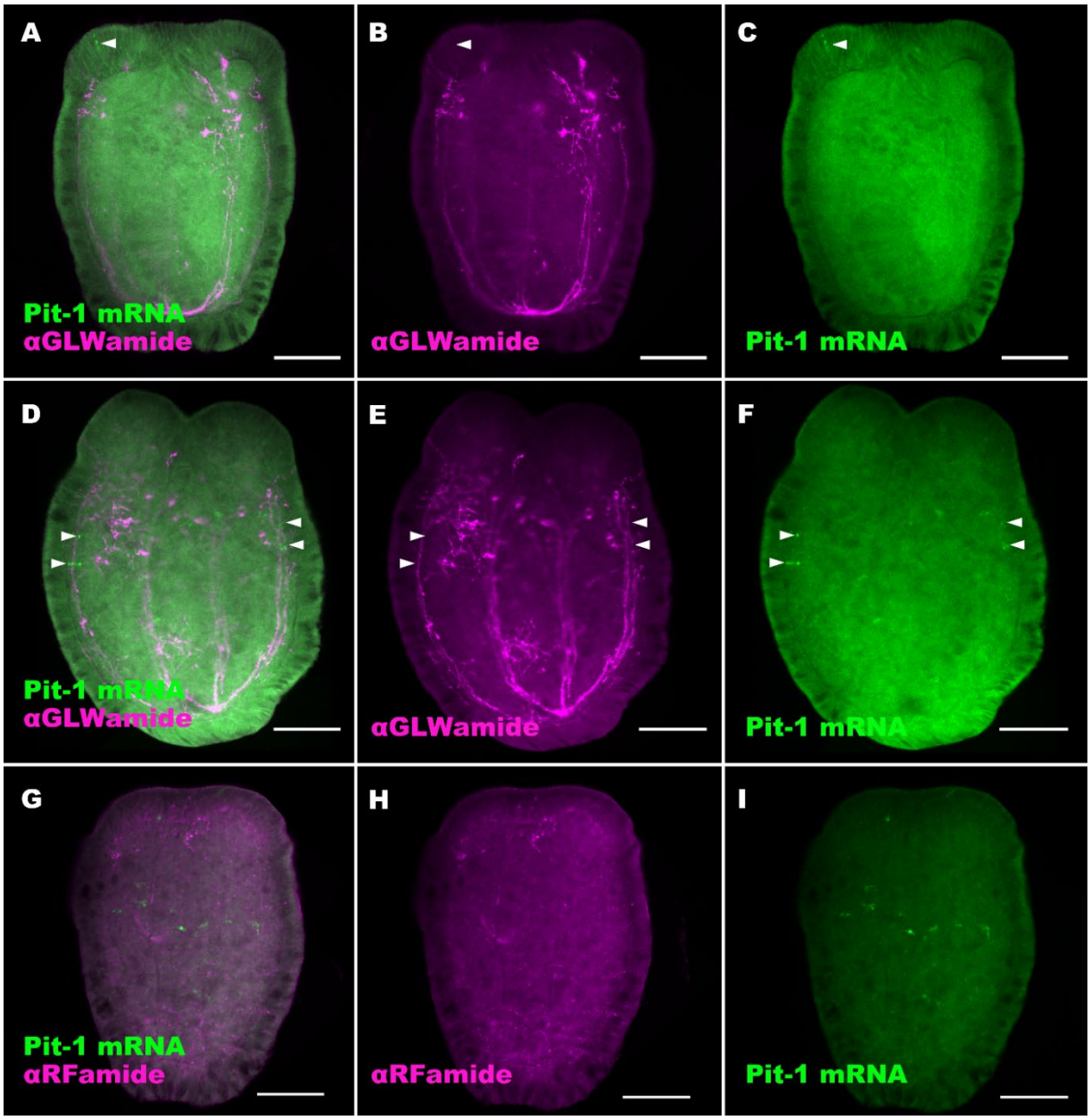

Supplementary Figure 10 – GLWamide and RFamide colocalization analysis with Pit1. **(A-F)** Apical arrowheads demonstrate no colocalization on ectodermal cells while central/equatorial arrowheads point to Pit1 expressing cells possibly colocalizing with GLWamide neurons, or in adjacent cells – further data at higher resolution is needed to clarify. **(G-I)** RFamide does not seem to colocalize with Pit1 but more data is required. Scale bars 50um

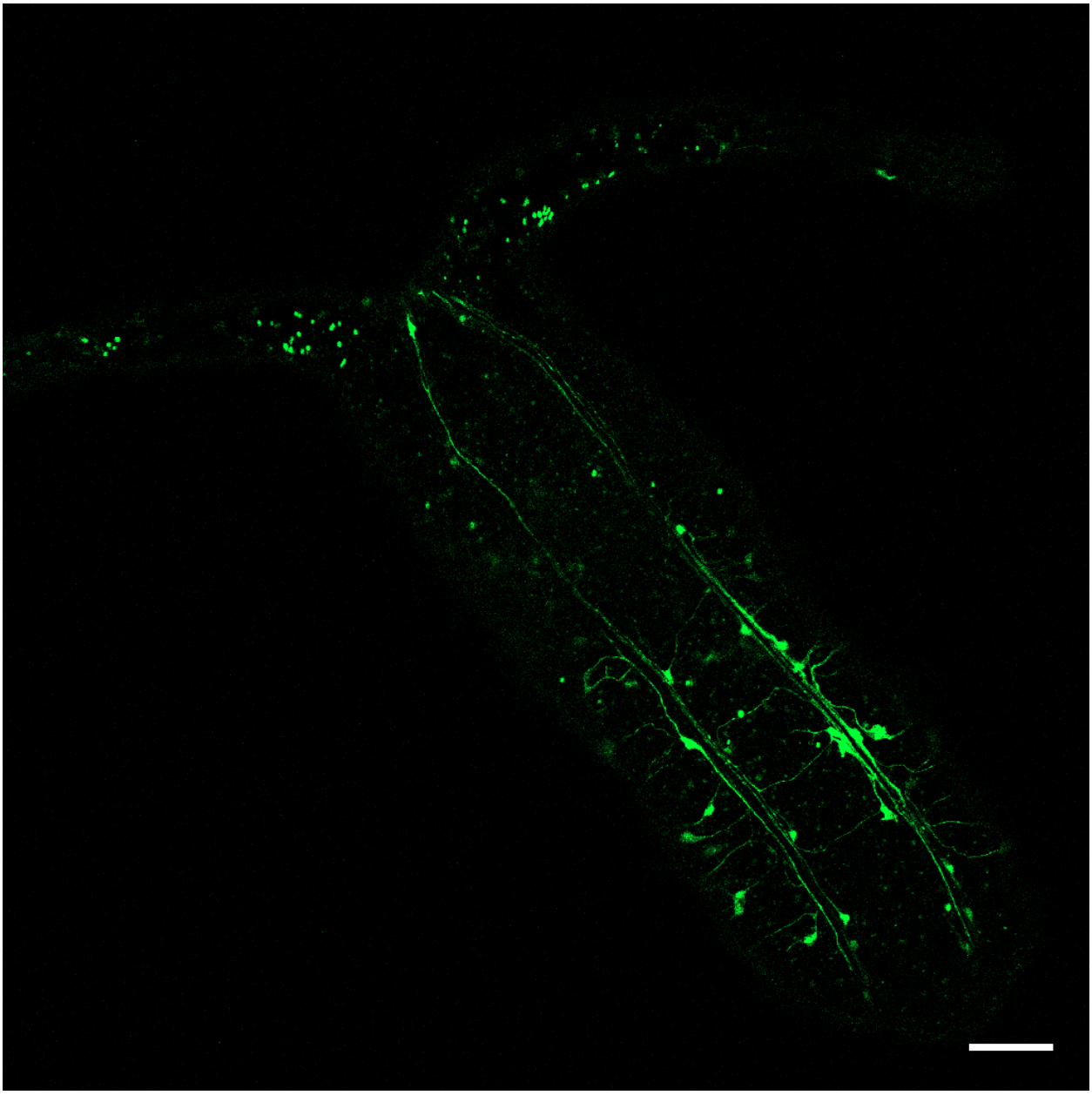

Supplementary Figure 11. Live imaging of Pit1::Kaede F2 polyps. Scale bar 50um.

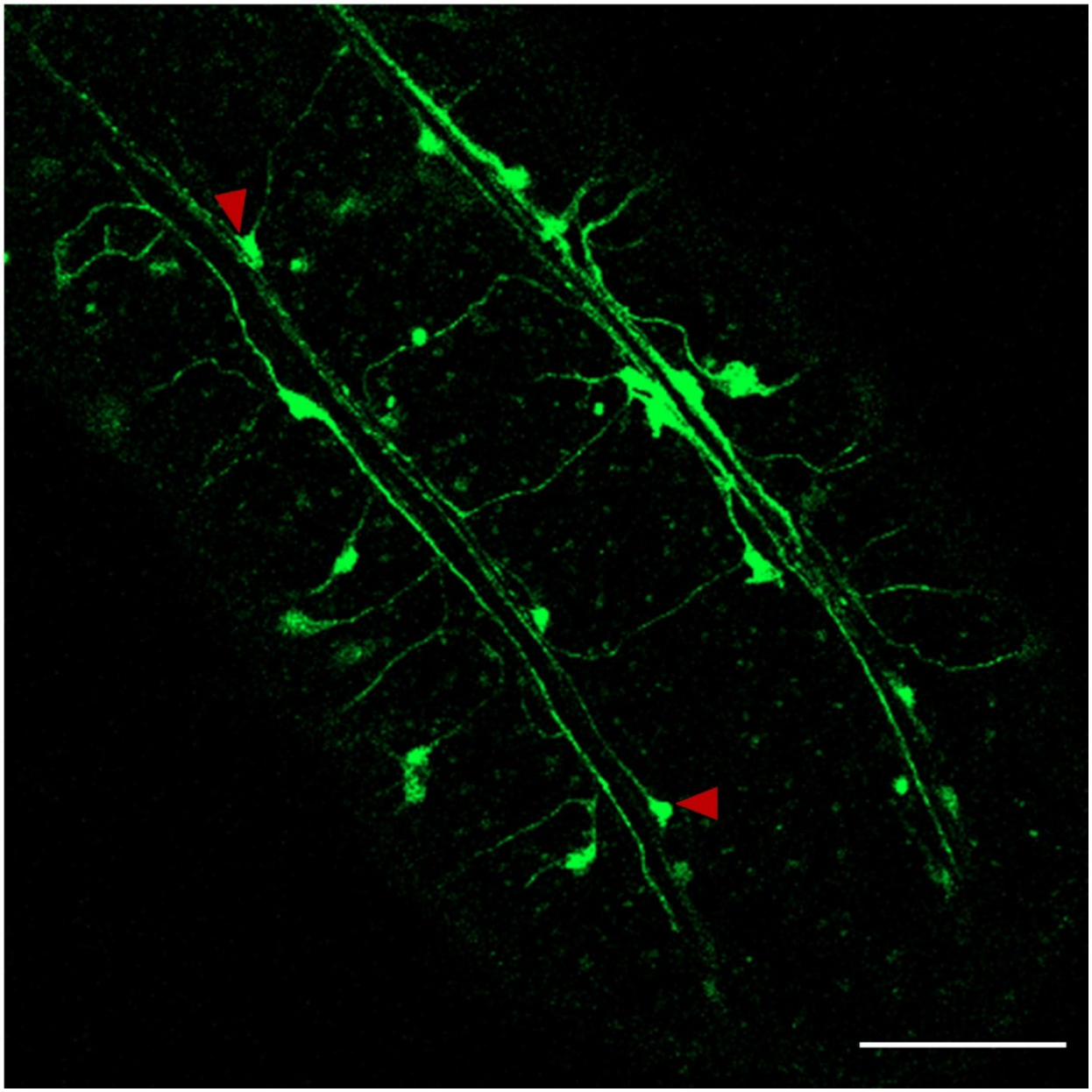

Supplementary Figure 12. Live imaging of Pit1::Kaede F2 polyps. Red arrowheads point at possible connecting ganglion neurons Scale bar 50um.

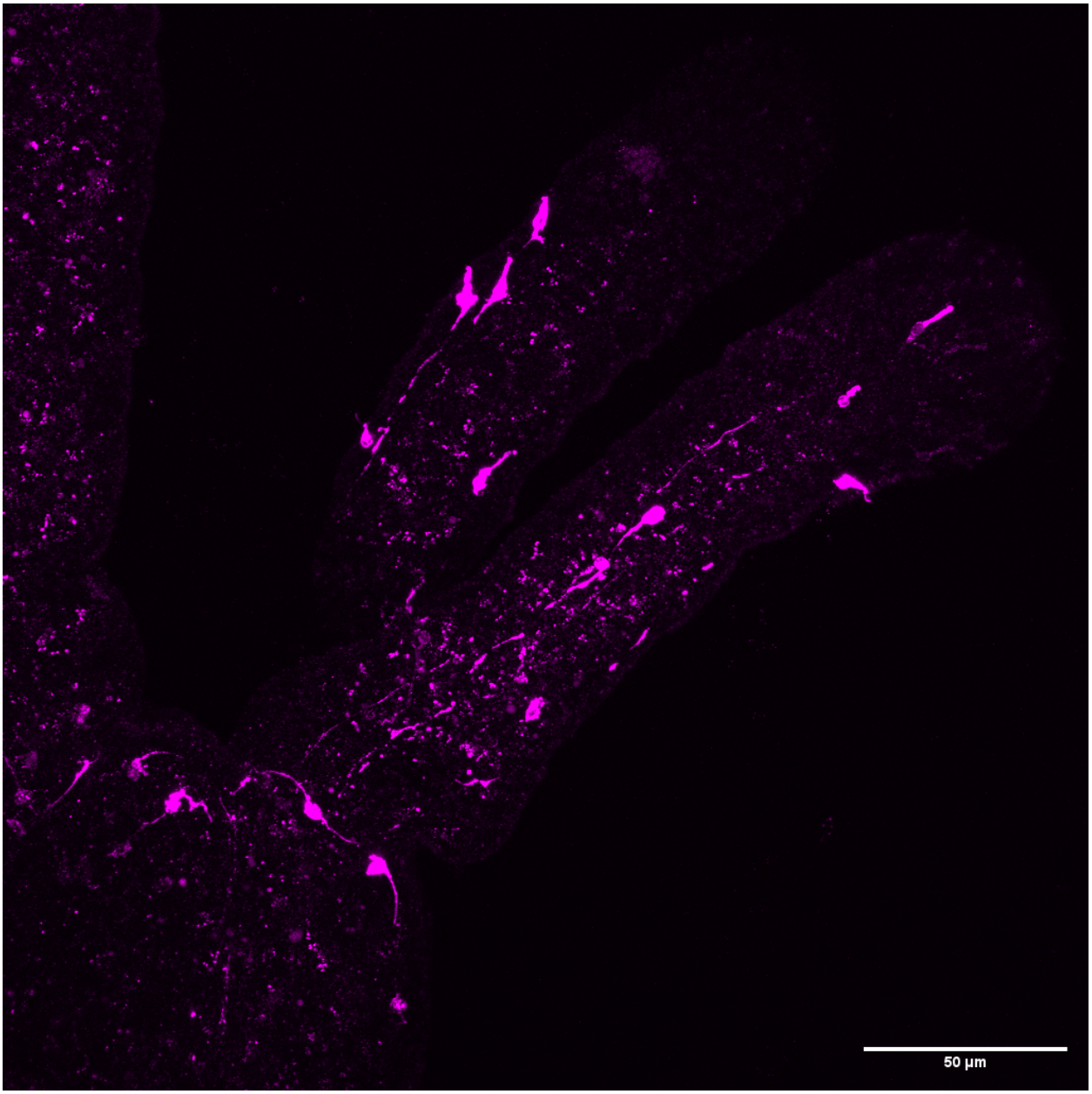

Supplementary Figure 13. Kaede stain on F2 Pit1::Kaede Transgenic polyps. Z-projection, reveals morphologically diverse sensory cells in the tentacles and ganglion cells at the base of the tentacle.

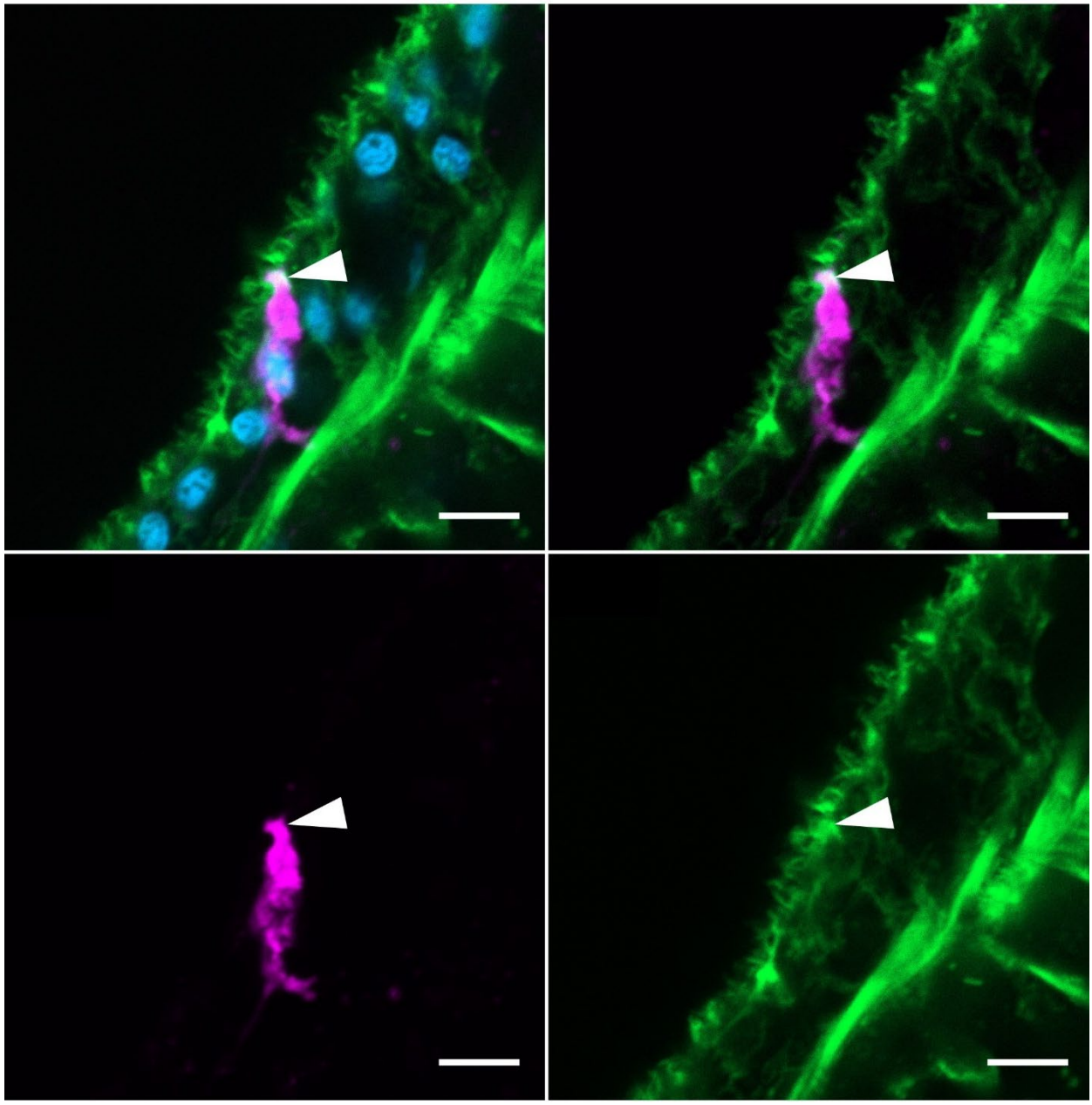

Supplementary Figure 14. Confocal section (z7) shows Pit1^{+} cells, with the apical tip of the cell rich in (or surrounded by) actin stereocilia.

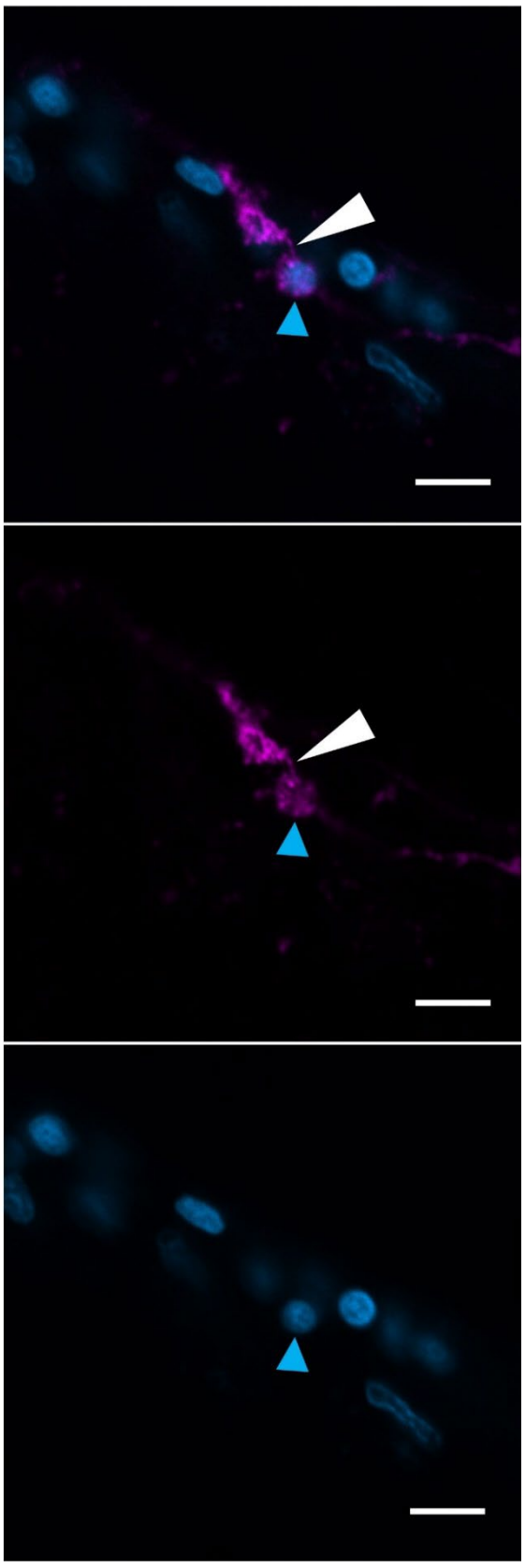

Supplementary Figure 15. Single confocal section clarifies that this cell is a single cell (see blue arrowhead), since only one nucleus is found. White arrowhead points at noticeable characteristic of a thin process extending from the soma to the apical tip of the cell. Scale bars: All 5um.

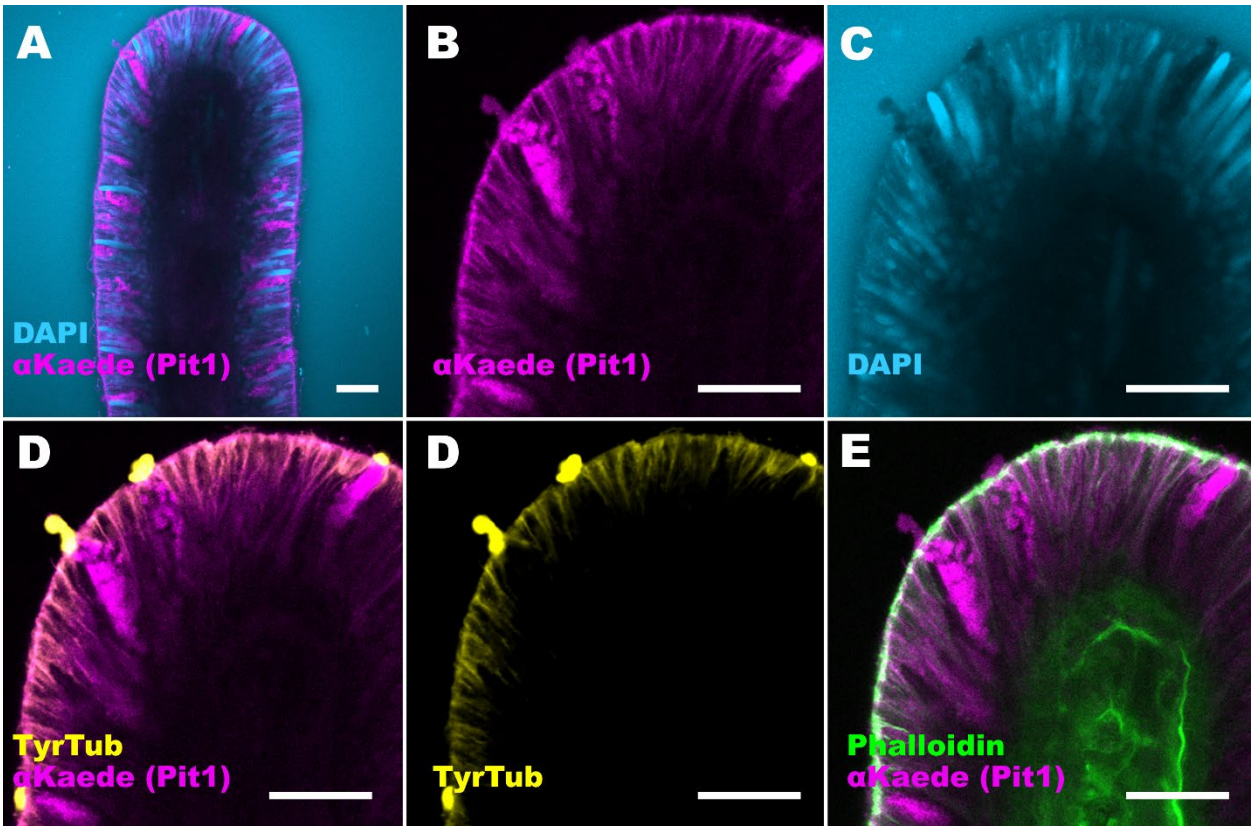

Supplementary Figure 16. Pit1::Kaede F1 animals stained with anti-Kaede and a cnidocyte specific DAPI staining revealed no expression of Pit1 in cnidocytes. Scale bars: All 10um.

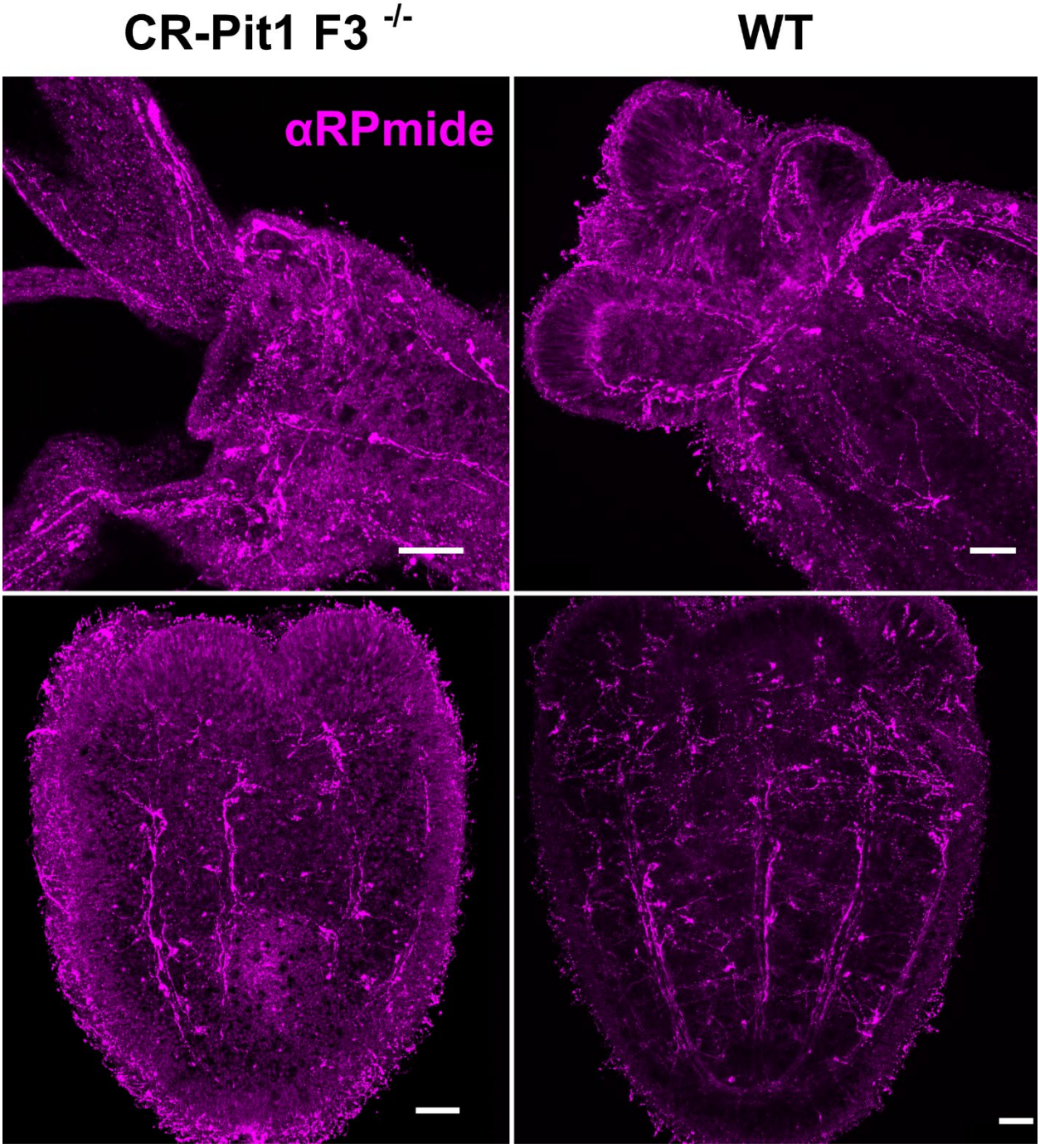

Supplementary Figure 17. Preliminary data of Staining of CR-Pit1 +/+ and -d/-d siblings did not reveal noticeable defects of RPamide neurons, but further investigation is required (n=1, for tentacle bud and polyp stage). Scale bars: All 20um.

CONCLUSION

Here, for the first time, the spatiotemporal gene expression pattern of Pit1 was described in *Nematostella vectensis*, revealing a dynamic expression beginning in the endoderm of the body column and subsequentially starting in the ectoderm of tentacles during metamorphosis. Analysis of Pit1::Kaede transgenic animals revealed a complex neuronal network of Pit1-positive neurons in the endoderm and diverse morphologies of sensory cells in the ectoderm of tentacles.

Based on comparative data from the 'moon jellyfish' *Aurelia*, I infer that Pit1 is expressed in sensorial cell types across Cnidaria, but analysis from other taxa is required. Furthermore, considering the hypothesis that the Pit1-positive Hatschek's pit has chemosensory functions in the lancelet *Branchiostma floridae*, and the diverse cellular morphologies here described in *Nematostella*, I raise the hypothesis that the ancestral function of Pit1 is to regulate the differentiation of chemosensory cells. Stable CRISPR-Cas9 knockout lines of Pit1 were generated and the experimental and conceptual foundations were laid for further functional studies of Pit1 in *Nematostella vectensis*. Furthermore, the genotyping protocol developed in Chapter 1 can be applied to non-sea anemone cnidarians allowing to gain insights into the evolution of the diverse developmental mechanisms of cnidarians.

Characterizing the function of neuronal and neuroendocrine regulators across Cnidarian and Bilaterian organisms is essential to understanding and reconstructing the ancestral nervous system of the last common ancestor and consequently to begin unveiling the origins of the animal mind. Hence, I here propound the idea that Cnidarians should be considered and examined through the lens of comparative cognitive sciences. This will provide a view of the core properties underlying the functional mind as we know it, and its primordial properties at basal levels of animal evolution.

It is thus implied that in some sense a rudimentary mind-like quality is present even at the level of particle physics, and that as we go to subtler levels, this mind-like quality becomes stronger and more developed.

– David Bohm (1990)

The laws of physics leave a place for mind in the description of every molecule… In other words, mind is already inherent in every electron, and the processes of human consciousness differ only in degree and not in kind.

– Freeman Dyson (1979)

Will it not turn out, with the further development of science, that the study of the universe and the study of consciousness will be inseparably linked, and that ultimate progress in the one will be impossible without progress in the other?

– Andrei Linde (1998)

REFERENCES

Bohm, D. (1990): A new theory of the relationship of mind and matter, Philosophical Psychology, 3:2-3, 271-286

Dyson, F. (1979). Disturbing the Universe; Basic Books: New York, NY, USA, 1979

Linde, A. (1998) Universe, Life, Consciousness. 1998. Available online: http://web.stanford.edu/~alinde/ SpirQuest.doc (accessed on 18 November 2019)

APPENDIX

UNIVERSITY OF ARKANSAS

Office of Research Compliance

August 26, 2021

MEMORANDUM

TO:	Dr. Nagayasu Nakanishi
FROM:	Ines Pinto, Biosafety Committee Chair
RE:	Protocol Renewal
PROTOCOL #:	18033
PROTOCOL TITLE:	Investigating the fundamental mechanisms of establishing neural cell identities in animals

APPROVED PROJECT PERIOD: **Start Date** July 13, 2017 **Expiration Date** July 12, 2023

The Institutional Biosafety Committee (IBC) has approved your request, dated August 5, 2021, to renew IBC # 18033, "Investigating the fundamental mechanisms of establishing neural cell identities in animals".

The IBC appreciates your assistance and cooperation in complying with University and Federal guidelines for research involving hazardous biological materials.

1424 W. Martin Luther King, Jr. • Fayetteville, AR 72701
Voice (479) 575-4572 • Fax (479) 575-6527